CrossMark

ORIGINAL ARTICLE

Identification of mutations in *FN1* leading to glomerulopathy with fibronectin deposits

Hiromi Ohtsubo[1] · Taro Okada[2] · Kandai Nozu[1] · Yutaka Takaoka[3] · Akemi Shono[1] ·
Katsuhiko Asanuma[4] · Lifang Zhang[2] · Koichi Nakanishi[5] · Mariko Taniguchi-Ikeda[1] ·
Hiroshi Kaito[1] · Kazumoto Iijima[1] · Shun-ichi Nakamura[2]

Abstract

Background Glomerulopathy with fibronectin deposits (GFND) is a rare autosomal dominant disease characterized by massive fibronectin deposits, leading to end-stage renal failure. Although mutations within the heparin-binding domains of the fibronectin 1 gene (*FN1*) have been associated with GFND, no mutations have been reported within the integrin-binding domains.
Methods In this study, *FN1* mutational analysis was conducted in 12 families with GFND. Biochemical and functional features of mutated proteins were examined using recombinant fibronectin fragments encompassing both the integrin- and heparin-binding domains.

Results We report six *FN1* mutations from 12 families with GFND, including five that are novel (p.Pro969Leu, p.Pro1472del, p.Trp1925Cys, p.Lys1953_Ile1961del, and p.Leu1974Pro). p.Pro1472del is localized in the integrin-binding domain of fibronectin, while the others are in heparin-binding domains. We detected p.Tyr973Cys, p.Pro1472del, and p.Leu1974Pro mutations in multiple families, and haplotype analysis implied that p.Pro1472del and p.Leu1974Pro are founder mutations. The protein encoded by the novel integrin-binding domain mutation p.Pro1472del showed decreased cell binding ability via the integrin-binding site. Most affected patients developed urine abnormalities during the first or second decade of life, and some mutation carriers were completely asymptomatic.
Conclusions This is the second large-scale analysis of GFND families and the first report of an integrin-binding domain mutation. These findings may help determine the pathogenesis of GFND.

Keywords Heparin-binding domain · Integrin-binding domain · GFND · Fibronectin · Nephropathy

Hiromi Ohtsubo, Taro Okada and Kandai Nozu should be regarded as joint first authors.

Electronic supplementary material The online version of this article (doi:10.1007/s00467-016-3368-7) contains supplementary material, which is available to authorized users.

✉ Kandai Nozu
  nozu@med.kobe-u.ac.jp

1   Department of Pediatrics, Kobe University Graduate School of Medicine, 7-5-1 Kusunoki-cho, Chuo, Kobe 650-0017, Japan

2   Department of Biochemistry and Molecular Biology, Kobe University Graduate School of Medicine, Kobe 658-0072, Japan

3   Division of Medical Informatics and Bioinformatics, Kobe University Hospital, Kobe 658-0072, Japan

4   Medical Innovation Center, TMK project, Kyoto University Graduate School of Medicine, Kyoto 606-8501, Japan

5   Department of Pediatrics, Wakayama Medical University, Wakayama 641-8509, Japan

Introduction

Fibronectin is an adhesive, multifunctional high-molecular-weight glycoprotein found in the plasma (pFN) and the extra-cellular matrix (cell-associated FN, cFN). Fibronectin participates in various physiological processes, such as cell migration, adhesion, cell cycle progression, and cell differentiation [1–3]. The biological activities of fibronectin are mediated via interactions with various members of the integrin family and cell surface proteoglycans. pFN is a dimer comprising two 220-kDa monomers joined by a disulfide bond at the C-

🖄 Springer

terminus. Each monomer comprises homologous repeating structural modules (Fig. 1) [1, 4].

Fibronectin is known to be involved in several interactions, including heparin binding and cell binding via integrins (Fig. 1). The type III repeat 10 (III_{10}) has been shown to bind integrins via an Arg–Gly–Asp (RGD) sequence [5], and repeat 9 contains a synergy site (PHSRN) that enhances interactions with integrins on the same face of fibronectin as the RGD segment [6]. In addition to integrin binding, heparin-binding sites have been reported within type III repeats 12–14 ($III_{12–14}$) [7–9]. The heparin-binding activity of fibronectin has been proposed to act in concert with integrins in the formation of focal adhesions [10–12].

Glomerulopathy with fibronectin deposits (GFND, OMIM: 601894) is a rare autosomal dominant disease characterized by proteinuria, microscopic hematuria, hypertension, and massive fibronectin deposits in the mesangium and subendothelial space, leading to end-stage renal failure. In immunolocalization studies, fibrillary deposits stained positively for an antibody detecting both pFN and cFN, but were only weakly stained for an antibody specific to cFN, suggesting that the fibrils are deposits of pFN [13]. GFND presents at different ages, although urinary abnormalities usually occur during the first decade of life. In the second to sixth decade, it may lead to end-stage renal failure. There is currently no specific treatment for this disease.

Until recently, the genetic background of GFND remained unclear. Castelletti et al. reported, for the first time, three heterozygous missense mutations in the fibronectin 1 gene (FN1) (p.Tyr973Cys, p.Trp1925Arg, and p.Leu1974Arg) that were associated with GFND [14]. These mutations were located in heparin-binding domain 2 or 3 (Fig. 1), and resulted in a lower affinity for fibronectin binding to heparin on the surface of endothelial cells and podocytes. However, no mutations within the integrin-binding domains have yet been reported, and the precise molecular pathogenesis underlying GFND remains to be clarified.

In the present study, we identified six FN1 mutations in 12 GFND families, including five novel FN1 mutations. We also

report, for the first time, a mutation localized in the integrin-binding domain (p.Pro1472del) in two families. Given that mutations associated with GFND in the integrin-binding domain are novel and may be important for understanding disease pathogenesis, we conducted physicochemical and functional studies using recombinant mutant fibronectin fragments encompassing both the integrin- and heparin-binding domains. Finally, we discuss a possible mechanism for how these mutations cause GFND, including the integrin-binding site mutation in fibronectin.

Concise methods

Complete methods are provided in Online Resource 1 (Supplementary Material).

Ethical considerations

All procedures were reviewed and approved by the Institutional Review Board of Kobe University School of Medicine and were conducted in accordance with the principles contained in the Declaration of Helsinki. All participants provided informed consent.

Patients and diagnosis

This study examined GFND patients and their family members. All patients underwent renal biopsies and were diagnosed with GFND by renal histological findings. None of the affected participants presented clinical or laboratory evidence of systemic lupus, cryoglobulinemia, diabetes mellitus, amyloidosis, or autoimmune disease.

DNA analysis

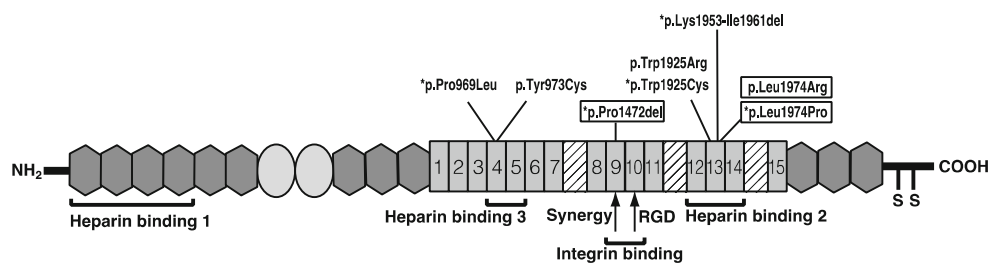Genomic DNA was prepared from peripheral blood according to standard procedures. Genomic DNA analysis using

Fig. 1 Domain structure of fibronectin. FN1 comprises type I (hexagons), II (ellipses), and III (rectangles, numbered 1–15; alternatively spliced sites are shown with a hatched pattern) repeats. The three main heparin-binding and integrin-binding domains are shown. Positions of the glomerulopathy with fibronectin deposits (GFND)-associated mutations are indicated. The novel mutations identified in the current study are indicated by *asterisks* and the mutations used in recombinant proteins are *boxed*. Note that the p.Pro1472del mutation is located in the domain that has a synergistic effect on integrin binding by the RGD motif in III_{10}. All other mutations are located in the heparin-binding domain

polymerase chain reaction (PCR) and direct sequencing of *FN1* was conducted to detect mutations.

Baculovirus constructs

Full-length fibronectin cDNA was subjected to PCR to amplify fibronectin fragments encoding the region encompassing repeats III_{8-14}. The PCR product was subcloned into the baculovirus expression vector pFastBac1 using *Not*I.

Production and analysis of recombinant proteins

Mutated fibronectin fragments (p.Pro1472del, p.Leu1974Arg, and p.Leu1974Pro) were generated using QuikChange site-directed mutagenesis (Agilent Technologies, Santa Clara, CA). His-tagged wild-type and mutant III_{8-14} fragments were expressed in Sf-9 cells using the Bac-to-Bac baculovirus expression system (Thermo Fisher Science, Waltham, MA) and purified by TALON metal affinity resin (Clontech).

Expression and functional studies

The three mutations were introduced into human cDNA encoding repeats III_{8-14} of fibronectin and expressed as His-tagged fusion proteins in Sf9 cells using the baculovirus system, according to the methods previously described by Castelletti et al. [14]. Binding of wild-type and mutant III_{8-14} recombinants to heparin was assessed by enzyme-linked immunosorbent assay (ELISA). The capability of wild-type and mutant III_{8-14} recombinants to bind to podocytes (immortalized mouse podocytes from Katsuhiko Asanuma, Kyoto University, Japan) was evaluated by confocal microscopy analysis.

For spreading assays, podocytes were seeded on glass coverslips coated with or without purified wild-type III_{8-14} and mutant recombinant proteins, and examined using inverted confocal laser microscopy.

Construction of 3-D structures of III_{7-10} domains and docking simulation of fibronectin and integrin $\alpha v \beta 3$

We analyzed the 3-D structures of III_7, EDB, III_8, III_9, and III_{10} domains for wild-type and p.P1472del mutant human fibronectin using homology modeling because the crystal structure of those domains of human fibronectin was not available.

Results

Clinical characteristics and *FN1* mutations in GFND families

The clinical features of our 12 GFND families are shown in Table 1, and their pedigrees were analyzed (Fig. 2). Detailed information for each patient is described in Online Resource 2. Interestingly, some mutation carriers were completely asymptomatic despite being older than the affected individuals; this finding has also been reported by Castelletti et al. in two families [14]. The DNA sequence of the candidate gene, *FN1*, was analyzed for each participant. Six different mutations were identified in all families (giving a mutation detection rate of 100 %): p.Pro969Leu (Family 8), p.Tyr973Cys (Families 1, 2, 5, 6, and 11), p.Pro1472del (Families 4 and 10), p.Trp1925Cys (Family 3), p.Lys1953_Ile1961del (Family 12), and p.Leu1974Pro (Families 7 and 9) (Online Resource 3 and Table 2). We detected four missense variants, which were all shown to be strongly evolutionarily conserved. Polyphen2 (http://genetics.bwh.harvard.edu/pph2/index.shtml) and SIFT (http://sift.jcvi.org) analyses estimated that the amino acid changes resulting from the mutations were damaging or probably damaging (Table 2). Moreover, these variants were not found in 100 ethnically matched healthy controls in the ExAC database (http://exac.broadinstitute.org), suggesting that they are not polymorphisms.

Five of the mutations identified were novel. Of these, p.Pro969Leu, p.Trp1925Cys, p.Leu1974Pro, and p.Lys1953_Ile1961del are localized within the heparin-binding domain and p.Pro1472del is within the integrin-binding domain (Fig. 1). Mutations located at identical sites in the heparin-binding domain (p.Trp1925Arg and p.Leu1974Arg) have been reported previously [14]. However, p.Pro1472del has not been reported before and is the first mutation to be identified in the integrin-binding domain in GFND patients.

To understand the physiological role of each binding domain in integrin signaling and the pathogenesis underlying GFND, we examined the biochemical features of fragments encompassing both the integrin- and heparin-binding domains containing p.Pro1472del, p.Leu1974Pro, and p.Leu1974Arg mutations.

Haplotype analysis

To identify any founder effect for the p.Pro1472del mutation in families 4 and 10, haplotypes were inferred by using eight markers: D2S117, D2S2358, D2S325, D2S2321, D2S2361, D2S2382, D2S163, and D2S126, which span 26.4 Mb centered on the *FN1* region on chromosome 2 (Online Resources 4 and 5). Because individual I-2 in family 4 was deceased, her genotypes and haplotypes were predicted based on those of her family members. A haplotype, shown in blue in Online Resource 4, spanning 8.9 Mb including *FN1* was conserved in both families, specifically in affected individuals I-2 and II-2 in Family 4 and II-8 and III-3 in Family 10, suggesting that the disease-associated segment was inherited from the same founder.

Table 1 Clinical data from glomerulopathy with fibronectin deposits (GFND)-affected participants

Family	Sex	Age (years)	Proteinuria onset (years)	Proteinuria (g/gCre)	eGFR (ml/min/ 1.73 m^2)	Hematuria	Blood pressure (mmHg)	Treatment
1	M	20	6	0.86	92.1	2+	110/57	ACE-I + ARB
2	F	13	9	1.6	115	−	113/64	ARB
3	F	35	26	ESRD at 34 years	ESRD	+	170/100	HD
4	F	54	13	ESRD at 49 years	ESRD	+/−	−	Renal transplantation
5	F	35	12	5.85	76.3	−	114/74	Dipyridamole
6	F	15	12	0.51	86.5	2+	152/90	ACE
7	F	53	20	11.8	48	−	158/96	ACE-I + ARB
8	M	16	15	0.44	124.07	−	124/91	−
9	M	74	61	3. 56	63	+	160/100	ARB
10	F	38	38	4.9	55.3	+/−	132/94	ARB + furosemide
11	F	14	11	10.1	123.4	2+	106/58	ARB
12	M	64	63	4.6	46.3	2+	146/64	−

M male, *F* female, *eGFR* estimated glomerular filtration rate, *OB* occult blood, *ACE-I* angiotensin converting enzyme, *ARB* angiotensin receptor blocker, *ESRD* end-stage renal disease, *HD* hemodialysis

Of note, the frequencies of alleles 1, 2, and 3 for D2S325 are 0.214286, 0.017857, and 0.089286, respectively, in the CEPH database; allele 2, with the lowest frequency, is the allele present in the disease-associated haplotype. Although individuals II-1 and II-4 in Family 4 also had the disease-associated haplotype, they presented with no proteinuria or

hematuria, and had normal blood urea nitrogen and creatinine levels at the ages of 28 and 22, respectively.

Mutation p.Tyr973Cys has previously been reported in several pedigrees from different ethnic backgrounds and is considered a mutation "hot spot" [14]. Haplotype analysis for this mutation revealed that it was not derived from a

Fig. 2 Pedigrees of 12 families with *FN1* mutations. Affected participants are indicated with *arrows*. Individuals with abnormal urinalysis are indicated with *filled squares*. Individuals with *FN1* mutations are indicated with an *asterisk*. ESRD: end-stage renal disease. 1. Family 1: p.Tyr973Cys. 2. Family 2: p.Tyr973Cys. 3. Family 3: p.Trp1925Cys. 4. Family 4: Pro1472del. 5. Family 5: p.Tyr973Cys. 6. Family 6: p.Tyr973Cys. 7. Family 7: Leu1974Pro. 8. Family 8: Pro969Leu. 9. Family 9: p.Leu1974Pro. 10. Family 10: p.Pro1472del. 11. Family 11: p.Tyr973Cys. 12. Family 12: p.Lys1953_Ile1962del
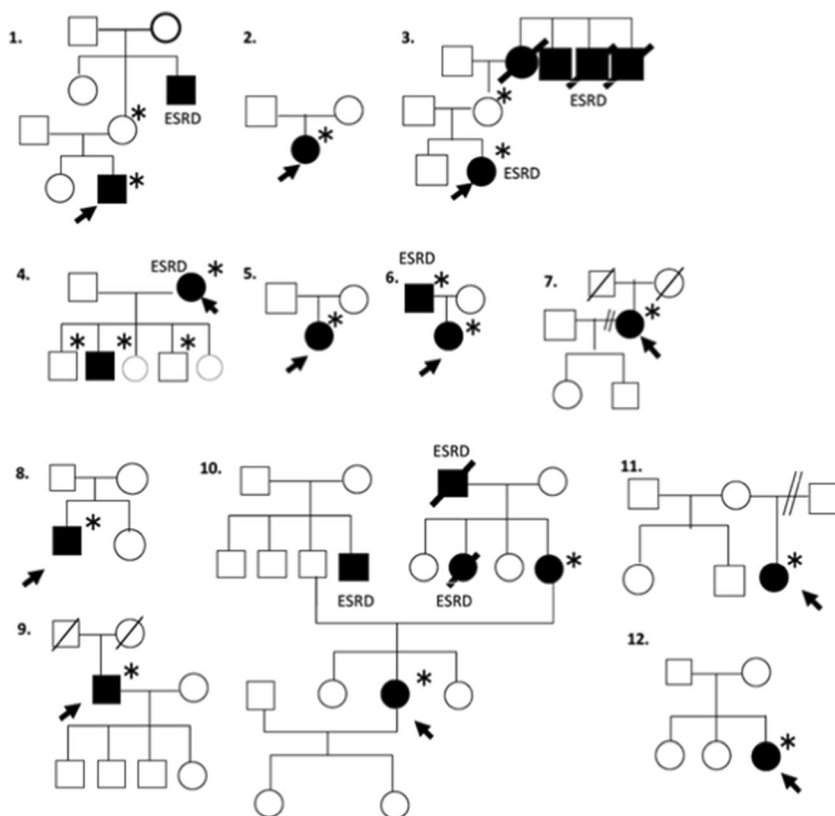
Table 2 *FN1* mutations found in glomerulopathy with fibronectin deposits (GFND)-affected participants

Family	Mutation	Amino acid change	Binding domain	Previous reports	Polyphen2 score	SIFT score
1	c.2918A>G	p.Tyr973Cys	Heparin binding 3	[14]	1.0 (Probably damaging)	0 (Damaging)
2	c.2918A>G	p.Tyr973Cys	Heparin binding 3	[14]	1.0 (Probably damaging)	0 (Damaging)
3	c.5775G>C	p.Trp1925Cys	Heparin binding 2	Novel (Trp1925Arg [14])	1.0 (Probably damaging)	0 (Damaging)
4	c.4414_4416del	p.Pro1472del	Integrin binding	Novel	–	–
5	c.2918A>G	p.Tyr973Cys	Heparin binding 3	[14]	1.0 (Probably damaging)	0 (Damaging)
6	c.2918A>G	p.Tyr973Cys	Heparin binding 3	[14]	1.0 (Probably damaging)	0 (Damaging)
7	c.5921T>C	p.Leu1974Pro	Heparin binding 2	Novel (Leu1974Arg [14])	0.993 (Probably damaging)	0 (Damaging)
8	c.2906C>T	p.Pro969Leu	Heparin binding 3	Novel	1.0 (Probably damaging)	0 (Damaging)
9	c.5921T>C	p.Leu1974Pro	Heparin binding 2	Novel (Leu1974Arg [14])	0.993 (Probably damaging)	0 (Damaging)
10	c.4414_4416del	p.Pro1472del	Integrin binding	Novel	–	–
11	c.2918A>G	p.Tyr973Cys	Heparin binding 3	[14]	1.0 (Probably damaging)	0 (Damaging)
12	c.5858_5884del	p.Lys1953_Ile1961del	Heparin binding 2	Novel	–	–

RefSeq NM_212482.1

All mutations are absent from the ExAC database, although 26 truncating variants (16 nonsense and 10 frameshift), 797 non-truncating variants (790 missense and seven in-frame), and 11 splice site variants have been submitted

common ancestor (Online Resource 6). We also conducted haplotype analysis for p.Leu1974Pro, and observed a founder effect for this variant (Online Resource 6).

Expression and functional studies

p.Pro1472del was within repeat III$_9$ in the integrin-binding domain, and substitution mutations p.Leu1974Pro and p.Leu1974Arg were within repeat III$_{13}$ in heparin-binding domain 2. Therefore, His-tagged recombinant fragments of fibronectin (III$_{8-14}$), including both the integrin- and heparin-binding domains and their mutations (p.Pro1472del, p.Leu1974Pro, and p.Leu1974Arg as a control), were expressed using the baculovirus expression system in Sf9 cells and were purified using an affinity column. Binding of the purified recombinant protein to immobilized heparin was measured by ELISA (Fig. 3a). The heparin-binding site mutants (p.Leu1974Pro and p.Leu1974Arg), but not the integrin-binding site mutant (p.Pro1472del), showed decreased binding to heparin, implying that these amino acids are important for binding to heparin, although the difference between WT and Leu1974Arg was not statistically significant. Additionally, binding of the purified recombinant protein to immobilized integrin was measured by ELISA (Fig. 3b). The integrin-binding site mutant (p.Pro1472del) showed decreased binding to integrin, but the heparin mutants (p.Leu1974Pro and p.Leu1974Arg) did not.

The binding ability of recombinant fragment proteins to immortalized mouse podocytes was also investigated. We found that neither the integrin- nor the heparin-binding domain mutants showed decreased binding. We expected p.Leu1974Pro and p.Leu1974Arg to have a lower binding ability, but they showed the same level as wild-type (Fig. 3c, left four bars). A previous study by Castelletti et al. reported a significantly lower cell-binding ability of fibronectin compared with controls for p.Leu1974Arg. The difference between this and our current finding is that the researchers in the former study constructed the recombinant fibronectin fragment to contain only the heparin-binding domain, whereas we used both the heparin- and integrin-binding sites. It is therefore possible that our findings reflect the fact that heparin and integrin binding sites affect each other's binding ability.

Interestingly, binding of the p.Pro1472del mutant to podocyte cells was strongly decreased in the presence of protamine, which itself binds to the heparin-binding domain in competition with heparin. This suggests that the binding ability of the p.Pro1472del mutant fragment through the integrin-binding domain was strongly impaired (Fig. 3c, right four bars), and that either the intact integrin-binding domain or the heparin-binding domain is sufficient for the binding of fibronectin fragment proteins to the podocyte cell surface.

To address whether these mutant fragment proteins retain the ability to transmit integrin signaling, a podocyte suspension was seeded on glass-bottomed dishes coated with wild-type or mutated recombinant fibronectin fragments and incubated for 2 h. All fibronectin fragments induced podocyte spreading, shown by well-developed actin stress-fiber formation, to a similar extent as the wild-type counterpart (Fig. 4a). This finding was consistent with the cell surface binding assay under 'without protamine' conditions (Fig. 3c).

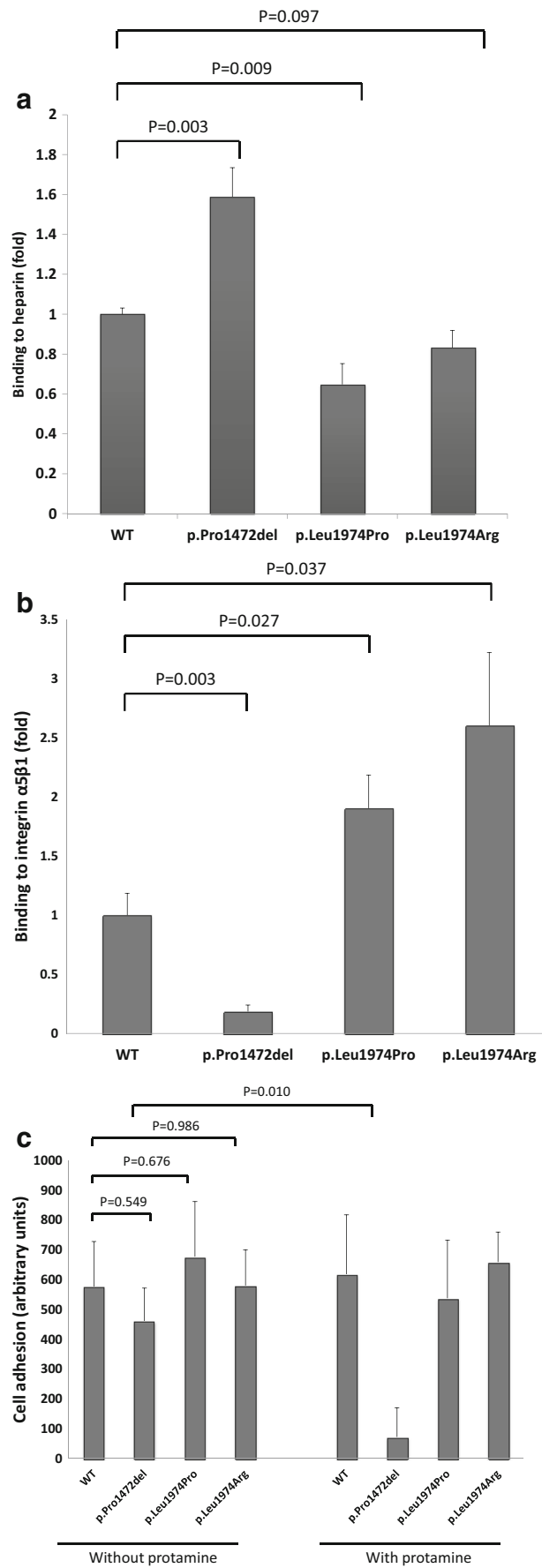The ability of fibronectin fragments to induce integrin-mediated intracellular signaling was also assessed by

◀ **Fig. 3** Binding of wild-type and mutated fibronectin fragments. **a** The binding of wild-type (WT), Pro1472del, Leu1974Pro, and Leu1974Arg fragments to heparin was assayed using ELISA. The binding data for each mutant fragment were normalized to the fold-change of the wild-type fragment. The data are representative of three independent experiments. *Error bars* show standard errors of means. **b** The binding of wild-type (WT), Pro1472del, Leu1974Pro, and Leu1974Arg fragments to integrin was assayed using ELISA. The binding data for each mutant fragment were normalized to the fold-change of the wild-type fragment. The data are representative of four independent experiments. *Error bars* show standard errors of means. **c** The binding of wild-type (WT), Pro1472del, Leu1974Pro, and Leu1947Arg fragments on mouse podocytes with or without protamine. His-tagged recombinants were added to the cells and stained with an anti-His antibody after fixation without permeabilization. The amount of each recombinant bound on the surface of podocytes was assayed as a fluorescent signal using confocal microscopy and ImageJ software. $N = 44$, 38, 44, and 63, respectively for without protamine assay and 20, 34, 20, 17, respectively, for with protamine assay. *Error bars* show standard errors of means

immunostaining using an anti-phosphotyrosine antibody. Both wild-type and mutant fragments elicited tyrosine phosphorylation at the typical focal adhesion-like structures, suggesting that either the integrin-binding domain or the heparin-binding domain is sufficient not only for association to the cell surface, but also for intracellular signal transduction (Fig. 4b).

Construction of 3-D structures and docking simulations

The mutant protein contained alterations in molecular conformation and electrostatic surface potentials, as well as significantly weaker integrin-docking compared with the wild-type fibronectin protein (Online Resource 7).

Discussion

Castelletti et al. previously reported that several mutations in *FN1* cause GFND [14]. These researchers detected *FN1* mutations in repeats III₄ and III₁₃, mapping to heparin-binding domains 3 and 2, respectively (Fig. 1). They constructed recombinant fibronectin fragments containing only the heparin-binding site (from repeats III₁₂₋₁₄) and found that mutant recombinant heparin-binding fragments showed weaker binding to heparin and to endothelial cells and podocytes compared with wild-type fragments, and also had an impaired capability to induce endothelial cell spreading and cytoskeletal reorganization.

In the current study, we found novel *FN1* mutations in repeats III₉ (p.Pro1472del) and III₁₃ (p.Trp1925Cys, p.Lys1953_Ile1961del, and p.Leu1974Pro). This brings the total number of mutations reported to date to eight, of which two were at position 1925 and two were at 1974. However, according to the ExAC database, 16 nonsense variants, 790
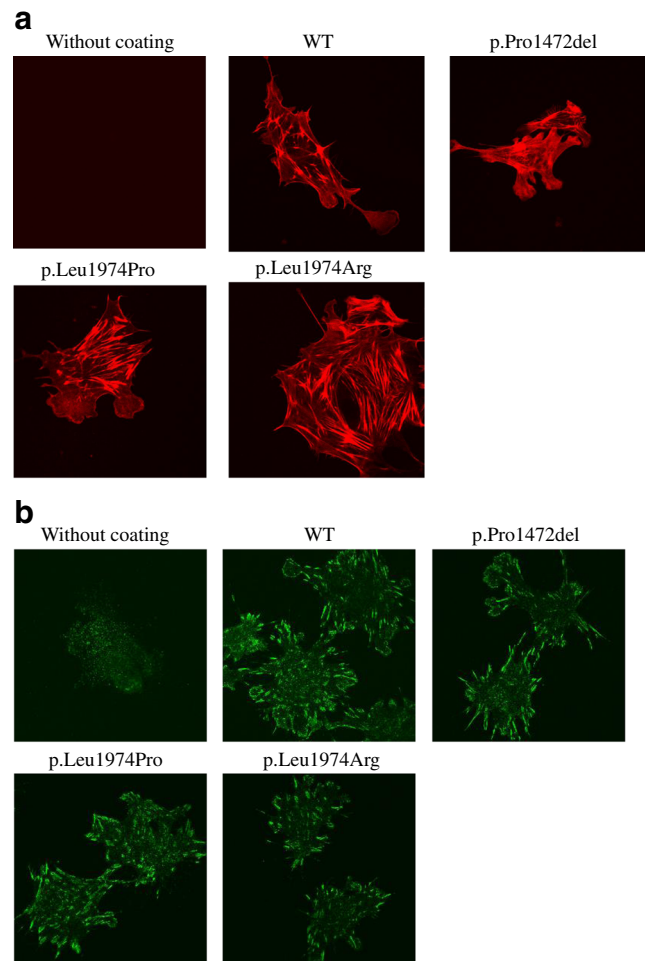
Fig. 4 Actin stress-fiber formation and Intracellular tyrosine phosphorylation induced by fibronectin fragments in podocytes. **a** Podocytes were trypsinized, seeded on non-coated or wild-type (WT) or mutant fibronectin fragment-coated glass-bottomed dishes, incubated at 37 °C for 2 h, fixed, permeabilized, and stained with rhodamine–phalloidin. Actin stress-fiber formation was analyzed by confocal microscopy. **b** Podocytes were trypsinized, seeded on non-coated or wild-type (WT) or mutant fibronectin fragment-coated glass-bottomed dishes, incubated at 37 °C for 2 h, fixed, permeabilized, immunostained using an anti-phosphotyrosine antibody, and analyzed using confocal microscopy. Almost no positive signals were observed in cells seeded on non-coated dishes

missense variants, and numerous silent variants have been reported. The fact that only eight pathogenic variants have been reported might be because variants at other locations do not cause disease involving fibronectin deposits in the glomerulus.

We also constructed a mutant recombinant that included both the heparin- and integrin-binding fragments (from repeats III₈₋₁₄). Because the synergy site in repeat III₉ cooperates with the RGD sequence in repeat III₁₀ for maximal α5β1 integrin-mediated matrix assembly, we studied functional characteristics using recombinant fragments that included both the integrin- and heparin-

binding domains (from repeats III$_{8-14}$). We found that both the integrin-binding mutation p.Pro1472del and the heparin-binding mutations p.Leu1974Pro and p.Leu1974Arg possessed a similar capacity to wild-type to induce actin filament rearrangement (Fig. 4a) and integrin signaling (Fig. 4b). However, each mutation caused a significant loss of binding ability of the heparin- or integrin-binding sites to immobilized heparin (Fig. 3a) or to integrins and the cell surface, respectively, in the presence of protamine (Fig. 3b and c). Additionally, 3-D modeling showed a significant reduction in the integrin-binding ability for the integrin-domain mutation (Online Resource 7).

From differences between the experimental designs used in our study and that of Castelletti et al. [14], it is suggested that either the integrin-binding domain or the heparin-binding domain is sufficient for cell surface binding and integrin signaling. This was also indicated following our in vitro podocyte binding assay using integrin $\alpha 5 \beta 1$ and heparin as binding partners to demonstrate the importance of Pro1472 and Leu1974, respectively. Either integrin or heparin binding was shown to be sufficient for recombinant fibronectin (III$_{8-14}$) to bind podocytes. Because p.Pro1472del binds more to heparin and p.Leu1974Pro and p.Leu1974Arg bind more to integrin $\alpha 5 \beta 1$ than the wild type, it is possible that the integrin- and heparin-binding domains interact with each other, and that this interaction is disturbed in these mutants. The physiological role of an intermolecular interaction should be clarified in future studies, while further experiments involving the construction of a double mutated protein are required to confirm if integrin and/or heparin binding is necessary for podocyte binding.

Our study failed to show an impaired capability to induce endothelial cell spreading and cytoskeletal reorganization. This is a possible limitation of the in vitro assay, and might not be an accurate reflection of GFND pathogenesis in vivo.

We detected some asymptomatic patients with *FN1* mutations at F1, F3, and F4. The observation of large intra-familial heterogeneity meant that no genotype–phenotype correlation was observed, so additional studies are required to determine any such correlation.

In conclusion, we detected a novel integrin-binding domain mutation in two unrelated families, and microsatellite marker analysis suggested the presence of a founder effect. This mutation caused decreased integrin-binding ability in both in vitro functional studies and 3-D modeling. These findings may contribute to an understanding of GFND pathogenesis. Although GFND is a very rare disease, most patients show proteinuria from childhood. It is therefore imperative that pediatric nephrologists are aware of this disorder, and that diagnosis is not delayed.

References

1. Ruoslahti E (1988) Fibronectin and its receptors. Annu Rev Biochem 57:375–413
2. Schwarzbauer JE (1991) Fibronectin: from gene to protein. Curr Opin Cell Biol 3:786–791
3. George EL, Georges-Labouesse EN, Patel-King RS, Rayburn H, Hynes RO (1993) Defects in mesoderm, neural tube and vascular development in mouse embryos lacking fibronectin. Development 119:1079–1091
4. Petersen TE, Thogersen HC, Skorstengaard K, Vibe-Pedersen K, Sahl P, Sottrup-Jensen L, Magnusson S (1983) Partial primary structure of bovine plasma fibronectin: three types of internal homology. Proc Natl Acad Sci U S A 80:137–141
5. Pierschbacher MD, Ruoslahti E (1984) Variants of the cell recognition site of fibronectin that retain attachment-promoting activity. Proc Natl Acad Sci U S A 81:5985–5988
6. Obara M, Kang MS, Yamada KM (1988) Site-directed mutagenesis of the cell-binding domain of human fibronectin: separable, synergistic sites mediate adhesive function. Cell 53:649–657
7. Benecky MJ, Kolvenbach CG, Amrani DL, Mosesson MW (1988) Evidence that binding to the carboxyl-terminal heparin-binding domain (Hep II) dominates the interaction between plasma fibronectin and heparin. Biochemistry 27:7565–7571
8. Ingham KC, Brew SA, Atha DH (1990) Interaction of heparin with fibronectin and isolated fibronectin domains. Biochem J 272:605–611
9. Barkalow FJ, Schwarzbauer JE (1991) Localization of the major heparin-binding site in fibronectin. J Biol Chem 266:7812–7818
10. Laterra J, Norton EK, Izzard CS, Culp LA (1983) Contact formation by fibroblasts adhering to heparan sulfate-binding substrata (fibronectin or platelet factor 4). Exp Cell Res 146:15–27

11. Woods A, Couchman JR, Johansson S, Hook M (1986) Adhesion and cytoskeletal organisation of fibroblasts in response to fibronectin fragments. EMBO J 5:665–670
12. Haugen PK, McCarthy JB, Skubitz AP, Furcht LT, Letourneau PC (1990) Recognition of the A chain carboxy-terminal heparin binding region of fibronectin involves multiple sites: two contiguous sequences act independently to promote neural cell adhesion. J Cell Biol 111:2733–2745
13. Strom EH, Banfi G, Krapf R, Abt AB, Mazzucco G, Monga G, Gloor F, Neuweiler J, Riess R, Stosiek P, HebertLA SDD, Gudat F, Mihatsch MJ (1995) Glomerulopathy associated with predominant fibronectin deposits: a newly recognized hereditary disease. Kidney Int 48:163–170
14. Castelletti F, Donadelli R, Banterla F, Hildebrandt F, Zipfel PF, Bresin E, Otto E, Skerka C, Renieri A, Todeschini M, Caprioli J, Caruso RM, Artuso R, Remuzzi G, Noris M (2008) Mutations in FN1 cause glomerulopathy with fibronectin deposits. Proc Natl Acad Sci U S A 105:2538–2543

Case study

Daughter and mother with orofaciodigital syndrome type 1 and glomerulocystic kidney disease☆,☆☆

Takashi Iijima MD[a], **Junichi Hoshino MD, MPH**[a,*], **Koki Mise MD**[a], **Keiichi Sumida MD**[a], **Tatsuya Suwabe MD, PhD**[a], **Noriko Hayami MD**[a], **Toshiharu Ueno MD, PhD**[a], **Kenmei Takaichi MD, PhD**[a,b], **Takeshi Fujii MD, PhD**[c], **Kenichi Ohashi MD, PhD**[c,e], **Naoya Morisada MD, PhD**[d], **Kazumoto Iijima MD, PhD**[d], **Yoshifumi Ubara MD, PhD**[a,b]

[a]Nephrology Center, Toranomon Hospital Kajigaya, Kanagawa 213-0015, Japan
[b]Okinaka Memorial Institute for Medical Research, Toranomon Hospital, Tokyo 105-0001, Japan
[c]Department of Pathology, Toranomon Hospital, Tokyo 105-0001, Japan
[d]Department of Pediatrics, Kobe University, Kobe 650-0017, Japan
[e]Department of Pathology, Yokohama City University, Graduate School of Medicine, Yokohama 236-0027, Japan

Summary A 35-year-old woman was admitted to our hospital for evaluation of end-stage renal failure. Diagnostic imaging, including ultrasonography and magnetic resonance imaging, showed polycystic kidneys and peribiliary hepatic cysts, but the renal cysts were isointense and her kidneys were smaller than the end-stage kidneys of patients with autosomal dominant polycystic kidney disease. Glomerulocystic kidney disease was diagnosed by renal biopsy. Clinical examination revealed findings such as a missing maxillary canine, lingual anomalies, and brachydactyly. Genetic testing gave a diagnosis of orofaciodigital syndrome type 1 with a 5 nucleotide deletion indicating a frameshift mutation in exon 9. The patient's mother had the same mutation and similar clinical findings. This case is useful for understanding kidney and liver involvement in orofaciodigital syndrome type 1.
© 2016 Elsevier Inc. All rights reserved.

1. Introduction

There are many causes of polycystic kidney disease other than autosomal dominant polycystic kidney disease (ADPKD) and autosomal recessive polycystic kidney disease, including

nephronophthisis, tuberous sclerosis, Caroli disease, and some types of glomerulocystic kidney disease (GCKD). Among them, GCKD was classified into 5 categories by Lennerz et al [1]. Type 1 GCKD is a variant of ADPKD or autosomal recessive polycystic kidney disease with glomerular cysts, whereas type 2 GCKD is a hereditary disease due to mutation of uromodulin, hepatocyte nuclear factor–1b, or other unspecified genes. Type 3 is defined as syndromic GCKD caused by various hereditary or acquired syndromes. Type 4 is due to urinary tract obstruction, and type 5 is due to ischemia and/or drugs or other factors. Orofaciodigital syndrome type 1 is

one of the type 3 GCKDs and has varying systemic manifestations [1].

The orofaciodigital syndromes (OFDs) are a group of at least 13 related conditions that affect development of the oral cavity (mouth and teeth), facial features, and digits (fingers and toes). OFD type 1 (OFD1) was first described by Papillon-Léage and Psaume in 1954. It is characterized by X-linked dominant inheritance, so almost all affected individuals are female. Renal involvement in OFD1 results in polycystic kidney disease [2]. The locus of OFD1 was first mapped by Feather et al [3], who used linkage analysis to identify a 19.8-cM interval in the Xp22 region flanked by crossovers with the markers DXS996 and DXS7105. Ferrante et al [4] reported that analysis of familial cases of OFD1 revealed a missense mutation, a 19–base pair deletion, and a single base pair deletion leading to frameshift, whereas sporadic cases showed missense, nonsense, splice, and frameshift mutations. The *OFD1* gene is located on Xp22, and its product is related to formation of primary cilia and establishment of the left-right axis [5]. The relation between OFD1 and polycystic kidneys remains unclear [6–10].

We encountered a 35-year-old Japanese woman with clinical features of OFD1, including a missing maxillary canine, lingual anomalies, and brachydactyly, as well as polycystic kidney disease of the glomerulocystic type. The patient's mother also had similar phenotypic characteristics. This report presents their imaging findings, renal histology, and gene analysis data, as well as discussing kidney involvement in OFD1.

2. Case presentation

In August 2013, a 35-year-old woman was admitted to our hospital for evaluation of end-stage renal failure. She had developed fatigue in March 2013, whereas dizziness, flu-like symptoms, and edema of the bilateral lower extremities were noted in May. At her local clinic, anemia (hemoglobin concentration, 6.6 g/dL) and renal dysfunction (serum creatinine, 10.2 mg/dL) were detected in June. Hemodialysis was started immediately, 2 U of red cell concentrate were transfused, iron and erythropoietin supplementation were initiated, and she was transferred to our hospital.

On admission, the patient was 148 cm tall and weighed 41.3 kg. Her blood pressure was 118/73 mm Hg. Her fingers (Fig. 1A and B) and toes were short, and she had mild edema of the lower legs. Her left maxillary canine was missing (Fig. 1C). She had a history of frenotomy as an infant because of difficulty with nursing due to dense adhesions between the tongue and floor of the mouth.

Laboratory parameters are shown in the Table. There were mild anemia (hemoglobin concentration, 11.5 g/dL), hypoalbuminemia (serum albumin, 3.4 g/dL), elevation of serum urea nitrogen (85 mg/dL), and elevation of serum creatinine (10.2 mg/dL). Urinalysis showed moderate proteinuria (24-hour protein excretion, 1.2 g).

Abdominal ultrasonography revealed numerous cysts in the bilateral kidneys and in the liver. The hepatic cysts were located parallel to the bile ducts (Fig. 1D). Magnetic resonance imaging (MRI) showed that both kidneys were largely replaced by iso-intense cysts and seemed smaller than ordinary end-stage kidneys of ADPKD patients (Fig. 1E). Renal volume was calculated from MRI data using the formula for an ellipsoid (long axis × short axis × short axis × $\pi/6$), revealing that the left kidney volume was 427 cm^3 (12.1 × 5.4 × 6.4 cm) and the right kidney volume was 332 cm^3 (10.5 × 5.4 × 5.7 cm).

Cystic kidney disease had previously been diagnosed in the patient's mother, so she was also investigated. On examination, she had congenital absence of the right maxillary canine, and her digits of both hands were short. The mother's laboratory data are also shown in the Table. Abdominal ultrasonography demonstrated peribiliary cysts in the liver, and MRI revealed numerous renal cysts similar to those in her daughter's kidneys (Fig. 1F).

2.1. Renal biopsy

Renal biopsy was performed because the time course of renal failure was unknown. Of the 32 glomeruli in the biopsy specimens, 8 showed global sclerosis accompanied by severe interstitial fibrosis, tubular atrophy, and marked cellular infiltration. Several cystic lesions with thick fibrous walls and a flat epithelial lining were observed, and collapsed glomeruli with dilation of Bowman space and glomerular cysts could be seen around these cystic lesions. A few dilated proximal tubules with thickened basement membrane were noted, but dilation of distal tubules and collecting ducts was not observed. The residual glomeruli were intact. Based on these findings, the cystic lesions were considered to have originated from glomerular cysts (Fig. 2A). Immunofluorescence microscopy and electron microscopy did not detect any immune deposits.

Her mother had also previously undergone renal biopsy for diagnosis. The biopsy specimens contained 27 glomeruli, and all of them showed global sclerosis with severe interstitial fibrosis, tubular atrophy, and inflammatory cell infiltration. Some small cystic lesions with thick fibrous walls and flat epithelial lining were also noted, which resembled her daughter's cystic lesions, but no glomerular cysts associated with collapsed glomeruli were found (Fig. 2B).

2.2. Gene analysis

Because of the characteristic findings revealed by renal biopsy and the presence of brachydactyly, we considered analysis of several genes related to glomerular cysts. Among them, the OFD1 gene was the most plausible candidate because the patient's history of frenotomy and her mother's renal cystic disease were considered to suggest an X-linked systemic condition.

We performed genetic analysis after obtaining written informed consent from the proband and her mother. All
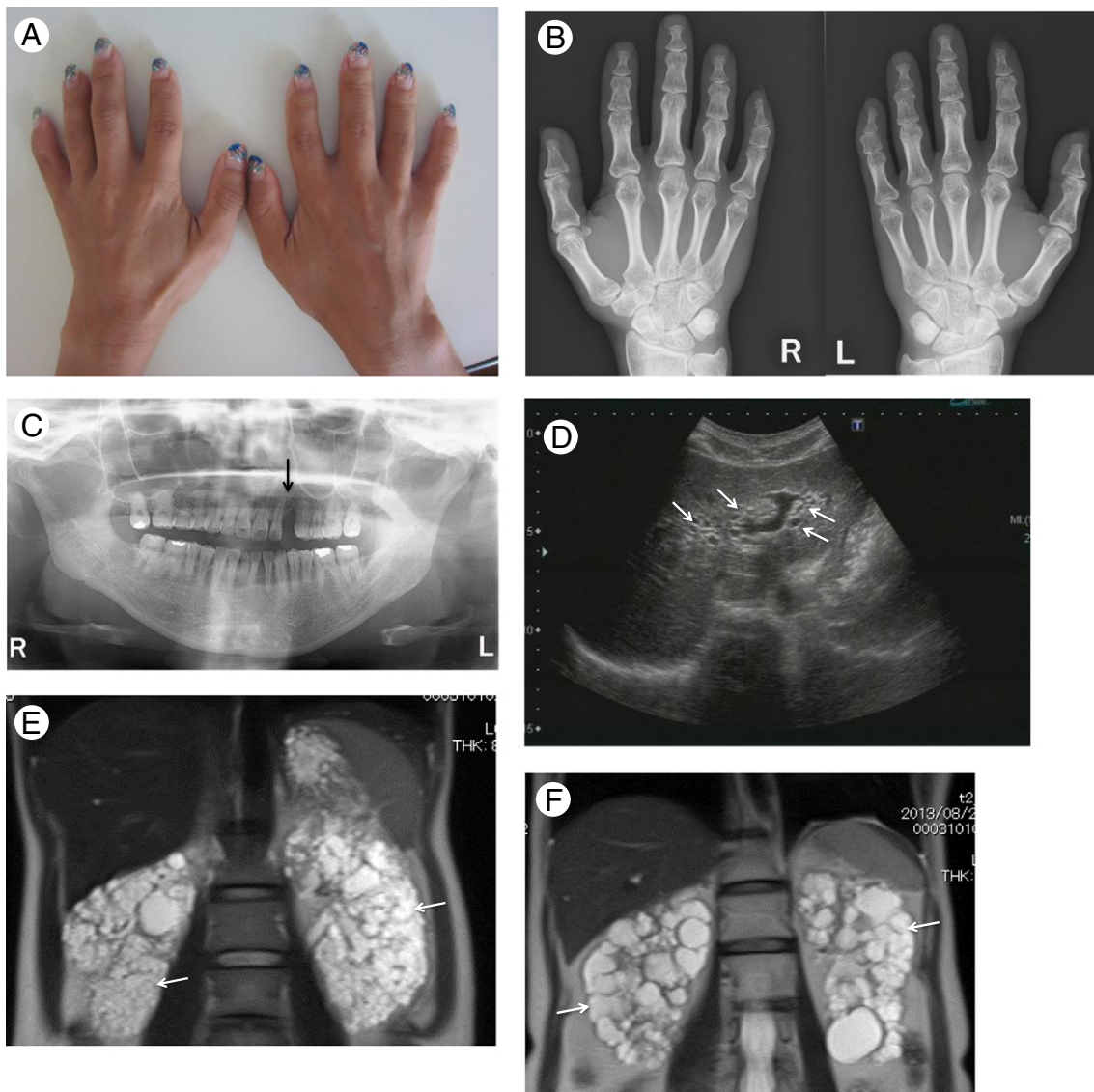
Fig. 1 Clinical and imaging findings. A and B, The patient has short fingers (brachydactyly). C, The left maxillary canine is missing (arrow). D, Abdominal ultrasonography reveals hepatic cysts parallel to the bile ducts (peribiliary cysts) (arrows). E, MRI shows that both kidneys (arrows) are largely replaced by isointense cysts and are smaller than the end-stage kidneys of ADPKD patients. F, MRI also reveals numerous cysts in the mother's kidneys (arrows).

procedures were reviewed and approved by the Institutional Review Board of Kobe University School of Medicine and were in accordance with the ethical standards of the 1964 Declaration of Helsinki. Genomic DNA was extracted from peripheral blood mononuclear cells using QuickGene whole blood kit S (Kurabo, Osaka, Japan) according to the manufacturer's instructions. Twenty-two pairs of oligonucleotide primers were generated to amplify all 23 coding exons of *OFD1*. Then, polymerase chain reaction was performed, and the products were purified with a DNA purification kit (Qiagen Japan, Tokyo, Japan), followed by direct sequencing with a 3100 Genetic Analyzer (Life Technologies Japan, Tokyo, Japan). Sequence alignment was performed with CLC Main Workbench software (CLC-bio, Aarhus, Denmark). In both the proband and her mother, we identified a 5 nucleotide deletion indicating a heterozygous

frameshift mutation in exon 9 (NM_003611.2 [OFD1]: c.840_844delAGAAA [p.Lys280AsnfsX27]), consistent with the genotype of *OFD1* (Fig. 2C). This mutation was considered to be causative in both patients.

3. Discussion

Patients with OFD1 can develop polycystic kidney disease. Renal cysts are considered to arise from both the tubules and glomeruli, although previous reports have not provided sufficient information about the mechanism of renal involvement. There have been 3 reports about the incidence of polycystic kidneys in OFD1. Saal et al [6] investigated renal findings in

Table Laboratory data of the patient and her mother

	Daughter	Mother	Normal limit and unit
Hematology			
White blood cells	6700	6000	3200-7900/mL
Hemoglobin	11.5	11.2	11.3-15.0 g/dL
Platelet count	167	166	$155\text{-}350 \times 10^3$/mL
Serum chemistry			
Total protein	6.3	7.7	6.7-8.3 g/dL
Albumin	3.4	4.0	4.0-5.0 g/dL
Aspartate aminotransferase	9	14	13-33 IU/L
Alanine aminotransferase	12	12	8-42 IU/L
Lactate dehydrogenase	170	184	119-229 IU/L
Alkaline phosphatase	289	239	I8-42 U/L
γ-Glutamyltransferase	15	17	10-46 IU/L
Urea nitrogen	85	39	8-22 mg/dL
Creatinine	10.2	4.6	0.6-0.8 mg/dL
Uric acid	7.9	3.8	3.6-7.0 mg/dL
Sodium	138	144	135-145 mmol/L
Potassium	5.2	4.7	3.5-4.9 mmol/L
Chloride	106	110	96-108 mmol/L
Calcium	8.3	8.9	8.7-10.1 mg/dL
Phosphate	5.3	4.6	2.8-4.6 mg/dL
C-reactive protein	0.0	0.0	<0.3 mg/dL
Ferritin	120	19	<12.0 μg/L
Immunoglobulin G	937	1235	870-1700 mg/dL
Immunoglobulin A	139.6	155.4	110-410 mg/dL
Immunoglobulin M	130.7	87	30-190 mg/dL
Antinuclear antibody	Negative	Negative	<40
Urinary analyses			
Red blood cells	1 to 5	<1	/HPF
White blood cells	<1	1 to 4	/HPF
Protein excretion	1.2	0.63	g/d
α-1 Microglobulin	103.1		g/day
β-2 Microglobulin	49,179	56,645	30-370 μg/d
M protein	Negative		Negative

Abbreviation: HPF, high-power field.

34 female patients with pathogenic mutation of the *OFD1* gene. Polycystic kidneys were diagnosed in 12 patients by ultrasonography, whereas 10 patients presented with renal impairment and 6 received kidney transplantation. The probability of developing renal failure was estimated as greater than 50% after the age of 36 years. Although their data revealed a high incidence of renal impairment in OFD1 syndrome, they could not find any genotype-phenotype correlation that was predictive of renal failure [6].

Bisschoff et al [7] studied 55 sporadic and 6 familial cases of suspected OFD1. Comprehensive gene analysis revealed mutations in 37 women from 30 families. They also found cystic kidney diseases in 6 of 23 patients investigated (26.1%), but the details were not reported.

Prattichizzo et al [8] performed mutation analysis in a cohort of 100 unrelated affected individuals collected worldwide with a clinical diagnosis of OFD1 syndrome. Most of the probands were from Europe (65%) and North America (21%), followed by Australia (6%), the Middle East (5%), and Asia (3%).

Cystic kidney disease was demonstrated by renal scans in 24 of 81 patients tested (29.6%). Renal cystic disease was present in 15 of 25 patients (60%) >18 years old who were examined.

According to our literature search, there are only 2 case reports showing the development of renal cysts from the glomeruli in OFD1 patients. Feather et al [3] performed histological examination at autopsy of a woman in her 50s who had end-stage renal failure and polycystic kidneys with cysts <1 cm in diameter. Cysts were not noted in any of her other organs. Most of the renal cysts were lined by flat epithelium and had fibrotic walls. Glomerular tufts were detected in the cyst lining, and many of the tufts within cysts contained open capillary loops. Mildly dilated tubules up to 100-200 micrometers in size were also noted [3]. Stapleton reported an 11-year-old girl with OFD1 who underwent bilateral nephrectomy before renal transplantation. Examination of the resected kidneys showed that the cortex was largely replaced by numerous cysts lined by flattened epithelium, many of which contained glomerular tufts [9].
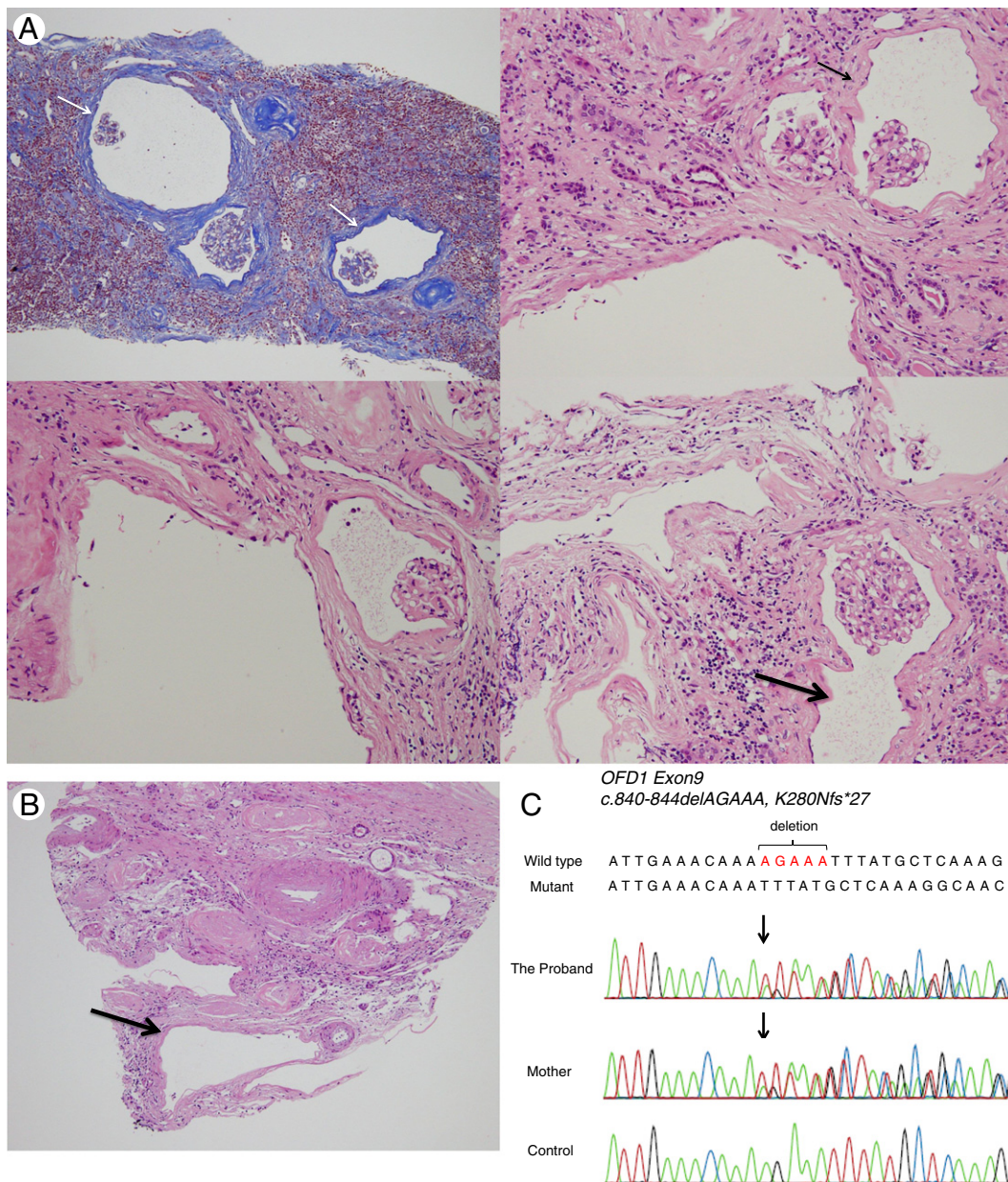
Fig. 2   Renal biopsy finding. A, Several cystic lesions with thick fibrous walls and flat epithelial lining were observed, and collapsed glomeruli with dilation of Bowman space and glomerular cysts (arrows) were seen around the cystic lesions. In some of the glomerular cysts, Bowman capsule was connected to the cystic lesions. A few dilated proximal tubules with thickened basement membrane (large arrow) were noted. B, The mother had similar cystic lesions (arrow) to those of her daughter. However, no glomerular cysts associated with collapsed glomeruli could be detected. C, Gene analysis revealed a 5 nucleotide deletion, indicating a frameshift mutation in exon 9 (NM_003611.2 [OFD1]: c.840_844delAGAAA [p.Lys280AsnfsX27]), which was consistent with the genotype of *OFD1*.

The imaging characteristics of renal cysts were reported by Scolari et al [10] in 2 generations of a family with OFD1 (mother and daughter). CT of the abdomen revealed polycystic kidneys in both patients. Renal cysts were more numerous and smaller in the 2 OFD1 patients compared with those in ADPKD patients, and their kidneys showed less enlargement without gross deformity of the renal contour.

Similarly, there have only been a few reports about hepatic cysts in patients with OFD1. Scolari et al [10] reported the co-existence of multiple liver and pancreatic cysts in OFD1, with

the liver containing peribiliary cysts along the principal branches of the biliary tree. Topra et al [11] reported a 20-year-old woman with polycystic kidneys and end-stage renal disease who was diagnosed as having coexistence of OFD1 and Caroli disease. Thus, it seems that hepatic cysts may be a rare manifestation of OFD1.

OFD1 needs to be differentiated from "acquired cystic disease" in end-stage renal disease patients. Acquired cystic disease can be diagnosed in patients on dialysis for more than 4 years. It features multiple cystic lesions that mainly originate from the proximal

tubules and exist throughout cortex and medulla, along with intra-cystic hemorrhage and calcium oxalate crystal deposition [12].

In conclusion, we encountered a 35-year-old woman with clinical features of OFD1 (missing maxillary canine, lingual anomalies, and brachydactyly) and polycystic kidney disease. Her mother also had similar clinical characteristics. In both women, gene analysis revealed a 5 nucleotide deletion of a frameshift mutation in exon 9, which was consistent with the diagnosis of OFD1. MRI showed that their kidneys contained isointense cysts and were smaller than the end-stage kidneys of ADPKD patients, whereas peribiliary cysts were noted in the livers of both women. Renal biopsy showed glomerulocystic polycystic kidney disease. This case suggests that OFD1 may be a possible alternative diagnosis in women with poly-cystic kidney disease and smaller cysts. Further clinical infor-mation about renal involvement in OFD1 may be obtained from detailed case series.

References

[1] Lennerz JK, Spence DC, Iskandar SS, Dehner LP, Liapis H. Glomerulo-cystic kidney: one hundred-year perspective. Arch Pathol Lab Med 2010; 134:583-605.

[2] Toriello HV. Oral-facial-digital syndromes. Clin Dysmorphol 1993;2: 95-105.

[3] Feather SA, Winyard PJ, Dodd S, Woolf AS. Oral-facial-digital syn-drome type 1 is another dominant polycystic kidney disease: clinical, ra-diological and histopathological features of a new kindred. Nephrol Dial Transplant 1997;12:1354-61.

[4] Ferrante MI, Giorgio G, Feather SA, et al. Identification of the gene for oral-facial-digital type I syndrome. Am J Hum Genet 2001;68:569-76.

[5] Ferrante MI, Zullo A, Barra A, et al. Oral-facial-digital type I protein is required for primary cilia formation and left-right axis specification. Nat Genet 2006;38:112-7.

[6] Saal S, Faivre L, Aral B, et al. Renal insufficiency, a frequent complica-tion with age in oral-facial-digital syndrome type I. Clin Genet 2010;77: 258-65.

[7] Bisschoff IJ, Zeschnigk C, Horn D, et al. Novel mutations including de-letions of the entire OFD1 gene in 30 families with type 1 orofaciodigital syndrome: a study of the extensive clinical variability. Hum Mutat 2013; 34:237-47.

[8] Prattichizzo C, Macca M, Novelli V, et al. Mutational spectrum of the oral-facial-digital type I syndrome: a study on a large collection of pa-tients. Hum Mutat 2008;29:1237-46.

[9] Stapleton FB, Bernstein J, Koh G, Roy III S, Wilroy RS. Cystic kidneys in a patient with oral-facial-digital syndrome type I. Am J Kidney Dis 1982;1:288-93.

[10] Scolari F, Valzorio B, Carli O, et al. Oral-facial-digital syndrome type I: an unusual cause of hereditary cystic kidney disease. Nephrol Dial Trans-plant 1997;12:1247-50.

[11] Toprak O, Uzum A, Cirit M, et al. Oral-facial-digital syndrome type 1, Caroli's disease and cystic renal disease. Nephrol Dial Transplant 2006;21:1705-9.

[12] Chang A, Vasilyev A. Acquired cystic disease. In: Chang A, Kambham N, Meehan AM, et al, editors. Diagnostic pathology, kidney diseases. 1st ed. Canada: Amirsys Inc.; 2011. p. 6.65-8.

SCIENTIFIC REP⚙RTS

Identification of rs671, a common variant of *ALDH2*, as a gout susceptibility locus

Masayuki Sakiyama[1,2,*], Hirotaka Matsuo[1,*], Hirofumi Nakaoka[3], Ken Yamamoto[4], Akiyoshi Nakayama[1], Takahiro Nakamura[5], Sayo Kawai[6], Rieko Okada[6], Hiroshi Ooyama[7], Toru Shimizu[8,9] & Nariyoshi Shinomiya[1]

Gout is a common disease resulting from hyperuricemia. Recently, a genome-wide association study identified an association between gout and a single nucleotide polymorphism (SNP) rs2188380, located on an intergenic region between *MYL2* and *CUX2* on chromosome 12. However, other genes around rs2188380 could possibly be gout susceptibility genes. Therefore, we performed a fine-mapping study of the *MYL2-CUX2* region. From 8,595 SNPs in the *MYL2-CUX2* region, 9 tag SNPs were selected, and genotyping of 1,048 male gout patients and 1,334 male controls was performed by TaqMan method. Eight SNPs showed significant associations with gout after Bonferroni correction. rs671 (Glu504Lys) of *ALDH2* had the most significant association with gout ($P = 1.7 \times 10^{-18}$, odds ratio = 0.53). After adjustment for rs671, the other 8 SNPs no longer showed a significant association with gout, while the significant association of rs671 remained. rs671 has been reportedly associated with alcohol drinking behavior, and it is well-known that alcohol drinking elevates serum uric acid levels. These data suggest that rs671, a common functional SNP of *ALDH2*, is a genuine gout-associated SNP in the *MYL2-CUX2* locus and that "A" allele (Lys) of rs671 plays a protective role in the development of gout.

Gout is a common disease resulting from hyperuricemia, and causes acute arthritis. Previous genetic and functional analyses revealed that *ABCG2* dysfunctional variants caused gout[1–3] due to decreased urate excretion in gut[4] and kidney[5]. Genome-wide association studies (GWASs) of gout also showed genome-wide significant associations with *ABCG2* and *GLUT9*[6–8]. Recently, we revealed for the first time that the following 3 loci were associated with gout at the genome-wide significance level: rs1260326 of *GCKR*, rs4073582 of *CNIH-2* and rs2188380 of *MYL2-CUX2*[8]. Among them, 2 SNPs are located in gene regions: rs1260326 is a nonsynonymous single nucleotide polymorphism (SNP) (Leu446Pro) of *GCKR*, and rs4073582 is an intronic SNP of *CNIH-2*. On the other hand, rs2188380 is located on an intergenic region between *MYL2* and *CUX2*[8]. Additionally, we detected many SNPs showing significant associations with gout across the chromosome 12q24 region which were in strong linkage disequilibrium (LD) with rs2188380. *MYL2* encodes a regulatory light chain associated with cardiac myosin β (or slow) heavy chain, and an association between *MYL2* variant and high-density lipoprotein cholesterol metabolism was previously reported[9]. *CUX2* regulates cell-cycle progression[10] and plays important roles in neural progenitor development in the central nervous system[10,11]. An association between *CUX2* and type 1 diabetes has also been reported[12]. However, there is a possibility that the other genes around rs2188380 of *MYL2-CUX2* can be gout susceptibility genes. Therefore, we performed fine-mapping of the *MYL2-CUX2* region and a further association analysis of gout.

[1]Department of Integrative Physiology and Bio-Nano Medicine, National Defense Medical College, 3-2 Namiki, Tokorozawa, Saitama 359-8513, Japan. [2]Department of Dermatology, National Defense Medical College, 3-2 Namiki, Tokorozawa, Saitama 359-8513, Japan. [3]Division of Human Genetics, Department of Integrated Genetics, National Institute of Genetics, 1111 Yata, Mishima, Shizuoka 411-0801, Japan. [4]Department of Medical Chemistry, Kurume University School of Medicine, 67 Asahi-machi, Kurume, Fukuoka 830-0011, Japan. [5]Laboratory for Mathematics, National Defense Medical College, 3-2 Namiki, Tokorozawa, Saitama 359-8513, Japan. [6]Department of Preventive Medicine, Nagoya University Graduate School of Medicine, 65 Tsurumai-cho, Showa-ku, Nagoya, Aichi 466-8550, Japan. [7]Ryougoku East Gate Clinic, 3-21-1 Ryougoku, Sumida-ku, Tokyo 130-0026, Japan. [8]Midorigaoka Hospital, 3-13-1 Makami-cho, Takatsuki, Osaka 569-1121, Japan. [9]Kyoto Industrial Health Association, 67 Kitatsuboi-cho, Nishinokyo, Nakagyo-ku, Kyoto 604-8472, Japan. *These authors contributed equally to this work. Correspondence and requests for materials should be addressed to H.M. (email: hmatsuo@ndmc.ac.jp)
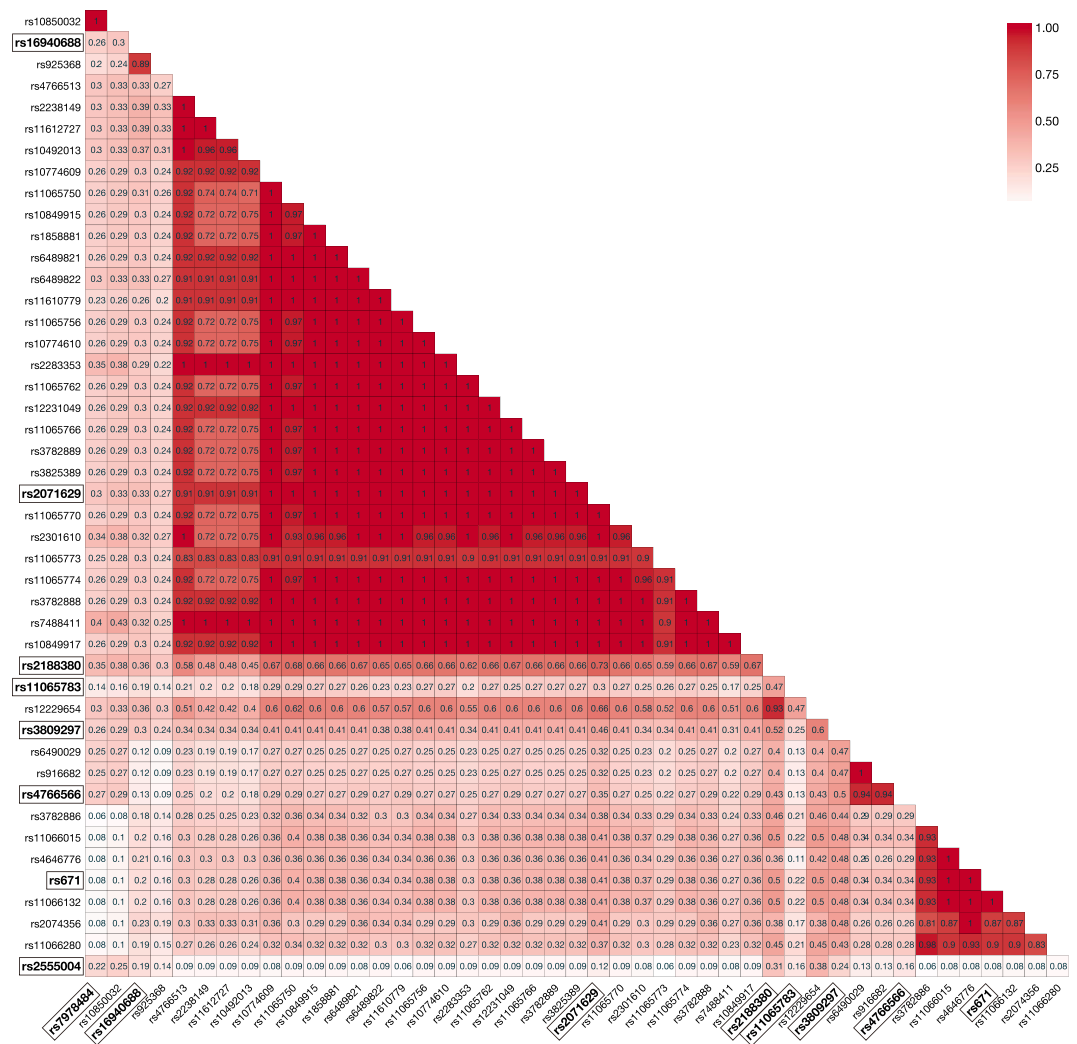
Figure 1. Linkage disequilibrium heat map of 46 SNPs. We examined the linkage disequilibrium (LD) between each pair of 46 SNPs and searched the SNPs that were tagging other SNPs with strong LD ($r^2 \geq 0.8$). The 9 tag SNPs (rs7978484, rs16940688, rs2071629, rs2188380, rs11065783, rs3809297, rs4766566, rs671 and rs2555004), which are shown in bold and boxes, were selected for association analysis.

Results

From 8,595 SNPs in the *MYL2-CUX2* region within 10 Mb across rs2188380, 45 SNPs in LD ($r^2 \geq 0.3$) with rs2188380 were selected (Supplementary Figure S1). Among these 45 SNPs and rs2188380, 9 tag SNPs were selected for association analysis (Fig. 1 and Supplementary Table S1). Genotyping results of the 9 tag SNPs for 1,048 gout patients and 1,334 controls were shown in Table 1. The call rates for the 9 SNPs were more than 95.0%. All the SNPs in the control group were in Hardy-Weinberg equilibrium ($P > 0.05$). Except for rs2555004, the other 8 SNPs showed significant associations at $P < 5.6 \times 10^{-3}$ ($= 0.05/9$) with the Bonferroni correction, and rs671 (Glu504Lys) of aldehyde dehydrogenase 2 (*ALDH2*) had the most significant association with gout ($P = 1.7 \times 10^{-18}$; odds ratio [OR] $= 0.53$; 95% confidence interval [CI]: 0.46–0.61, Table 1 and Supplementary Figure S2A).

Next, the multivariate logistic regression analyses were performed to evaluate whether there was an additional association signal after the adjustment for the most significantly associated SNP rs671. We set the significance threshold as $\alpha = 6.3 \times 10^{-3}$ ($= 0.05/8$) with the Bonferroni correction. While the significant association of rs671 remained, the other 8 SNPs no longer showed a significant association with gout after the adjustment for rs671 (Table 2 and Supplementary Figure S2B). Among rs671 and 6 tagged SNPs (rs3782886, rs11066015, rs4646776, rs11066132, rs2074356 and rs11066280) shown in Supplementary Table S2, rs671 is the most promising functional SNP because only rs671 is a nonsynonymous variant (Glu504Lys). rs4766566 had a nominally significant association ($P = 0.032$), but did not pass the significant threshold for multiple hypothesis testing (Table 2). Additionally, the OR for rs4766566 became closer to 1.0 after the adjustment for rs671 (from 0.59 to 0.82; Tables 1 and 2). These data suggest that rs671 (Glu504Lys) of *ALDH2* is a genuine gout-associated SNP in the *MYL2-CUX2* locus.

SNP[*]	Position[†]	Gene	$r^{2\ddagger}$	$D'^{\ddagger}$	A1/A2[§]	MAF		P value[¶]	OR (95% CI)	Reciprocal OR (95% CI)
						Cases	Controls			
rs2188380	111386127	MYL2-CUX2	–	–	T/C	0.14	0.22	**7.1×10^{-12}**	0.58 (0.50–0.68)	1.72 (1.47–2.00)
rs7978484	109738076	FOXN4	0.35	0.65	G/A	0.14	0.17	**4.8×10^{-3}**	0.79 (0.67–0.93)	1.26 (1.07–1.49)
rs16940688	110360321	TCHP-GIT2	0.36	0.85	G/A	0.07	0.13	**6.2×10^{-9}**	0.55 (0.45–0.67)	1.82 (1.49–2.23)
rs2071629	111351186	MYL2	0.73	0.90	G/A	0.17	0.25	**3.7×10^{-11}**	0.60 (0.52–0.70)	1.65 (1.42–1.92)
rs11065783	111396249	MYL2-CUX2	0.47	1.00	A/G	0.25	0.31	**2.8×10^{-5}**	0.76 (0.66–0.86)	1.32 (1.16–1.51)
rs3809297	111609727	CUX2	0.52	0.79	G/T	0.17	0.28	**6.7×10^{-16}**	0.55 (0.48–0.64)	1.82 (1.57–2.10)
rs4766566	111706877	CUX2	0.43	1.00	T/C	0.25	0.36	**1.2×10^{-15}**	0.59 (0.52–0.67)	1.69 (1.48–1.92)
rs671	112241766	ALDH2	0.50	0.91	G/A	0.18	0.29	**1.7×10^{-18}**	0.53 (0.46–0.61)	1.88 (1.63–2.16)
rs2555004	114686645	RBM19-TBX5	0.31	0.82	A/G	0.21	0.20	0.22	1.09 (0.95–1.26)	0.91 (0.79–1.06)

Table 1. Association analysis of gout. Abbreviation: MAF = minor allele frequency; OR = odds ratio; CI = confidence interval. [*]dbSNP rs number. [†]SNP positions are based on NCBI human genome reference sequence Build 37. [‡]r^2 and D' indicate the pairwise linkage disequilibrium with rs2188380. [§]A1 is a major allele and A2 is a minor allele. [¶]P values smaller than 5.6×10^{-3} (adjusting for 9 tests with the Bonferroni correction) are shown in bold letters.

SNP A	SNP A		rs671	
	P value[*]	OR (95% CI)	P value[†]	OR (95% CI)
rs7978484	0.390	0.94 (0.74–1.19)	**2.6×10^{-16}**	0.57 (0.46–0.70)
rs16940688	0.054	0.93 (0.78–1.10)	**1.6×10^{-11}**	0.54 (0.47–0.63)
rs2071629	0.228	0.80 (0.63–1.00)	**7.8×10^{-10}**	0.57 (0.49–0.67)
rs2188380	0.593	0.89 (0.73–1.08)	**2.1×10^{-7}**	0.56 (0.47–0.67)
rs11065783	0.195	1.11 (0.95–1.31)	**6.8×10^{-16}**	0.48 (0.41–0.58)
rs3809297	0.213	0.85 (0.66–1.10)	**3.1×10^{-5}**	0.59 (0.46–0.76)
rs4766566	0.032	0.82 (0.68–0.98)	**3.2×10^{-6}**	0.61 (0.50–0.75)
rs2555004	0.353	1.07 (0.93–1.24)	**9.4×10^{-19}**	0.52 (0.45–0.60)

Table 2. Multivariate logistic regression analysis of gout including rs671 and each of the 8 SNPs. Abbreviation: OR = odds ratio; CI = confidence interval. [*]P values of each of the 8 SNPs (SNP A) adjusted by rs671. [†]P values of rs671 adjusted by SNP A. P values smaller than 6.3×10^{-3} (adjusting for 8 tests with the Bonferroni correction) are shown in bold letters.

It is well-known that individuals with rs671 heterozygotes (A/G; Lys/Glu) have only 6.25% of enzyme activity of those with normal ALDH2 (G/G; Glu/Glu), and those with homozygotes (A/A; Lys/Lys) show almost no activity[13]. Therefore, it is expected that dominant model (G/G v.s. A/G or A/A) is the most likely genetic model for the association between rs671 and gout. Actually, the statistical significance of the association between rs671 and gout was improved by applying the dominant model ($P = 2.9 \times 10^{-21}$; OR = 0.44; 95% CI: 0.37–0.52) compared with the result from the allelic model ($P = 1.7 \times 10^{-18}$; OR = 0.53; 95% CI: 0.46–0.61; Table 1). These findings indicate that "A" allele (Lys) of rs671 plays a protective role in the development of gout.

Discussion

In this study, among 9 tag SNPs selected from 8,595 SNPs in the *MYL2-CUX2* locus, only the association of rs671 of *ALDH2* remained significant after the adjustment for each SNP with the Bonferroni correction (Table 2). Together with the fact that rs671 (Glu504Lys) is a well-known dysfunctional SNP, we therefore concluded that rs671 is a genuine gout-associated SNP. Indeed, a previous Japanese study with 180 gout cases and 49 controls has indicated that the frequency of homozygotes (A/A; Lys/Lys) of rs671 was lower in gout patients than in controls[14]. The fine-mapping study for the associational signal on chromosome 12 identified by our GWAS reached the consistent result with the previous finding showing the association between *ALDH2* and gout[14].

ALDH2 is a crucial enzyme in the alcohol metabolism. Alcohol is oxidized to acetaldehyde by alcohol dehydrogenase, and acetaldehyde is further metabolized to acetate by aldehyde dehydrogenase[15], which largely depends on ALDH2. rs671 (Glu504Lys), a common missense SNP of *ALDH2* gene, severely decreases the activity of ALDH2 enzyme[13]. When acetate is metabolized to acetyl-coenzyme A, adenosine triphosphate (ATP) hydrolyzes to adenosine monophosphate (AMP) which is ultimately metabolized to uric acid. This alcohol metabolism is one of the reasons why alcohol drinking elevates serum uric acid (SUA) levels. Thus, the association between rs671 and gout is partly due to alcohol drinking.

The allele frequencies of rs671 of *ALDH2* differ among populations: the 504Lys allele ("A" allele) is common in East Asians including Japanese, but quite rare in other populations such as European and African descendants[16]. Therefore, it is reasonable that this SNP has not been detected in the previous GWASs of gout in Europeans and African Americans due to its low frequency. We showed that rs671 of *ALDH2* is an influential genetic factor for

Japanese as the other 4 previously reported loci[8] (*ABCG2*, *SLC2A9*, *GCKR* and *CNIH-2*) of gout, and further investigations in East Asian populations will be able to warrant these findings.

In summary, Glu504Lys polymorphism (rs671), a common dysfunctional SNP of *ALDH2*, is identified as a genuine gout-associated polymorphism in the *MYL2-CUX2* locus, and "A" allele (Lys) of rs671 plays a protective role in the development of gout.

Methods

Study participants.   This study was approved by the institutional ethical committees (National Defense Medical College and Nagoya University), and all procedures involved in this study were performed in accordance with the Declaration of Helsinki with written informed consent from each subject.

1,048 gout cases were assigned from the Japanese male outpatients at the gout clinics of Kyoto Industrial Health Association (Kyoto, Japan), or Ryougoku East Gate Clinic (Tokyo, Japan). All patients were clinically diagnosed as primary gout according to the criteria established by the American College of Rheumatology[17]. Patients with inherited metabolism disorders including Lesch–Nyhan syndrome were excluded. For the control group, 1,334 Japanese males with normal SUA (≤ 7.0 mg/dl) and without a history of gout were collected from the participants in the Shizuoka area in the Japan Multi-Institutional Collaborative Cohort Study (J-MICC Study)[18,19]. The details of participants in this study are shown in Supplementary Table S3.

Selection of SNPs.   First, 8,595 SNPs within 10 Mb across rs2188380 were selected using HapMap phase III JPT samples (http://hapmap.ncbi.nlm.nih.gov/)[20]; then, the pairwise LD was calculated between rs2188380 and the 8,595 SNPs (Supplementary Figure S1). After 8,550 SNPs in weak LD were excluded, the other 45 SNPs showing moderate to strong LD ($r^2 \geq 0.3$) with rs2188380 remained. Next, we examined the LD between each pair of these 46 SNPs (Fig. 1), and searched for the SNPs that were tagging other SNPs with strong LD ($r^2 \geq 0.8$). Finally, in addition to rs2188380, we selected 8 SNPs (rs7978484, rs16940688, rs2071629, rs11065783, rs3809297, rs4766566, rs671 and rs2555004) for association analysis (Supplementary Table S1).

Genetic analysis.   Genomic DNA was extracted from whole peripheral blood cells[21]. Genotyping of the 8 SNPs was performed by the TaqMan method (Life Technologies Corporation, Carlsbad, CA USA) with a LightCycler 480 (Roche Diagnostics, Mannheim, Germany)[22]. To confirm their genotypes, DNA sequencing analyses were performed with the primers shown in Supplementary Table S4. Direct sequencing was performed with a 3130xl Genetic Analyzer (Life Technologies Corporation)[22]. The deviation from Hardy-Weinberg equilibrium in control samples was evaluated by chi-square test using the software R (version 3.1.1) (http://www.r-project.org/).

Statistical analyses.   The associations between SNPs and gout were examined with logistic regression analyses. For the robustness of the statistical test, random re-sampling methods with computer simulation are often applied[23,24]. In this study, the permutation test[24] was used for random re-sampling in a case-control study with replacement for 1,000,000 times, and the robustness of statistics was confirmed. All the logistic regression analyses and chi-square tests were performed with SPSS v.22.0J (IBM Japan Inc., Tokyo, Japan) and the software R (version 3.1.1) (http://www.r-project.org/). We examined the pairwise LD using PLINK v1.07[25].

References

1. Woodward, O. M. *et al.* Identification of a urate transporter, ABCG2, with a common functional polymorphism causing gout. *Proc. Natl. Acad. Sci. USA* **106,** 10338–10342 (2009).
2. Matsuo, H. *et al.* Common defects of ABCG2, a high-capacity urate exporter, cause gout: a function-based genetic analysis in a Japanese population. *Sci. Transl. Med.* **1,** 5ra11 (2009).
3. Matsuo, H. *et al.* Common dysfunctional variants in ABCG2 are a major cause of early-onset gout. *Sci. Rep.* **3,** 2014 (2013).
4. Ichida, K. *et al.* Decreased extra-renal urate excretion is a common cause of hyperuricemia. *Nat. Commun.* **3,** 764 (2012).
5. Matsuo, H. *et al.* ABCG2 dysfunction causes hyperuricemia due to both renal urate underexcretion and renal urate overload. *Sci. Rep.* **4,** 3755 (2014).
6. Sulem, P. *et al.* Identification of low-frequency variants associated with gout and serum uric acid levels. *Nat. Genet.* **43,** 1127–1130 (2011).
7. Köttgen, A. *et al.* Genome-wide association analyses identify 18 new loci associated with serum urate concentrations. *Nat. Genet.* **45,** 145–154 (2013).
8. Matsuo, H. *et al.* Genome-wide association study of clinically defined gout identifies multiple risk loci and its association with clinical subtypes. *Ann. Rheum. Dis.* **75,** 652–659 (2016).
9. Kim, Y. J. *et al.* Large-scale genome-wide association studies in East Asians identify new genetic loci influencing metabolic traits. *Nat. Genet.* **43,** 990–995 (2011).
10. Iulianella, A., Sharma, M., Durnin, M., Vanden Heuvel, G. B. & Trainor, P. A. Cux2 (Cutl2) integrates neural progenitor development with cell-cycle progression during spinal cord neurogenesis. *Development* **135,** 729–741 (2008).
11. Franco, S. J. *et al.* Fate-restricted neural progenitors in the mammalian cerebral cortex. *Science* **337,** 746–749 (2012).
12. Huang, J., Ellinghaus, D., Franke, A., Howie, B. & Li, Y. 1000 Genomes-based imputation identifies novel and refined associations for the Wellcome Trust Case Control Consortium phase 1 Data. *Eur. J. Hum. Genet.* **20,** 801–805 (2012).
13. Matsuo, K. *et al.* Alcohol dehydrogenase 2 His47Arg polymorphism influences drinking habit independently of aldehyde dehydrogenase 2 Glu487Lys polymorphism: analysis of 2,299 Japanese subjects. *Cancer Epidemiol. Biomarkers Prev.* **15,** 1009–1013 (2006).
14. Yamanaka, H. *et al.* Analysis of the genotypes for aldehyde dehydrogenase 2 in Japanese patients with primary gout. *Adv. Exp. Med. Biol.* **370,** 53–56 (1994).
15. Takeuchi, F. *et al.* Confirmation of ALDH2 as a major locus of drinking behavior and of its variants regulating multiple metabolic phenotypes in a Japanese population. *Circ. J.* **75,** 911–918 (2011).
16. Goedde, H. W. *et al.* Distribution of ADH2 and ALDH2 genotypes in different populations. *Hum. Genet.* **88,** 344–346 (1992).
17. Wallace, S. L. *et al.* Preliminary criteria for the classification of the acute arthritis of primary gout. *Arthritis Rheum.* **20,** 895–900 (1977).

18. Hamajima, N. & J-MICC Study Group. The Japan Multi-Institutional Collaborative Cohort Study (J-MICC Study) to detect gene-environment interactions for cancer. *Asian Pac. J. Cancer Prev.* **8,** 317–323 (2007).
19. Asai, Y. *et al.* Baseline data of Shizuoka area in the Japan Multi-Institutional Collaborative Cohort Study (J-MICC Study). *Nagoya J. Med. Sci.* **71,** 137–144 (2009).
20. International HapMap, C. The International HapMap Project. *Nature* **426,** 789–796 (2003).
21. Matsuo, H. *et al.* Mutations in glucose transporter 9 gene SLC2A9 cause renal hypouricemia. *Am. J. Hum. Genet.* **83,** 744–751 (2008).
22. Sakiyama, M. *et al.* Common variant of leucine-rich repeat-containing 16A (LRRC16A) gene is associated with gout susceptibility. *Hum. Cell* **27,** 1–4 (2014).
23. Li, J. *et al.* Identification of high-quality cancer prognostic markers and metastasis network modules. *Nat. Commun.* **1,** 34 (2010).
24. Efron, B. & Tibshirani, R. J. In *An Introduction to the Bootstrap* (eds Cox,. D. R. *et al.*) 202–219 (Chapman & Hall, 1993).
25. Purcell, S. *et al.* PLINK: a tool set for whole-genome association and population-based linkage analyses. *Am. J. Hum. Genet.* **81,** 559–575 (2007).

Acknowledgements

Author Contributions

M.S., H.M., H.N. and A.N. conceived and designed this study. S.K., R.O., H.O. and T.S. collected samples and analyzed clinical data. M.S., H.M., K.Y. and A.N. performed genetic analysis. M.S., H.N. and T.N. performed statistical analyses. K.Y. and N.S. provided intellectual input and assisted with the preparation of the manuscript. M.S., H.M. and H.N. wrote the manuscript. M.S. and H.M. contributed equally to this work.

Additional Information

Supplementary information accompanies this paper at http://www.nature.com/srep

Competing financial interests: Yes, there is potential competing interest: H.M. and N.S. have a patent pending based on the work reported in this paper.

How to cite this article: Sakiyama, M. *et al.* Identification of rs671, a common variant of *ALDH2*, as a gout susceptibility locus. *Sci. Rep.* **6**, 25360; doi: 10.1038/srep25360 (2016).

Genetic, Clinical, and Pathologic Backgrounds of Patients with Autosomal Dominant Alport Syndrome

Naohiro Kamiyoshi,* Kandai Nozu,* Xue Jun Fu,* Naoya Morisada,* Yoshimi Nozu,* Ming Juan Ye,* Aya Imafuku,[†] Kenichiro Miura,[‡] Tomohiko Yamamura,* Shogo Minamikawa,* Akemi Shono,* Takeshi Ninchoji,* Ichiro Morioka,* Koichi Nakanishi,[§] Norishige Yoshikawa,[§] Hiroshi Kaito,* and Kazumoto Iijima*

Abstract

Background and objectives Alport syndrome comprises a group of inherited heterogeneous disorders involving CKD, hearing loss, and ocular abnormalities. Autosomal dominant Alport syndrome caused by heterozygous mutations in *collagen 4A3* and/or *collagen 4A4* accounts for <5% of patients. However, the clinical, genetic, and pathologic backgrounds of patients with autosomal dominant Alport syndrome remain unclear.

Design, setting, participants, & measurements We conducted a retrospective analysis of 25 patients with genetically proven autosomal dominant Alport syndrome and their family members (a total of 72 patients) from 16 unrelated families. Patients with suspected Alport syndrome after pathologic examination who were referred from anywhere in Japan for genetic analysis from 2006 to 2015 were included in this study. Clinical, laboratory, and pathologic data were collected from medical records at the point of registration for genetic diagnosis. Genetic analysis was performed by targeted resequencing of 27 podocyte-related genes, including Alport–related *collagen* genes, to make a diagnosis of autosomal dominant Alport syndrome and identify modifier genes or double mutations. Clinical data were obtained from medical records.

Results The median renal survival time was 70 years, and the median age at first detection of proteinuria was 17 years old. There was one patient with hearing loss and one patient with ocular lesion. Among 16 patients who underwent kidney biopsy, three showed FSGS, and seven showed thinning without lamellation of the glomerular basement membrane. Five of 13 detected mutations were reported to be causative mutations for autosomal recessive Alport syndrome in previous studies. Two families possessed double mutations in both *collagen 4A3* and *collagen 4A4*, but no modifier genes were detected among the other podocyte–related genes.

Conclusions The renal phenotype of autosomal dominant Alport syndrome was much milder than that of autosomal recessive Alport syndrome or X–linked Alport syndrome in men. It may, thus, be difficult to make an accurate diagnosis of autosomal dominant Alport syndrome on the basis of clinical or pathologic findings. No modifier genes were identified among the known podocyte–related genes.
Clin J Am Soc Nephrol 11: 1441–1449, 2016. doi: 10.2215/CJN.01000116

*Department of Pediatrics, Kobe University Graduate School of Medicine, Kobe, Japan; [†]Department of Nephrology, Toranomon Hospital, Tokyo, Japan; [‡]Department of Pediatrics, The University of Tokyo, Tokyo, Japan; and [§]Department of Pediatrics, Wakayama Medical University, Wakayama, Japan

Correspondence:
Dr. Kandai Nozu, Department of Pediatrics, Kobe University Graduate School of Medicine, 7-5-1 Kusunoki-cho, Chuo, Kobe 6500017, Japan. Email: nozu@med.kobe-u.ac.jp

Introduction

Alport syndrome is a hereditary disorder involving CKD progressing to ESRD, sensorineural hearing loss, and ocular abnormalities (1). Alport syndrome has three genetic modes of inheritance: X–linked Alport syndrome (XLAS), autosomal recessive Alport syndrome (ARAS), and autosomal dominant Alport syndrome (ADAS). XLAS is caused by mutations in the *collagen 4A5* (*COL4A5*) gene encoding the type 4 collagen α5–chain and accounts for approximately 80% of patients with the disease. ARAS occurs in about 15% of patients as a result of homozygous or compound heterozygous mutations in the *COL4A3* or *COL4A4* gene, whereas ADAS occurs in <5% of patients and arises as a result of heterozygous mutations in the *COL4A3* and/or *COL4A4* gene encoding the type 4 collagen α3– or α4–chain, respectively (2). However, heterozygous mutations in *COL4A3* or *COL4A4* are also found in about 40% of patients with thin basement membrane nephropathy (TBMN) (3). Although most affected individuals develop hematuria in childhood, proteinuria, renal failure, and extrarenal disorders are not observed in patients with TBMN, and the molecular mechanisms responsible for the different clinical courses of ADAS and TBMN remain unclear. Recent studies have revealed correlations between FSGS and heterozygous mutations in *COL4A3* or *COL4A4* (3,4), and 10% of patients diagnosed with familial FSGS showed heterozygous mutations in these two genes (5). A recent study using next generation sequencing (NGS) analysis revealed high proportions of mutations in *COL4A3* and *COL4A4* and a higher incidence of ADAS than previously reported (6). However, studies of ADAS are limited, and the clinical phenotype and genetic and pathologic backgrounds remain unclear (7–12). In this study, we provide the first clarification of

the genetic, clinical, and pathologic backgrounds of ADAS in a relatively large number of patients.

Materials and Methods
Diagnostic Criteria for ADAS
All patients diagnosed with ADAS in this study satisfied one of the following criteria: (1) hematuria and proteinuria or ESRD with renal pathology showing thickening and thinning with lamellation in the glomerular basement membrane (GBM; basket weave change [BWC]) and heterozygous mutations in COL4A3 and/or COL4A4; (2) hematuria and proteinuria with renal pathology showing thin basement membrane (TBM) and a family history of ESRD, with heterozygous mutations in COL4A3 and/or COL4A4; and (3) siblings or consanguineous family members of patients with ADAS diagnosed with criteria 1 or 2 and at least showing hematuria, including patients for whom genetic tests were not available. These criteria ensured that at least one person in the family had received a kidney biopsy and had TBM leading to a pathologic diagnosis of ADAS.

Patients
Patients with suspected Alport syndrome after pathologic examination who were referred to our hospital for genetic diagnosis from 2006 to 2015 were included in this study. Clinical, laboratory, and pathologic data were collected from medical records at the point of registration for genetic diagnosis. Detailed family histories were gathered from the patients and/or their parents. Information on hearing loss was obtained from medical records. All patients were evaluated for ocular lesions by an ophthalmologist before genetic analysis. In Japan, annual urinary screening is available for all students and most adults, and family members with urinary abnormalities of at least hematuria were included in the analysis of renal survival. Patient age was determined at the time of registration for genetic testing. We conducted a retrospective study of 72 patients with renal manifestations, including 25 genetically diagnosed patients with ADAS and 47 family members from 16 unrelated families. The family trees for all families are shown in Supplemental Figure 1. Age at registration for genetic analysis, age at reaching ESRD, or age at death without ESRD are shown for all 72 patients. Of these 72 patients, 19 (26%) had already developed ESRD. Clinical and laboratory data and pathologic findings were obtained from medical records. The degree of urinary protein excretion was evaluated by urinary protein-to-creatinine ratio. eGFRs were calculated using the Schwartz equation (13,14) or GFR-estimating equations for Japanese individuals (15) for patients <18 and ≥18 years old, respectively.

Genetic Analyses
Sanger Sequencing. Sanger sequencing for COL4A3 and COL4A4 was performed by PCR and direct sequencing of genomic DNA for all exons and exon-intron boundaries. Most patients in this study had undergone Sanger sequencing for the diagnosis of ADAS before NGS analysis. Blood samples were collected from patients and family members, and genomic DNA was isolated from peripheral blood leukocytes using the Quick Gene Mini 80 System (Fujifilm, Tokyo, Japan) according to the manufacturer's instructions. For genomic DNA analysis, all 52 specific exons of COL4A3 and 48 exons of COL4A4 were amplified by PCR as described previously (16). The PCR-amplified products were then purified and subjected to direct sequencing using a Dye Terminator Sequencing Kit (Amersham Biosciences, Piscataway, NJ) with an automatic DNA sequencer (model ABI Prism 3130; PerkinElmer, Waltham, MA).

Targeted Resequencing. NGS samples were prepared using a HaloPlex Target Enrichment System Kit by following the manufacturer's instruction (Agilent Technologies, Santa Clara, CA). Briefly, digested 225 ng genomic DNA were hybridized at 54°C for 16 hours with custom–designed NGS probes to capture 27 genes, such as COL4A3, COL4A4, COL4A5, and other FSGS–causative genes. Amplified target libraries were sequenced with 150-bp pair-end reads on a MiSeq Platform (Illumina, San Diego, CA) followed by variant analysis on a SureCall 3.0 (Agilent Technologies).

We analyzed 25 patients with ADAS, including at least one from each of 16 families.

Haplotype Analyses. Haplotype analysis was performed for families 122 and 140, both of which possessed double mutations in both COL4A3 and COL4A4 with identical substitutions and were, thus, suspected of having a common ancestor. The target fragments on chromosome 2 were amplified by AmpliTaq Gold (Thermo Fisher Scientific, Vernon Hills, IL) using microsatellite markers D2S163, D2S126, D2S133, D2S2354, D2S362, D2S396, D2s233, and D2s206. PCR fragment size was analyzed using an ABI PRISM 310 Genetic Analyzer (Applied Biosystems, Foster City, CA) followed by allele binning using GeneMapper (Thermo Fisher Scientific).

Statistical Analyses
Statistical analysis was performed using JMP (JMP, Version 11 Package for Windows; SAS Institute Inc., Cary, NC). The occurrence of events (age at detection of proteinuria and age at ESRD) was analyzed according to the Kaplan–Meier method. We defined the outcomes as age at ESRD for renal survival analysis and detection of proteinuria for proteinuria–free survival analysis. We considered patients who died without ESRD as censored patients. Deaths in patients who had already developed ESRD were treated as having reached the outcome at the age of developing ESRD. Patients who had not reached ESRD at the point of registration for genetic analysis were also treated as censored patients.

Ethical Considerations
All procedures were reviewed and approved by the Institutional Review Board of Kobe University School of Medicine. Informed consent was obtained from all patients or their parents.

Results
Clinical Features
The clinical features of the 25 patients with genetically proven ADAS are shown in Table 1, and all family trees are shown in Supplemental Figure 1. The cohort included 11 men and 14 women, with a mean age of 33.4 years old (range =5–82 years old). Proteinuria was detected in

Table 1. Clinical findings

Patient ID	Age, yr	Sex	Height, cm	BW, kg	Proteinuria Detected Age, yr	ESRD Detected Age, yr	Hearing Loss Detection Age, yr	Ocular Lesion	sCr, mg/dl	sAlb, g/dl	U-P/C, g/g	eGFR, ml/min per 1.73 m²
72	14	W	155.6	47.4	—	—	—	—	0.49	4.8	0.04	131.1
122	35	M	183	66.0	9	—	—	—	1.27	4.3	0.45	53.8
122A	39	W	156	51.0	2	—	—	—	ND	ND	ND	ND
122C	62	M	163	66.0	17	57	—	—	ND	ND	ND	ND
124	45	W	158	40.0	17	—	—	—	0.74	4.0	0.73	66.8
129	43	M	170	77.0	42	—	—	—	0.77	4.7	0.22	88.3
140	16	M	180.4	105.3	6	—	—	—	0.81	4.2	0.92	80.9
140A	47	M	172	89.8	9	33	—	—	ND	ND	ND	ND
148	46	W	153.6	38.7	35	—	—	—	0.69	3.7	2.1	71.7
148A	20	W	149	40.7	—	—	—	—	0.57	4.5	0.02	112.2
148B	18	W	164.7	50.4	—	—	—	—	0.51	4.5	0.02	130.6
148C	11	M	150.4	35.4	—	—	—	—	0.62	4.5	0.03	84.9
153	48	W	154.5	49.3	9	—	—	—	0.9	3.8	1.86	53.0
153E	82	M	160	44.0	32	63	—	AMD	8.84	3.2	ND	ND
154	26	W	161	67	16	—	—	—	0.68	4.8	0.71	86.8
161	26	M	177	74.0	5	—	—	—	0.9	4.6	1.5	83.7
175	31	W	159.6	54.4	5	—	—	—	0.92	3.6	1.0	58.1
175A	5	W	100.9	15.5	—	—	—	—	0.34	4.4	0.0	103.8
175B	5	W	106	17.5	—	—	—	—	0.28	4.6	0.0	132.5
198	36	M	167	62	11	—	—	—	3.0	3.6	2.0	20.9
205	45	M	174.3	67.0	20	—	—	—	1.67	3.9	1.0	37
279	29	M	175.0	72.0	17	—	—	—	0.91	3.8	1.3	81.8
285	25	W	152.0	46.0	—	—	—	—	0.41	4.2	0.0	155
297	11	W	143.8	26.5	6	—	—	—	0.60	3.9	0.4	98.8
305	69	W	157.0	51.0	44	—	65	—	1.76	3.6	3.6	22.9

ID, identification; BW, body weight; sCr, serum creatinine level; sAlb, serum albumin level; U-P/C, urinary protein-to-creatinine ratio; W, woman or girl; M, man or boy; ND, not detected until now; AMD, age–related macular degeneration.
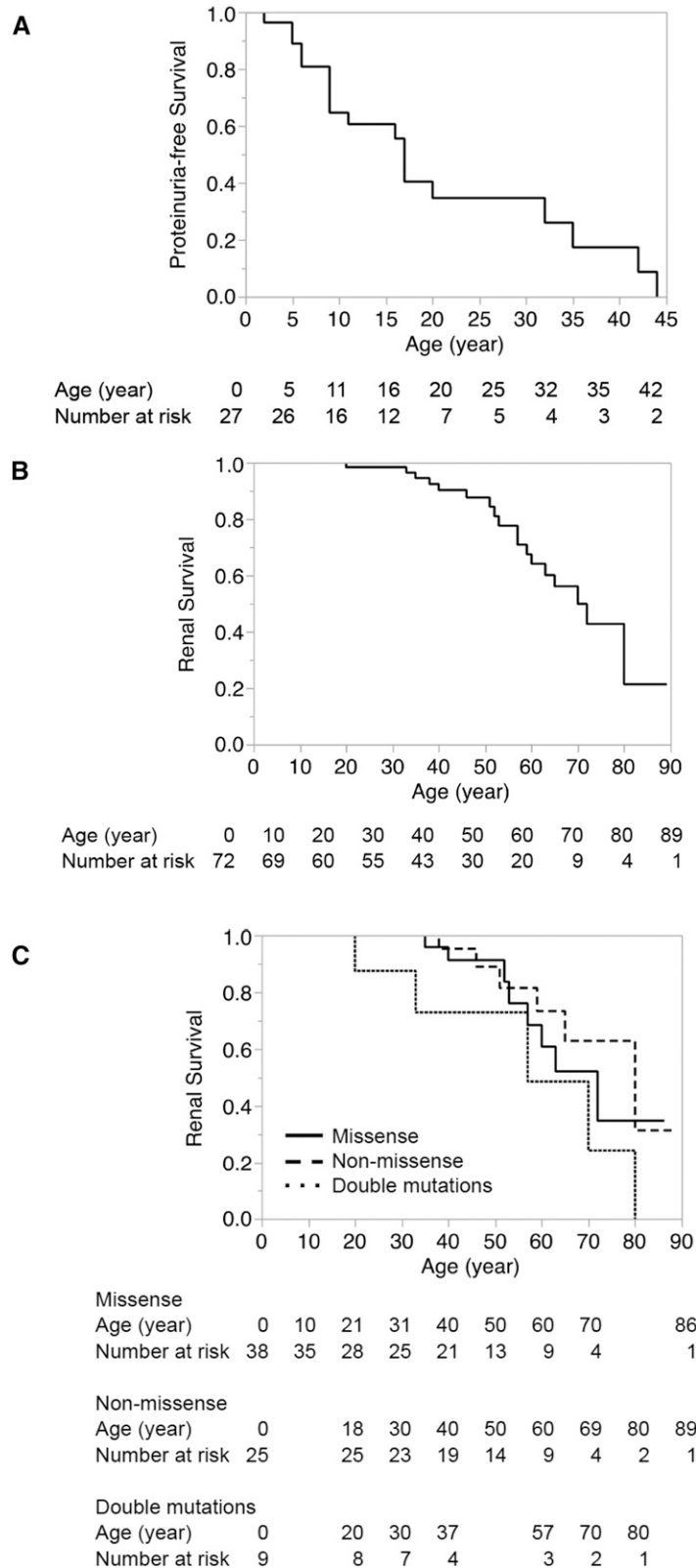
Figure 1. | Probability of each clinical sign in autosomal dominant Alport syndrome cases. (A) Probability of developing proteinuria in 24 patients. (B) Probability of developing ESRD in 72 patients. (C) Probability of developing ESRD according to the type of mutation (38 missense, 25 nonmissense, and nine double mutations). The median ages for developing proteinuria and ESRD were 17 and 70 years old, respectively. Differences between types of mutation were not significant (*P*=0.18).

18 patients, and the median age for developing proteinuria was 17.0 years old (Figure 1A). Although the proteinuria–free survival curve shows the time to proteinuria detection rather than time to onset, all students in Japan receive urinary screening every year, and most adults also receive urinary screening through their employers or public health organizations. The age at detection of proteinuria is, thus, relatively accurate. Seven patients showed normal renal function (age range =5–25 years old), 14 showed mild to severe renal dysfunction, and three patients reached ESRD at 33, 57, and 63 years old (Table 1). One patient had hearing loss, and one ocular lesion was detected. We also assessed a total of 172 patients with ADAS and family members for renal disease and detected renal disorders in 72 individuals, including ESRD in 19 patients. The median renal survival time in this study was 70.0 years (Figure 1B).

Pathologic Findings

The pathologic findings are shown in Table 2. Renal biopsy was performed in 16 patients from 16 families. All of these patients had both hematuria and proteinuria at the time of kidney biopsy. The mean age at renal biopsy was 32.3 years old (range =11–61 years old). Five biopsies showed minimal glomerular change, eight showed diffuse mesangial proliferation, and three showed FSGS, by light microscopy. Immunofluorescence staining revealed IgM deposits in three patients and IgA and C3 deposits in two patients. BWC was detected by electron microscopy in nine patients, and seven patients showed isolated TBM. Immunohistochemical staining of collagen-α5(4) showed normal expression in 15 patients and was not examined in one patient. Seven patients underwent multiple renal biopsies before diagnosis.

Mutation Detection

The detected mutations are shown in Table 3. Thirteen different mutations, including 10 missense mutations leading to glycine substitutions, an 18-bp deletion mutation, a splice-site mutation, and a 1-bp deletion mutation were identified, all in the collagenic domain. Eight of the mutations were novel mutations. Among the 16 families with ADAS, six had mutations in COL4A3, eight had mutations in COL4A4, and two had mutations in both COL4A3 and COL4A4 with identical substitutions suspicious of a common ancestor. Five mutations were reported to be causative mutations for ARAS in previous studies (17,18).

NGS Analyses

We conducted comprehensive analyses of 25 patients from 16 families by targeted resequencing. We targeted 27 causative genes for inherited FSGS and Alport syndrome (Supplemental Table 1). Identical variants in COL4A3 and/or COL4A4 were detected by both Sanger method and targeted resequencing in all patients. We also detected 168 variants in exonic region in 26 genes (Supplemental Table 2), and those were not pathogenic variants.

We failed to identify any other variants considered to be modifier genes or double mutations that might have increased the severity of the phenotype.

Haplotype Analyses

Two families had double mutations in both COL4A3 and COL4A4, with identical substitutions of p.Gly1406Glu in COL4A3 and p.Gly957Arg in COL4A4. We, therefore, performed microsatellite analysis to identify any founder effect between these two families using eight markers spanning 22.5 Mb centered on the COL4A3 and COL4A4 region on chromosome 2. A haplotype (gray in Figure 2) spanning 13.4 Mb including COL4A3 and COL4A4 was conserved in both families, suggesting that the disease-associated segment might have been inherited from the same founder.

Table 2. Pathologic findings						
Patient ID	Age at Biopsy, yr	Light Microscopy	Immunofluorescence Staining	Electron Microscopy	α5-Staining	No. of Biopsies
72	14	MGA	Negative	TBM, BWC	Positive	1
122	35	DMP	Negative	TBM	Positive	1
124	45	MGA	IgM	TBM	Positive	2
129	43	DMP	ND	TBM	Positive	1
140	16	FSGS	IgM	TBM	Positive	1
148	46	FSGS	Negative	TBM, BWC	Positive	1
153	48	DMP	ND	TBM, BWC	Positive	1
154	24	DMP	IgA, C3	BWC	Positive	2
161	26	MGA	Negative	TBM, BWC	Positive	1
175	31	DMP	Negative	TBM, BWC	Positive	4
198	17	DMP	Negative	TBM, BWC	ND	4
205	45	FSGS	IgM, Fib	TBM	Positive	2
279	30	MGA	IgA, C3	TBM	Positive	2
285	25	DMP	Negative	TBM	Positive	1
297	11	MGA	IgG, C1q	TBM, BWC	Positive	1
305	61	DMP	Negative	TBM, BWC	Positive	2

ID, identification; MGA, minimal glomerular abnormality; TBM, thin basement membrane; BWC, basket weave change; DMP, diffuse mesangial proliferation; Fib, fibrinogen; ND, not determined.

Table 3.   Collagen 4A3 and collagen 4A4 mutations

Patient ID	Mutation 1				Mutation 2				Previous Report of ARAS
	Gene	Position (Exon)	Nucleotide Change	Amino Acid Change	Gene	Position (Exon)	Nucleotide Change	Amino Acid Change	
72	COL4A4	29	c.2510G>C	p.Gly837Ala					Yes
122	COL4A3	47	c.4217G>A[a]	p.Gly1406Glu	COL4A4	32	c.2869G>A	p.Gly957Asp	Yes
124	COL4A4	22	c.1323_1340del[a]	18-bp Deletion					
129	COL4A3	35	c.2980+2T>A[a]	Exon skipping					
140	COL4A3	47	c.4217G>A[a]	p.Gly1406Glu	COL4A4	32	c.2869G>A	p.Gly957Asp	Yes
148	COL4A4	25	c.1808A>G[a]	p.Asp603Gly					
153	COL4A4	24	c.1733G>T	p.Gly577Val					Yes
154	COL4A4	31	c.2726G>A[a]	p.Gly909Glu					
161	COL4A3	26	c.1855G>A	pGly619Arg					Yes
175	COL4A3	40	c.3499G>A	p.Gly1167Arg					Yes
198	COL4A3	26	c.1901G>A	p.Gly634Glu					
205	COL4A3	26	c.1855G>A	p.Gly619Arg					Yes
279	COL4A4	20	c.1323_1340del[a]	18-bp Deletion					
285	COL4A4	30	c.2641del C[a]	p.His881fs					
297	COL4A4	27	c.2084G>A[a]	p.Gly695Asp					
305	COL4A3	40	c.3464G>A[a]	p.Gly1155Asp					

ID, identification; ARAS, autosomal recessive Alport syndrome; COL4A4, collagen 4A4; COL4A3, collagen 4A3.
[a]Novel mutation.
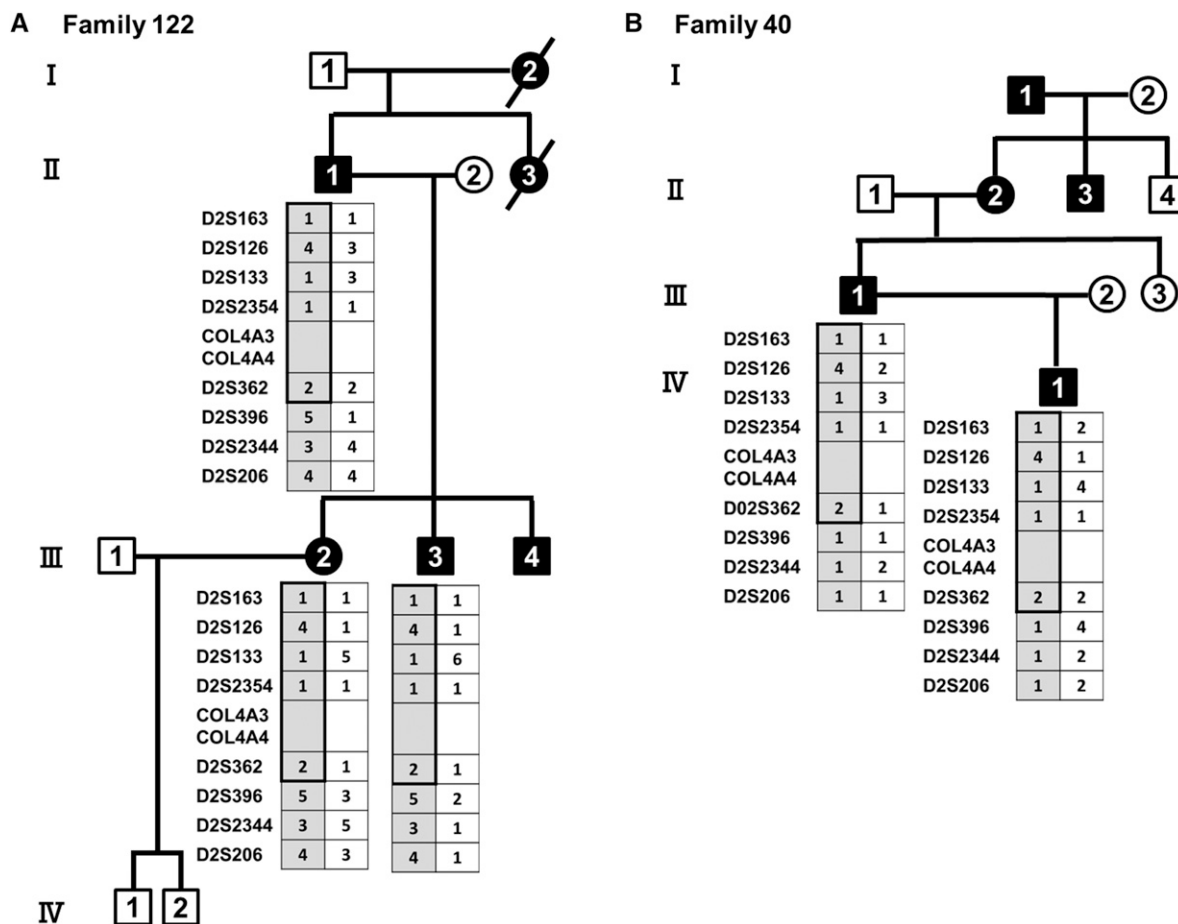
Figure 2. | Haplotype analysis of two families harboring p.Gly1406Glu in *collagen 4A3* (*COL4A3*) and p.Gly957Arg in *COL4A4* mutations. Haplotypes of (A) family 122 and (B) family 140. The haplotype from D2S163 to D2S362 (gray with black frame), spanning 13.4 Mb, was conserved in both families. Squares indicate men, and circles indicate women. lack symbols indicate affected individuals, oblique bars indicate deceased individuals, roman numerals represent generations, and numbers identify family members.

Genotype-Phenotype Correlations

We compared renal survival curves for patients with missense mutations, nonmissense mutations, and double mutations (Figure 1C). There were no significant differences among these three groups (*P*=0.18).

Discussion

This study is one of the largest to examine the clinical manifestations, pathologic characteristics, and genetic backgrounds of patients with ADAS. We conducted genetic analyses in patients with clinical manifestations, pathologic findings, and family histories consistent with Alport syndrome throughout Japan. To date, we have confirmed a genetic diagnosis of Alport syndrome in 305 families and detected ADAS in 16 families, giving a proportion of ADAS of 5.25%, consistent with a previous report (2).

In our study, the median age for developing proteinuria was 17 years old, and the median renal survival time was 70 years. In contrast, previous studies reported median renal survival rates in men with XLAS or ARAS of 25 and 21 years old, respectively (18,19). Marcocci *et al.* (10) observed proteinuria in 50% of patients with ADAS, but only

one patient developed proteinuria at younger than 20 years old; however, nine patients reached ESRD, and only one reached ESRD before 40 years of age, consistent with our results. Overall, these results indicate that renal manifestations in individuals with ADAS are mild and slowly progressive compared with those in men with XLAS and individuals with ARAS.

Only one patient in our cohort developed hearing loss (at age 61 years old), and one developed suspected age–related macular degeneration (at age 82 years old). Marcocci *et al.* (10) reported that 13.3% of patients with ADAS developed sensorineural hearing loss and that only one developed bilateral cataract, which was assumed to be caused by postrenal transplantation steroid treatment. Jais *et al.* (19) reported hearing loss and specific ocular changes in 79% and 35.2%, respectively, among men with XLAS, whereas Oka *et al.* (18) reported hearing loss in 40% and ocular lesions in 10% of Japanese patients with ARAS. These results indicate that extrarenal manifestations are relatively rare in patients with ADAS. Overall, the clinical manifestations in patients with ADAS, especially in younger patients, seem to be much milder than those in men with XLAS and patients with ARAS.

Sixteen patients in this study (one from each family) underwent kidney biopsy. Light microscopy revealed FSGS in three of these 16 patients. Previous studies of large Greek Cypriot pedigrees led to the suggestion of a causal relationship between heterozygous *COL4A3/COL4A4* mutations and FSGS (20,21). Malone *et al.* (5) analyzed a familial FSGS cohort and found *COL4A3* or *COL4A4* variants in seven of 70 families. Xie *et al.* (4) identified heterozygous *COL4A3* mutations in five (12.5%) FSGS families, whereas Gast *et al.* (22) reported *COL4A3* or *COL4A4* variants in four patients from three families among a total of 80 patients (5%) with FSGS. This suggests that some patients with ADAS might be diagnosed as having familial FSGS. Immunohistochemical staining of α5(4) showed normal expression in glomeruli in all patients in this study. We previously also showed normal expression of α5(4) in GBM in 29% of patients with XLAS and 20% of patients with ARAS (16,18). A normal distribution of α5(4) cannot, thus, be used to establish the inheritance mode for ADAS. Although GBM alterations were detected in all patients by electron microscopy, seven patients showed isolated TBM. The mean ages at renal biopsy were 34.1 years old (range =16–45 years old) in patients with isolated TBM and 30.9 years old (range =11–61 years old) in patients with BWC, suggesting that the different findings between TBM and BWC are unlikely to be caused by different ages at renal biopsy in patients with ADAS. Furthermore, multiple renal biopsies were performed before reaching a definite diagnosis in seven of the 16 patients. These results indicate that it may be difficult to make a precise diagnosis of Alport syndrome on the basis of clinical and pathologic findings.

Six patients in this study had heterozygous mutations in *COL4A3*, eight patients had heterozygous mutations in *COL4A4*, and two patients had heterozygous mutations in both *COL4A3* and *COL4A4*. The mutation sites were scattered throughout the genes with no accumulation in any specific region as in the previous study (10). Broad differences in phenotypes were observed among unrelated families, even among families with identical variants, and we were unable to establish any genotype-phenotype correlations in this cohort. Two families had double mutations with identical substitutions in both genes in the *cis* position, and microsatellite analysis in these families identified a founder effect. Mencarelli *et al.* (23) recently reported that digenic inheritance in ADAS was associated with a poorer prognosis, intermediate between ADAS and ARAS. The two families in our study comprised eight patients, five of whom developed ESRD at the ages of 20, 33, 57, 70, and 80 years old. Renal phenotype, thus, varied in these families, and we were unable to identify any correlation between phenotype severity and double mutations.

Five mutations detected in patients with ADAS in this study were previously reported as causative mutations for ARAS (11,18). Interestingly, the heterozygous carrier parents of these mutations in those reports were asymptomatic or only presented with microhematuria. Strasser *et al.* (24) reported that digenic mutations in *COL4A5* and *MYH9* affected severity of Alport syndrome symptoms. We, therefore, conducted targeted resequencing to search for modifier genes among podocyte-related genes reported as causative genes of familial FSGS or congenital nephrotic syndrome. As a result, we could not identify any variants likely to act as modifier genes in this study (Supplemental Table 2). These findings indicate that the heterozygous mutations in *COL4A3* or *COL4A4* may cause ESRD on their own, although secondary factors, such as environmental factors or unknown genetic changes, might also contribute to the phenotype of kidney disease in patients with ADAS.

In conclusion, the results of this study clarify the natural history of ADAS. Patients with ADAS show nonspecific clinical manifestations, except for hematuria at a young age. Pathologically, one half of the examined patients showed isolated TBM, and all showed normal α5(4), highlighting the difficulty of establishing a precise diagnosis of ADAS on the basis of clinical and pathologic findings, especially in the early phase of the disease. Some patients with ADAS may be incorrectly diagnosed with familial FSGS or even IgA nephropathy. The phenotype of ADAS varies, regardless of the genetic background, with no identifiable phenotype-genotype correlations, indicating the existence of secondary factors affecting the phenotype of kidney disease in patients with ADAS.

References

1. Kashtan CE, Michael AF: Alport syndrome. *Kidney Int* 50: 1445–1463, 1996
2. Kashtan CE: Alport syndrome and the X chromosome: Implications of a diagnosis of Alport syndrome in females. *Nephrol Dial Transplant* 22: 1499–1505, 2007
3. Papazachariou L, Demosthenous P, Pieri M, Papagregoriou G, Savva I, Stavrou C, Zavros M, Athanasiou Y, Ioannou K, Patsias C, Panagides A, Potamitis C, Demetriou K, Prikis M, Hadjigavriel M, Kkolou M, Loukaidou P, Pastelli A, Michael A, Lazarou A, Arsali M, Damianou L, Goutziamani I, Soloukides A, Yioukas L, Elia A, Zouvani I, Polycarpou P, Pierides A, Voskarides K, Deltas C: Frequency of COL4A3/COL4A4 mutations amongst families segregating glomerular microscopic hematuria and evidence for activation of the unfolded protein response. Focal and segmental glomerulosclerosis is a frequent development during ageing. *PLoS One* 9: e115015, 2014

4. Xie J, Wu X, Ren H, Wang W, Wang Z, Pan X, Hao X, Tong J, Ma J, Ye Z, Meng G, Zhu Y, Kiryluk K, Kong X, Hu L, Chen N: COL4A3 mutations cause focal segmental glomerulosclerosis. *J Mol Cell Biol* 6: 498–505, 2014

5. Malone AF, Phelan PJ, Hall G, Cetincelik U, Homstad A, Alonso AS, Jiang R, Lindsey TB, Wu G, Sparks MA, Smith SR, Webb NJ, Kalra PA, Adeyemo AA, Shaw AS, Conlon PJ, Jennette JC, Howell DN, Winn MP, Gbadegesin RA: Rare hereditary COL4A3/ COL4A4 variants may be mistaken for familial focal segmental glomerulosclerosis. *Kidney Int* 86: 1253–1259, 2014

6. Morinière V, Dahan K, Hilbert P, Lison M, Lebbah S, Topa A, Bole-Feysot C, Pruvost S, Nitschke P, Plaisier E, Knebelmann B, Macher MA, Noel LH, Gubler MC, Antignac C, Heidet L: Improving mutation screening in familial hematuric nephropathies through next generation sequencing. *J Am Soc Nephrol* 25: 2740–2751, 2014

7. Ciccarese M, Casu D, Ki Wong F, Faedda R, Arvidsson S, Tonolo G, Luthman H, Satta A: Identification of a new mutation in the alpha4(IV) collagen gene in a family with autosomal dominant Alport syndrome and hypercholesterolaemia. *Nephrol Dial Transplant* 16: 2008–2012, 2001

8. Jefferson JA, Lemmink HH, Hughes AE, Hill CM, Smeets HJ, Doherty CC, Maxwell AP: Autosomal dominant Alport syndrome linked to the type IV collage alpha 3 and alpha 4 genes (COL4A3 and COL4A4). *Nephrol Dial Transplant* 12: 1595–1599, 1997

9. Kharrat M, Makni S, Makni K, Kammoun K, Charfeddine K, Azaeiz H, Jarraya F, Ben Hmida M, Gubler MC, Ayadi H, Hachicha J: Autosomal dominant Alport's syndrome: Study of a large Tunisian family. *Saudi J Kidney Dis Transpl* 17: 320–325, 2006

10. Marcocci E, Uliana V, Bruttini M, Artuso R, Silengo MC, Zerial M, Bergesio F, Amoroso A, Savoldi S, Pennesi M, Giachino D, Rombolà G, Fogazzi GB, Rosatelli C, Martinhago CD, Carmellini M, Mancini R, Di Costanzo G, Longo I, Renieri A, Mari F: Autosomal dominant Alport syndrome: Molecular analysis of the COL4A4 gene and clinical outcome. *Nephrol Dial Transplant* 24: 1464–1471, 2009

11. Pescucci C, Mari F, Longo I, Vogiatzi P, Caselli R, Scala E, Abaterusso C, Gusmano R, Seri M, Miglietti N, Bresin E, Renieri A: Autosomal-dominant Alport syndrome: Natural history of a disease due to COL4A3 or COL4A4 gene. *Kidney Int* 65: 1598–1603, 2004

12. van der Loop FT, Heidet L, Timmer ED, van den Bosch BJ, Leinonen A, Antignac C, Jefferson JA, Maxwell AP, Monnens LA, Schröder CH, Smeets HJ: Autosomal dominant Alport syndrome caused by a COL4A3 splice site mutation. *Kidney Int* 58: 1870–1875, 2000

13. Schwartz GJ, Haycock GB, Edelmann CM Jr., Spitzer A: A simple estimate of glomerular filtration rate in children derived from body length and plasma creatinine. *Pediatrics* 58: 259–263, 1976

14. Schwartz GJ, Gauthier B: A simple estimate of glomerular filtration rate in adolescent boys. *J Pediatr* 106: 522–526, 1985

15. Matsuo S, Imai E, Horio M, Yasuda Y, Tomita K, Nitta K, Yamagata K, Tomino Y, Yokoyama H, Hishida A; Collaborators developing the Japanese equation for estimated GFR: Revised equations for estimated GFR from serum creatinine in Japan. *Am J Kidney Dis* 53: 982–992, 2009

16. Hashimura Y, Nozu K, Kaito H, Nakanishi K, Fu XJ, Ohtsubo H, Hashimoto F, Oka M, Ninchoji T, Ishimori S, Morisada N, Matsunoshita N, Kamiyoshi N, Yoshikawa N, Iijima K: Milder clinical aspects of X-linked Alport syndrome in men positive for the collagen IV α5 chain. *Kidney Int* 85: 1208–1213, 2014

17. Heidet L, Arrondel C, Forestier L, Cohen-Solal L, Mollet G, Gutierrez B, Stavrou C, Gubler MC, Antignac C: Structure of the human type IV collagen gene COL4A3 and mutations in autosomal Alport syndrome. *J Am Soc Nephrol* 12: 97–106, 2001

18. Oka M, Nozu K, Kaito H, Fu XJ, Nakanishi K, Hashimura Y, Morisada N, Yan K, Matsuo M, Yoshikawa N, Vorechovsky I, Iijima K: Natural history of genetically proven autosomal recessive Alport syndrome. *Pediatr Nephrol* 29: 1535–1544, 2014

19. Jais JP, Knebelmann B, Giatras I, De Marchi M, Rizzoni G, Renieri A, Weber M, Gross O, Netzer KO, Flinter F, Pirson Y, Verellen C, Wieslander J, Persson U, Tryggvason K, Martin P, Hertz JM, Schröder C, Sanak M, Krejcova S, Carvalho MF, Saus J, Antignac C, Smeets H, Gubler MC: X-linked Alport syndrome: Natural history in 195 families and genotype- phenotype correlations in males. *J Am Soc Nephrol* 11: 649–657, 2000

20. Pierides A, Voskarides K, Athanasiou Y, Ioannou K, Damianou L, Arsali M, Zavros M, Pierides M, Vargemezis V, Patsias C, Zouvani I, Elia A, Kyriacou K, Deltas C: Clinico-pathological correlations in 127 patients in 11 large pedigrees, segregating one of three heterozygous mutations in the COL4A3/ COL4A4 genes associated with familial haematuria and significant late progression to proteinuria and chronic kidney disease from focal segmental glomerulosclerosis. *Nephrol Dial Transplant* 24: 2721–2729, 2009

21. Voskarides K, Damianou L, Neocleous V, Zouvani I, Christodoulidou S, Hadjiconstantinou V, Ioannou K, Athanasiou Y, Patsias C, Alexopoulos E, Pierides A, Kyriacou K, Deltas C: COL4A3/COL4A4 mutations producing focal segmental glomerulosclerosis and renal failure in thin basement membrane nephropathy. *J Am Soc Nephrol* 18: 3004–3016, 2007

22. Gast C, Pengelly RJ, Lyon M, Bunyan DJ, Seaby EG, Graham N, Venkat-Raman G, Ennis S: Collagen (COL4A) mutations are the most frequent mutations underlying adult focal segmental glomerulosclerosis [published online ahead of print September 7, 2015]. *Nephrol Dial Transplant*

23. Mencarelli MA, Heidet L, Storey H, van Geel M, Knebelmann B, Fallerini C, Miglietti N, Antonucci MF, Cetta F, Sayer JA, van den Wijngaard A, Yau S, Mari F, Bruttini M, Ariani F, Dahan K, Smeets B, Antignac C, Flinter F, Renieri A: Evidence of digenic inheritance in Alport syndrome. *J Med Genet* 52: 163–174, 2015

24. Strasser K, Hoefele J, Bergmann C, Büscher AK, Büscher R, Hoyer PF, Weber S: COL4A5-associated X-linked Alport syndrome in a female patient with early inner ear deafness due to a mutation in MYH9. *Nephrol Dial Transplant* 27: 4236–4240, 2012

CrossMark

Clinical guides for atypical hemolytic uremic syndrome in Japan

Hideki Kato[1] · Masaomi Nangaku[1] · Hiroshi Hataya[2] · Toshihiro Sawai[3] ·
Akira Ashida[4] · Rika Fujimaru[5] · Yoshihiko Hidaka[6] · Shinya Kaname[7] ·
Shoichi Maruyama[8] · Takashi Yasuda[9] · Yoko Yoshida[1] · Shuichi Ito[10] ·
Motoshi Hattori[11] · Yoshitaka Miyakawa[12] · Yoshihiro Fujimura[13] ·
Hirokazu Okada[14] · Shoji Kagami[15] · The Joint Committee for the Revision of Clinical
Guides of Atypical Hemolytic Uremic Syndrome in Japan

Abstract Atypical hemolytic uremic syndrome (aHUS) is a rare disease characterized by the triad of microangiopathic hemolytic anemia, thrombocytopenia, and acute kidney injury. In 2013, we developed diagnostic criteria to enable early diagnosis and timely initiation of appropriate treatment for aHUS. Recent clinical and molecular findings have resulted in several proposed classifications and definitions of thrombotic microangiopathy and aHUS. Based on recent advances in this field and the emerging international consensus to exclude secondary TMAs from the definition of aHUS, we have redefined aHUS and proposed diagnostic algorithms, differential diagnosis, and therapeutic strategies for aHUS.

Keywords Atypical hemolytic uremic syndrome · Thrombotic microangiopathy · Eculizumab · Alternative complement pathway

✉ Shoji Kagami
kagami@tokushima-u.ac.jp

1   Division of Nephrology and Endocrinology, The University of Tokyo Graduate School of Medicine, Bunkyo, Tokyo, Japan

2   Department of Nephrology, Tokyo Metropolitan Children's Medical Center, Fuchu, Tokyo, Japan

3   Department of Pediatrics, Shiga University of Medical Science, Otsu, Shiga, Japan

4   Department of Pediatrics, Osaka Medical College, Takatsuki, Osaka, Japan

5   Department of Pediatrics, Osaka City General Hospital, Miyakojima, Osaka, Japan

6   Department of Pediatrics, Shinshu University School of Medicine, Matsumoto, Nagano, Japan

7   First Department of Internal Medicine, Kyorin University School of Medicine, Mitaka, Tokyo, Japan

8   Department of Nephrology, Nagoya University Graduate School of Medicine, Nagoya, Aichi, Japan

9   Kichijoji Asahi Hospital, Musashino, Tokyo, Japan

10   Department of Pediatrics, Graduate School of Medicine, Yokohama City University, Kanazawa, Yokohama, Japan

11   Department of Pediatric Nephrology, Tokyo Women's Medical University, Shinjuku, Tokyo, Japan

12   Department of General Internal Medicine, Faculty of Medicine, Saitama Medical University, Iruma, Saitama, Japan

13   Department of Blood Transfusion Medicine, Nara Medical University, Kashihara, Nara, Japan

Introduction

Thrombotic microangiopathy (TMA) is a pathophysiological process characterized by the triad of microangiopathic hemolytic anemia (MAHA), consumptive thrombocytopenia, and platelet-mediated microvascular occlusion, leading to organ failure. Classic forms of TMA include hemolytic uremic syndrome (HUS) and thrombotic thrombocytopenic

purpura (TTP). TMAs caused by Shiga toxin-producing *Escherichia coli* (STEC) are termed STEC-HUS, while TMAs caused by severely reduced activity (levels less than 10 % of normal) of a disintegrin-like metalloproteinase with thrombospondin type 1 repeat motifs 13 (ADAMTS13) are termed TTP.

Approximately 90 % of patients presenting with HUS symptoms have STEC infection with bloody diarrhea. The remaining 10 % do not present with diarrhea and their samples are negative for Shiga toxins; such cases were previously classified as diarrhea-negative HUS (D(-)HUS). In 1981, the first case of D(-)HUS accompanied by complement factor H (CFH) deficiency was reported [1]. Warwicker et al. suggested CFH gene mutations as a possible cause of HUS in a linkage analysis study performed in 1998 [2], one of the earliest works to propose genetic involvement in atypical HUS (aHUS). Subsequently, a series of studies indicated that aHUS pathogenesis involved genetic abnormalities of the complements, such as *C3*, complement factor B (*CFB*), complement factor I (*CFI*), membrane cofactor protein (*MCP* or *CD46*), and thrombomodulin (*THBD*). In addition, an acquired form of aHUS with positive anti-CFH antibodies has been identified.

Patients with aHUS have also been reported in Japan [3], and a series of cases prompted the Japanese Society of Nephrology and the Japan Pediatric Society to jointly develop the aHUS diagnostic criteria in 2013 [4, 5]. These criteria broadly defined aHUS as a TMA condition unrelated to STEC-HUS or TTP; thus, the definition included aHUS with complement regulation abnormality and TMA with coexisting diseases (secondary TMA; also called other TMA). However, the international consensus to exclude secondary TMAs from the definition of aHUS [6–8] suggested the need to revise the 2013 edition. This article explains the diagnosis and treatment guides for aHUS, which have incorporated diagnostic algorithms and therapeutic recommendations to assist in clinical practice.

Definitions of TMA and aHUS

Originally, TMA was used to describe pathologic conditions involving systemic microvascular thrombosis and endothelial injury. Currently, TMA also refers to the clinical conditions with the triad of MAHA, consumptive thrombocytopenia, and platelet-mediated microvascular occlusion, leading to organ failures. Common forms of TMA include TTP, STEC-HUS, complement-related aHUS, and secondary TMA. Different types of TMA cause thrombosis in preferential organs, and renal impairment is the most frequent with STEC-HUS and aHUS.

There is currently no international consensus regarding the classification of diseases under TMA. According to the definition of the aHUS diagnostic criteria jointly proposed by the Japanese Society of Nephrology and the Japan Pediatric Society in 2013, aHUS involved the triad of MAHA, thrombocytopenia, and acute kidney failure in the absence of Shiga toxins and TTP [4, 5].

Quoting the diagnostic criteria established by the UK aHUS Rare Disease Group, Scully and Goodship [7] proposed to exclude the following from aHUS: STEC-HUS, TTP, and secondary TMAs resulting from drugs, infection, transplantation, cobalamin deficiency, systemic lupus erythematosus, antiphospholipid syndrome, scleroderma, and other causes.

The definitions of aHUS and TMA have been considerably revised in the current aHUS clinical guides, based on findings reported by several publications [7–9]. Specifically, aHUS associated with congenital and acquired "complement regulation abnormality", as defined in the 2013 version, has been termed "aHUS (complement-mediated HUS)" in the current edition. In addition, TMAs arising from other causes have been defined as "secondary TMAs."

More specifically, aHUS defined in the current version relates to one of the following:

1. Congenital genetic abnormalities (known as of 2015) in seven complement component and complement regulatory genes; i.e., abnormalities in the *CFH*, *CFI*, *CD46* (*MCP*), *C3*, *CFB*, *THBD*, and diacylglycerol kinase ε (*DGKE*) genes. Note that several researchers do not regard DGKE abnormalities as a cause of aHUS because of the absence of compelling evidence of the interplay between the DGKE and complement systems. Further, plasminogen (*PLG*) gene mutations have been suggested to contribute to the etiology of aHUS, but warrant further investigation.
2. Anti-CFH autoantibody positivity (a cause of acquired aHUS).
3. Patients who have none of the genetic mutations mentioned above, but whose clinical manifestations suggest aHUS that cannot be classified as STEC-HUS, TTP, or secondary TMA.

Epidemiology

The exact incidence rates of aHUS are unknown. It is estimated that 2 per million adults and 3.3 per million children develop aHUS each year [10]. Approximately

14   Department of Nephrology, Faculty of Medicine, Saitama Medical University, Iruma, Saitama, Japan

15   Department of Pediatrics, Graduate School of Medical Sciences, Tokushima University, 3-18-15 Kuramoto-cho, Tokushima, Tokushima 770-8503, Japan

40 % of patients who are newly diagnosed with aHUS are under 18 years of age [9, 11]. A one-year prospective study conducted in the United Kingdom reported that the incidence rate was 0.4 patients per million population [12]. In Japan, current estimates suggest that 100 to 200 patients are diagnosed with aHUS.

Etiology and pathophysiology

Complement-mediated HUS is caused by dysregulation of the alternative pathway of the complement system. The genetic causes of aHUS can be divided into loss-of-function and gain-of-function mutations. Loss-of-function mutations relate to the *CFH*, *CFI*, *CD46*, and *THBD* genes. Anti-CFH antibody also results in CFH dysfunction. Gain-of-function mutations relate to the *CFB* and *C3* genes. Loss-of-function and gain-of-function mutations both cause hyperactivation of the alternative complement pathway, which in turn induces aHUS by triggering endothelial damage and platelet aggregation.

Anti-CFH autoantibodies have been detected in approximately 10 % of patients with aHUS [13]. These antibodies bind to the C-terminal domain of CFH and impair CFH-mediated cell surface protection by interfering with the interaction between CFH and its surface ligands.

Recent genetic studies of patients with TMA have identified abnormalities in the *THBD*, *DGKE*, and *PLG* encoding components of the coagulation and fibrinolytic pathways [14, 15]. However, the details of the involvement of these mutations in TMA pathogenesis remain to be clarified. While THBD is a key mediator of anticoagulant response, it also induces C3b inactivation by binding to C3b or CFH. In the current clinical guides, patients with THBD, DGKE, and PLG abnormalities are categorized as having aHUS.

Diagnosis

Clinical manifestations

According to a UK national survey, the onset of many cases of aHUS is either idiopathic or secondary to infection and other disease triggers [16]. Similar to STEC-HUS, aHUS is frequently accompanied by hemolytic anemia, thrombocytopenia, and renal failure. The clinical manifestations may also include central neuropathy, cardiac failure, respiratory disorders, enterocolitis, hypertension, and other conditions affecting multiple organs or systems. Patients with aHUS may present with ischemic enterocolitis and other gastrointestinal problems. In addition, aHUS may be precipitated by microbial or viral infections of the digestive system. Therefore, attention should be paid to the fact that the presence of diarrhea does not exclude the diagnosis of aHUS [16].

Clinical diagnostic criteria

Patients with TMA are clinically diagnosed with aHUS if the following diagnoses can be excluded: STEC-HUS, TTP, TMA secondary to metabolism-related, infection, drug-induced, autoimmune diseases, malignant tumors, hemolysis, elevated liver enzymes, and low platelets (HELLP) syndrome, transplantation, or other known causes. TMA typically, but not necessarily, involves the following conditions:

1. **MAHA with hemoglobin levels below 10 g/dL**. In addition to blood hemoglobin levels, elevation of serum lactate dehydrogenase (LDH) level, notable decrease of serum haptoglobin level, and the presence of schistocytes on a peripheral blood smear should be taken into consideration to confirm the diagnosis of MAHA. Detection of schistocytes is not a necessary criterion for diagnosis of MAHA.
2. **Thrombocytopenia with platelet counts less than 150,000/μL** [9].
3. **Acute kidney injury (AKI)**. In pediatric patients, AKI is defined as serum creatinine levels at least 1.5 times the upper limit of the age- and sex-specific pediatric reference range defined by the Japanese Society for Pediatric Nephrology [17]. For adult patients, the diagnosis of AKI should be made according to well-established diagnostic guidelines [18].

Differential diagnosis

Patients with TMA should be clinically diagnosed with aHUS after confirming that they do not meet the criteria for the following: first, STEC-HUS or TTP, and then, TMA secondary to known causative underlying conditions [7, 19]. It should be noted that some cases of secondary TMA have been reported to have complement gene mutations and anti-CFH antibodies. Future research should investigate the extent of the involvement of abnormal complement activation in the etiology of secondary TMA, the proportion of patients with complement gene mutations among the population with secondary TMA, and the effectiveness of eculizumab for treating secondary TMA.

Clinicians should strongly suspect aHUS if the patient's family history includes individuals with the following diagnoses: aHUS; HUS, TTP, or TMA in the era when aHUS was not well recognized; or renal failure of unknown cause.

1. Differentiation between TMA and similar conditions

   - **Diagnosis of hemolytic anemia and differentiation of MAHA from other forms of hemolytic anemia**. Elevated LDH level, schistocytes in blood smears, and marked decreases in haptoglobin levels are consistent with the diagnosis of hemolytic anemia. The Coombs test is helpful in diagnosing autoimmune hemolytic anemia.
   - **Differentiation between TMA and other disorders causing AKI**.
   - **Differentiation of disseminated intravascular coagulation (DIC)**. Physicians should use well-established diagnostic criteria for DIC. For this purpose, appropriate parameters should be evaluated, such as prothrombin time (PT), activated partial thromboplastin time (APTT), and fibrin degradation product (FDP), D-dimer, and fibrinogen levels. In general, DIC occurs secondary to sepsis, malignant tumors, hematologic disorders, trauma, and other underlying causes.
   - **Differentiation of pernicious anemia**. Pernicious anemia has been reported to present with clinical manifestations similar to those of TMA [20]. Measurements of vitamin B12 and folic acid levels are helpful for its identification. Patients with pernicious anemia frequently have low reticulocyte counts.
   - **Differentiation of heparin-induced thrombocytopenia (HIT)**.

2. **Differentiation of STEC-HUS**
   Results of stool culture assays, direct detection of Shiga toxins in feces, and anti-lipopolysaccharide (LPS) immunoglobulin (Ig) M antibody measurements assist the diagnosis of STEC infection. Approximately 80 % of patients with STEC-HUS have bloody diarrhea, which is often severe. Ultrasound scans typically show extreme wall thickening of the ascending colon with elevated echogenicity. In pediatric patients, STEC-HUS accounts for approximately 90 % of all TMA cases. Therefore, STEC-HUS should be primarily suspected in children aged 6 months or older presenting with severe bloody diarrhea and other common gastrointestinal complications.

3. **Differentiation of TTP**
   Patients who have less than 10 % of normal ADAMTS13 activity and are positive for anti-ADAMTS13 neutralizing antibodies (inhibitors) are diagnosed with acquired TTP. Congenital TTP is suspected if ADAMTS13 activity is less than 10 % and anti-ADAMTS13 inhibitors are not present [21]. To confirm the diagnosis of congenital TTP, *ADAMST13* gene analysis is necessary. TMAs other than TTP, such

as aHUS, HUS, and secondary TMA, are occasionally associated with decreased ADAMTS13 activity; however, in most such cases, ADAMTS13 activity does not decrease below 20 % of normal [22].

4. **Differentiation of Secondary TMA**

   - **Cobalamin C deficiency** (particularly in infants). Disorders of cobalamin metabolism are frequently detected in infants less than 12 months of age presenting with feeding problems, vomiting, poor growth, enervation, hypotonia, and convulsions. Cobalamin C deficiency has also been reported in adults in recent years. This disease presents with hyperhomocysteinemia, decreased plasma methionine levels, and methylmalonic aciduria [23].
   - **Autoimmune diseases and connective tissue diseases**, in particular, systemic lupus erythematosus, scleroderma renal crisis, antiphospholipid syndrome, multiple myositis/dermatomyositis, and vasculitis. These disorders often present with signs and symptoms similar to TMA. The following assessments should be conducted, as appropriate: antinuclear antibodies, antiphospholipid antibodies, anti-DNA antibodies, anti-centromere antibodies, anti-Scl-70 antibodies, C3, C4, CH50, immunoglobulin (Ig)G, IgA, IgM, and anti-neutrophil cytoplasmic antibodies (ANCA).
   - **Accelerated or malignant hypertension**. Patients with accelerated or malignant hypertension often present with TMA. Patients with aHUS sometimes present with accelerated or malignant hypertension; thus, when TMA persists after treatment of hypertension, efforts should be made to differentiate aHUS from these disorders.
   - **Malignant tumors**. Advanced malignant tumors often cause TMA. In a review of cancer-related TMA cases reported in the literature, more than 90 % had advanced cancers, including tumors of the gastrointestinal tract, breast, prostate, and lung [24].
   - **Infections**. Pneumococcal infections, particularly invasive pneumococcal infections, cause TMA mostly in children. Therapeutic plasma exchange may aggravate the condition. Approximately 90 % of patients with pneumococcus-associated HUS have positive direct Coombs test results [25]. In addition to pneumococcal infection, infections with human immunodeficiency virus (HIV), influenza A H1N1 virus, hepatitis C virus, and cytomegalovirus, as well as pertussis, varicella, and severe streptococcal infection, have been reported to cause TMA [16, 26, 27]. Attention should be paid to the

cases where infections with influenza virus and other infections often trigger the onset of aHUS [28].

- **Pregnancy-induced HELLP syndrome and eclampsia**. HELLP syndrome and eclampsia usually resolve quickly after delivery. However, cases of TTP and aHUS triggered by pregnancy have been reported in the literature. In a cohort study, patients with aHUS developed HELLP syndrome primarily postpartum [29]; however, the incidence of aHUS among patients with HELLP syndrome or postpartum HELLP syndrome is unknown.
- **Drug-induced TMA**. Anti-tumor agents, anti-platelet drugs, immunosuppressive agents, and other medications may cause TMA (Table 1) [30]. Agents suspected of causing TMA should be tapered or discontinued wherever possible.
- **Acute pancreatitis**. Acute pancreatitis is a possible or probable precipitating event for TMA episodes [31]. In a review of seven cases of TMA precipitated by acute pancreatitis, patients responded well to therapeutic plasma exchange [32].
- **Post-transplant TMA subsequent to hematopoietic stem cell or organ transplantation**. Post-transplant TMA following hematopoietic stem cell transplantation has been widely documented. In patients with post-transplant TMA, ADAMTS13 activities usually do not fall below 10 % of normal, and plasma exchange is not very effective. Typical interventions include discontinuation or dose reduction of immunosuppressive calcineurin inhibitors [33]. Recent research revealed a high prevalence of anti-CFH autoantibodies in pediatric patients with hematopoietic stem cell transplant-associated TMA [34]; however, the involvement of complement dysregulation in the pathogenesis of TMA following hematopoietic stem cell transplant requires further investigation.

Patients with end-stage renal disease due to aHUS who are undergoing kidney transplant are at high risk of TMA recurrence and graft loss. It is therefore advisable to conduct genetic testing preoperatively in prospective kidney recipients suspected of having aHUS. TMAs occurring subsequent to kidney transplant (*de novo*) involve new onset of aHUS, with complement abnormalities [35], as well as transplant-induced TMA [30]. The clinical approaches for patients with aHUS undergoing kidney transplantation and TMA after kidney transplantation are beyond the scope of this guide; please see the current consensus [8]. The occurrence of TMA has been documented not only in patients with kidney transplants, but in those receiving liver, heart, lung, and small intestine transplants [36].

Considerations concerning pediatric diagnosis

STEC-HUS should primarily be suspected in children with TMA aged 6 months or older who manifest severe bloody diarrhea, because STEC-HUS accounts for approximately 90 % of all pediatric TMA cases. Conditions that predispose pediatric patients to TMA, not accompanied by diarrhea or bloody stool include pneumococcal and other infections in infants, and systemic lupus erythematosus and antiphospholipid syndrome. When a pediatric patient is diagnosed with TMA, the physician should immediately examine the possibility of TTP and determine whether existing medical conditions or oral medications are causing TMA. If these possibilities are ruled out, the physician should initiate eculizumab therapy while continuing to investigate whether rarer etiologies are responsible for TMA.

Laboratory confirmation of aHUS diagnosis

Besides the laboratory data supporting the diagnosis of TMA mentioned above, low C3 and normal C4 levels strongly suggest activation of the alternative pathway, and hence aHUS. However, previous data show that low C3 levels are detected in approximately half of patients with aHUS, and normal C3 levels do not necessarily rule out its diagnosis. To establish a diagnosis of aHUS, several studies recommend analyses of CFH, CFI, and CFB levels, and leukocyte expression levels of CD46 in addition to routine blood C3 and C4 measurements. However, the levels of these alternative complement molecules do not necessarily lead to the diagnosis of aHUS [6]. Quantitative hemolytic assay protocols using sheep erythrocytes are highly sensitive methods for detecting patients with genetic CFH abnormalities and anti-CFH antibodies [37, 38]. However, these protocols are still not practical for use in routine clinical settings. Urological examination in many patients with aHUS shows hematuria and proteinuria.

Confirmatory diagnosis of aHUS requires genetic testing for known causative genes and analysis of anti-CFH antibodies. However, the absence of causative genetic mutations does not always exclude the diagnosis of aHUS, because approximately 40 % of patients show no known genetic abnormalities.

Physicians caring for patients with suspected aHUS in Japan are advised to contact the Division of Nephrology and Endocrinology, University of Tokyo Hospital (ahus-office@umin.ac.jp), which will conduct hemolytic assay, anti-CFH antibody screening and genetic assays in

Table 1 Examples of medications that may cause TMA (adopted from References [9, 30])

Antiplatelets	Ticlopidine, clopidogrel
Antibacterials	Quinine
Antivirals	Valacyclovir
Interferons	
Antitumor agents	Mitomycin C, gemcitabine, cisplatin, vascular endothelial growth factor (VEGF) inhibitors, tyrosine kinase inhibitors
Immunosuppressants	Cyclosporin, tacrolimus, sirolimus
Oral contraceptives	

collaboration with the National Cerebral and Cardiovascular Center, Research Institute, Osaka, Japan. These researches are supported as the government-subsidized program, "Observational Study of Atypical Hemolytic Uremic Syndrome in Japan".

Treatments

Therapeutic considerations

Since the 1980s, plasma exchange therapy has been the mainstay method for management of aHUS. This therapy aims to eliminate abnormal complement regulatory proteins and anti-CFH antibodies, while supplementing normal complement regulatory proteins. Eculizumab is a humanized monoclonal antibody that binds to C5 complement protein. Eculizumab suppresses C5 cleavage to C5a and C5b and thereby prevents the production of the membrane attack complement complex (MAC).

In practical terms, when a patient presents with TMA and is negative for STEC-HUS and invasive pneumococcal infection (the latter of which is not indicated for plasma exchange), the treating physician should start the empirical treatments described below, while continuing diagnostic efforts. Physicians should also pay attention to systemic management such as fluid and electrolyte control, blood pressure control, and supportive therapies for AKI.

If the physician considers plasma exchange appropriate, it should be started immediately. Daily sessions followed by gradual tapering of the plasma therapy are recommended. Plasma infusion may be implemented in pediatric patients in whom plasma exchange is technically difficult to perform, as well as in situations where plasma exchange cannot be performed. The tapering of the plasma therapy will generally be based on improvements in platelet count, LDH and hemoglobin levels [39]. Although plasma infusion and plasma exchange can achieve hematological remission in approximately 70 % of patients with aHUS, long-term outcomes include high incidences of TMA recurrence, progression to end-stage renal failure, and death [40].

If the patient is clinically diagnosed with aHUS after STEC-HUS, and if TTP and secondary TMA are ruled out, the physician should consider eculizumab therapy [7]. Eculizumab is recommended in the early stages of treatment of pediatric patients with clinically diagnosed aHUS because pediatric patients have a lower incidence of secondary TMA than adults and a higher rate of complications related to catheterization for plasma exchange and plasma infusion [8].

Decreased platelet counts observed in patients with aHUS usually resolve after 1 to 2 weeks of eculizumab therapy [41–43].

In anti-CFH antibody-positive patients, plasma exchange combined with immunosuppressants or steroids, as compared to plasma exchange alone, yielded better outcomes with reduced antibody titers [11]. Eculizumab may be considered for treating aHUS accompanied by extra-renal organ injury [8].

Warnings and precautions for eculizumab use

Eculizumab has been shown to elevate the risk of meningococcal infection, and patients should be immunized with meningococcal vaccine at least two weeks prior to receiving eculizumab. If situations require immediate eculizumab administration in a patient who has not been immunized with meningococcal vaccine, the physician must administer appropriate prophylactic antibiotics.

Discontinuation of eculizumab

No expert consensus has been reached regarding the timing of eculizumab withdrawal after achievement of remission.

One study reviewed 20 cases of aHUS involving eculizumab therapy discontinuation [8]. Patients with *CFH* mutations and anti-CFH antibody-positive patients had a higher rate of recurrence. However, among patients with *CD46* or *CFI* mutations and those without known causative genes, no recurrence was observed during the study period. In a similar review of 24 patients who terminated eculizumab therapy [44], the incidence rate was 25 %, and

recurrences were noted more frequently in patients with *CFH* mutation and those positive for anti-CFH antibodies.

Available vaccines are insufficient for completely preventing meningococcal and other types of infections in patients receiving eculizumab. Eculizumab therapy requires patients to visit the hospital once every two weeks, a requirement that considerably affects their quality of life. Long-term repeated intravenous administration often leads to compromised vascular access. In addition, cost-benefit analyses should be considered for eculizumab, one of the most expensive drugs on the market. Future research on the relationship between genetic mutations and treatment outcomes, and markers for early detection of recurrence, will shed light on ways of overcoming these problems [8, 44].

Outcome

The literature has reported gene-specific differences in response to therapeutic plasma exchange and in graft survival after kidney transplant [11]. While eculizumab therapy has been shown to improve treatment outcomes, its gene-specific outcomes are not well known.

References

1. Thompson RA, Winterborn MH. Hypocomplementaemia due to a genetic deficiency of beta 1H globulin. Clin Exp Immunol. 1981;46(1):110–9.
2. Warwicker P, Goodship TH, Donne RL, Pirson Y, Nicholls A, Ward RM, et al. Genetic studies into inherited and sporadic hemolytic uremic syndrome. Kidney Int. 1998;53(4):836–44. doi:10.1111/j.1523-1755.1998.00824.x.
3. Mukai S, Hidaka Y, Hirota-Kawadobora M, Matsuda K, Fujihara N, Takezawa Y, et al. Factor H gene variants in Japanese: its relation to atypical hemolytic uremic syndrome. Mol Immunol. 2011;49(1–2):48–55. doi:10.1016/j.molimm.2011.07.017.
4. Sawai T, Nangaku M, Ashida A, Fujimaru R, Hataya H, Hidaka Y, et al. Diagnostic criteria for atypical hemolytic uremic syndrome proposed by the Joint Committee of the Japanese Society of Nephrology and the Japan Pediatric Society. Clin Exp Nephrol. 2014;18(1):4–9. doi:10.1007/s10157-013-0911-8.
5. Sawai T, Nangaku M, Ashida A, Fujimaru R, Hataya H, Hidaka Y, et al. Diagnostic criteria for atypical hemolytic uremic syndrome proposed by the Joint Committee of the Japanese Society of Nephrology and the Japan Pediatric Society. Pediatr Int. 2014;56(1):1–5. doi:10.1111/ped.12274.
6. Loirat C, Fremeaux-Bacchi V. Atypical hemolytic uremic syndrome. Orphanet J Rare Dis. 2011;6:60. doi:10.1186/1750-1172-6-60.
7. Scully M, Goodship T. How I treat thrombotic thrombocytopenic purpura and atypical haemolytic uraemic syndrome. Br J Haematol. 2014;164(6):759–66. doi:10.1111/bjh.12718.
8. Loirat C, Fakhouri F, Ariceta G, Besbas N, Bitzan M, Bjerre A, et al. An international consensus approach to the management of atypical hemolytic uremic syndrome in children. Pediatr Nephrol. 2016;31(1):15–39. doi:10.1007/s00467-015-3076-8.
9. Campistol JM, Arias M, Ariceta G, Blasco M, Espinosa M, Grinyo JM, et al. An update for atypical haemolytic uraemic syndrome: diagnosis and treatment. A consensus document. Nefrologia. 2013;33(1):27–45. doi:10.3265/Nefrologia.pre2012.Nov.11781.
10. Mele C, Remuzzi G, Noris M. Hemolytic uremic syndrome. Semin Immunopathol. 2014;36(4):399–420. doi:10.1007/s00281-014-0416-x.
11. Fremeaux-Bacchi V, Fakhouri F, Garnier A, Bienaime F, Dragon-Durey MA, Ngo S, et al. Genetics and outcome of atypical hemolytic uremic syndrome: a nationwide French series comparing children and adults. Clin J Am Soc Nephrol. 2013;8(4):554–62. doi:10.2215/CJN.04760512.
12. Sheerin NS, Kavanagh D, Goodship TH, Johnson S. A national specialized service in England for atypical haemolytic uraemic syndrome-the first year's experience. QJM. 2015;109(1):27–33. doi:10.1093/qjmed/hcv082.
13. Hofer J, Janecke AR, Zimmerhackl LB, Riedl M, Rosales A, Giner T, et al. Complement factor H-related protein 1 deficiency and factor H antibodies in pediatric patients with atypical hemolytic uremic syndrome. Clin J Am Soc Nephrol. 2013;8(3):407–15. doi:10.2215/CJN.01260212.
14. Lemaire M, Fremeaux-Bacchi V, Schaefer F, Choi M, Tang WH, Le Quintrec M, et al. Recessive mutations in DGKE cause atypical hemolytic-uremic syndrome. Nat Genet. 2013;45(5):531–6. doi:10.1038/ng.2590.
15. Bu F, Maga T, Meyer NC, Wang K, Thomas CP, Nester CM, et al. Comprehensive genetic analysis of complement and

coagulation genes in atypical hemolytic uremic syndrome. J Am Soc Nephrol. 2014;25(1):55–64. doi:10.1681/ASN.2013050453.

16. Johnson S, Stojanovic J, Ariceta G, Bitzan M, Besbas N, Frieling M, et al. An audit analysis of a guideline for the investigation and initial therapy of diarrhea negative (atypical) hemolytic uremic syndrome. Pediatr Nephrol. 2014;29(10):1967–78. doi:10.1007/s00467-014-2817-4.

17. Uemura O, Honda M, Matsuyama T, Ishikura K, Hataya H, Yata N, et al. Age, gender, and body length effects on reference serum creatinine levels determined by an enzymatic method in Japanese children: a multicenter study. Clin Exp Nephrol. 2011;15(5):694–9. doi:10.1007/s10157-011-0452-y.

18. KDIGO. Clinical practice guideline for acute kidney injury. Kidney Int Suppl. 2012;2:1–138.

19. Kato H, Yoshida Y, Nangaku M. Pathogenesis of complement-mediated and coagulation-mediated atypical hemolytic uremic syndrome. Nihon Jinzo Gakkai Shi. 2014;56(7):1058–66.

20. Tadakamalla AK, Talluri SK, Besur S. Pseudo-thrombotic thrombocytopenic purpura: a rare presentation of pernicious anemia. N Am J Med Sci. 2011;3(10):472–4. doi:10.4297/najms.2011.3472.

21. Fujimura Y, Isonishi A. Pathophysiology of thrombotic thrombocytopenic purpura. Nihon Jinzo Gakkai Shi. 2014;56(7):1043–51.

22. Shah N, Rutherford C, Matevosyan K, Shen YM, Sarode R. Role of ADAMTS13 in the management of thrombotic microangiopathies including thrombotic thrombocytopenic purpura (TTP). Br J Haematol. 2013;163(4):514–9. doi:10.1111/bjh.12569.

23. Hattori M. Pathogenesis and clinical features of HUS and aHUS. Nihon Jinzo Gakkai Shi. 2014;56(7):1052–7.

24. Lechner K, Obermeier HL. Cancer-related microangiopathic hemolytic anemia: clinical and laboratory features in 168 reported cases. Medicine (Baltimore). 2012;91(4):195–205. doi:10.1097/MD.0b013e3182603598.

25. von Vigier RO, Seibel K, Bianchetti MG. Positive Coombs test in pneumococcus-associated hemolytic uremic syndrome. A review of the literature. Nephron. 1999;82(2):183–4.

26. Allen U, Licht C. Pandemic H1N1 influenza A infection and (atypical) HUS–more than just another trigger? Pediatr Nephrol. 2011;26(1):3–5. doi:10.1007/s00467-010-1690-z.

27. Shimizu M, Yokoyama T, Sakashita N, Sato A, Ueno K, Akita C, et al. Thomsen-Friedenreich antigen exposure as a cause of Streptococcus pyogenes-associated hemolytic-uremic syndrome. Clin Nephrol. 2012;78(4):328–31.

28. Fan X, Yoshida Y, Honda S, Matsumoto M, Sawada Y, Hattori M, et al. Analysis of genetic and predisposing factors in Japanese patients with atypical hemolytic uremic syndrome. Mol Immunol. 2013;54(2):238–46. doi:10.1016/j.molimm.2012.12.006.

29. Fakhouri F, Roumenina L, Provot F, Sallee M, Caillard S, Couzi L, et al. Pregnancy-associated hemolytic uremic syndrome revisited in the era of complement gene mutations. J Am Soc Nephrol. 2010;21(5):859–67. doi:10.1681/ASN.2009070706.

30. Matsui K, Yasuda T. Drug/transplant-induced atypical hemolytic uremic syndrome. Nihon Jinzo Gakkai Shi. 2014;56(7):1067–74.

31. Swisher KK, Doan JT, Vesely SK, Kwaan HC, Kim B, Lammle B, et al. Pancreatitis preceding acute episodes of thrombotic thrombocytopenic purpura-hemolytic uremic syndrome: report of five patients with a systematic review of published reports. Haematologica. 2007;92(7):936–43.

32. McDonald V, Laffan M, Benjamin S, Bevan D, Machin S, Scully MA. Thrombotic thrombocytopenic purpura precipitated by acute pancreatitis: a report of seven cases from a regional UK TTP registry. Br J Haematol. 2009;144(3):430–3. doi:10.1111/j.1365-2141.2008.07458.x.

33. Matsumoto M. Pathophysiology and management of transplantation associated TMA. Rinsho Ketsueki. 2013;54(10):1958–65.

34. Jodele S, Licht C, Goebel J, Dixon BP, Zhang K, Sivakumaran TA, et al. Abnormalities in the alternative pathway of complement in children with hematopoietic stem cell transplant-associated thrombotic microangiopathy. Blood. 2013;122(12):2003–7. doi:10.1182/blood-2013-05-501445.

35. Le Quintrec M, Lionet A, Kamar N, Karras A, Barbier S, Buchler M, et al. Complement mutation-associated de novo thrombotic microangiopathy following kidney transplantation. Am J Transplant. 2008;8(8):1694–701. doi:10.1111/j.1600-6143.2008.02297.x.

36. Verbiest A, Pirenne J, Dierickx D. De novo thrombotic microangiopathy after non-renal solid organ transplantation. Blood Rev. 2014;28(6):269–79. doi:10.1016/j.blre.2014.09.001.

37. Roumenina LT, Roquigny R, Blanc C, Poulain N, Ngo S, Dragon-Durey MA, et al. Functional evaluation of factor H genetic and acquired abnormalities: application for atypical hemolytic uremic syndrome (aHUS). Methods Mol Biol. 2014;1100:237–47. doi:10.1007/978-1-62703-724-2_19.

38. Yoshida Y, Miyata T, Matsumoto M, Shirotani-Ikejima H, Uchida Y, Ohyama Y, et al. A novel quantitative hemolytic assay coupled with restriction fragment length polymorphisms analysis enabled early diagnosis of atypical hemolytic uremic syndrome and identified unique predisposing mutations in Japan. PLoS One. 2015;10(5):e0124655. doi:10.1371/journal.pone.0124655.

39. Sakai N, Wada T. Therapeutic strategy and thrombotic microangiopathy. Nihon Jinzo Gakkai Shi. 2014;56(7):1082–9.

40. Noris M, Caprioli J, Bresin E, Mossali C, Pianetti G, Gamba S, et al. Relative role of genetic complement abnormalities in sporadic and familial aHUS and their impact on clinical phenotype. Clin J Am Soc Nephrol. 2010;5(10):1844–59. doi:10.2215/CJN.02210310.

41. Legendre CM, Licht C, Muus P, Greenbaum LA, Babu S, Bedrosian C, et al. Terminal complement inhibitor eculizumab in atypical hemolytic-uremic syndrome. N Engl J Med. 2013;368(23):2169–81. doi:10.1056/NEJMoa1208981.

42. Licht C, Greenbaum LA, Muus P, Babu S, Bedrosian CL, Cohen DJ, et al. Efficacy and safety of eculizumab in atypical hemolytic uremic syndrome from 2-year extensions of phase 2 studies. Kidney Int. 2015;87(5):1061–73. doi:10.1038/ki.2014.423.

43. Ito N, Hataya H, Saida K, Amano Y, Hidaka Y, Motoyoshi Y, et al. Efficacy and safety of eculizumab in childhood atypical hemolytic uremic syndrome in Japan. Clin Exp Nephrol. 2015;20(2):265–72. doi:10.1007/s10157-015-1142-y.

44. Nester CM. Managing atypical hemolytic uremic syndrome: chapter 2. Kidney Int. 2015;87(5):882–4. doi:10.1038/ki.2015.60.

SCIENTIFIC REP🞉RTS

OPEN

Hyperuricemia in acute gastroenteritis is caused by decreased urate excretion *via* ABCG2

Hirotaka Matsuo[1,*], Tomoyuki Tsunoda[2,*], Keiko Ooyama[3,*], Masayuki Sakiyama[1,4,*], Tsuyoshi Sogo[2], Tappei Takada[5], Akio Nakashima[6], Akiyoshi Nakayama[1], Makoto Kawaguchi[1,7], Toshihide Higashino[1], Kenji Wakai[8], Hiroshi Ooyama[3], Ryota Hokari[9], Hiroshi Suzuki[5], Kimiyoshi Ichida[6,10], Ayano Inui[2], Shin Fujimori[11] & Nariyoshi Shinomiya[1]

To clarify the physiological and pathophysiological roles of intestinal urate excretion *via* ABCG2 in humans, we genotyped *ABCG2* dysfunctional common variants, Q126X (rs72552713) and Q141K (rs2231142), in end-stage renal disease (hemodialysis) and acute gastroenteritis patients, respectively. ABCG2 dysfunction markedly increased serum uric acid (SUA) levels in 106 hemodialysis patients ($P = 1.1 \times 10^{-4}$), which demonstrated the physiological role of ABCG2 for intestinal urate excretion because their urate excretion almost depends on intestinal excretion *via* ABCG2. Also, ABCG2 dysfunction significantly elevated SUA in 67 acute gastroenteritis patients ($P = 6.3 \times 10^{-3}$) regardless of the degree of dehydration, which demonstrated the pathophysiological role of ABCG2 in acute gastroenteritis. These findings for the first time show ABCG2-mediated intestinal urate excretion in humans, and indicates the physiological and pathophysiological importance of intestinal epithelium as an excretion pathway besides an absorption pathway. Furthermore, increased SUA could be a useful marker not only for dehydration but also epithelial impairment of intestine.

Hyperuricemia is a common disease which induces gout, and can lead to renal disorder, hypertension, cardiovascular or cerebrovascular diseases[1]. ATP-binding cassette transporter, subfamily G, member 2 (*ABCG2/BCRP*) is a high-capacity urate transporter[2] and expresses in both intestine[3] and kidney[4]. We and others previously demonstrated that ABCG2 dysfunction by its common variants causes gout[2,5,6] and hyperuricemia[2,7] by decreasing urate excretion. However, the evaluation of intestinal urate excretion in humans is very difficult due to urate degradation by intestinal bacterial flora. Thus, our previous study[8] has revealed the importance of ABCG2 for intestinal urate excretion using *Abcg2*-knockout mice, but not in humans. In this study, to clarify the physiological role of intestinal urate excretion *via* ABCG2 in humans, we performed genotyping of *ABCG2* dysfunctional variants in end-stage renal disease (hemodialysis) patients whose serum uric acid (SUA) levels are extremely elevated[9,10] and urate excretion almost depends on intestinal excretion *via* ABCG2 because of their almost complete absence of renal urate excretion. Furthermore, to investigate the pathophysiological role of intestinal urate excretion *via*

[1]Department of Integrative Physiology and Bio-Nano Medicine, National Defense Medical College, Tokorozawa, Saitama 359-8513, Japan. [2]Department of Pediatric Hepatology and Gastroenterology, Saiseikai Yokohamashi Tobu Hospital, Yokohama, Kanagawa 230-0012, Japan. [3]Ryougoku East Gate Clinic, Sumida-ku, Tokyo 130-0026, Japan. [4]Department of Dermatology, National Defense Medical College, Tokorozawa, Saitama 359-8513, Japan. [5]Department of Pharmacy, The University of Tokyo Hospital, Bunkyo-ku, Tokyo 113-8655, Japan. [6]Division of Kidney and Hypertension, Department of Internal Medicine, Jikei University School of Medicine, Minato-ku, Tokyo 105-8471, Japan. [7]Department of Urology, National Defense Medical College, Tokorozawa, Saitama 359-8513, Japan. [8]Department of Preventive Medicine, Nagoya University Graduate School of Medicine, Nagoya, Aichi 461-8673, Japan. [9]Department of Internal Medicine, National Defense Medical College, Tokorozawa, Saitama 359-8513, Japan. [10]Department of Pathophysiology, Tokyo University of Pharmacy and Life Sciences, Hachioji, Tokyo 192-0392, Japan. [11]Department of Internal Medicine, Teikyo University School of Medicine, Itabashi-ku, Tokyo 173-8605, Japan. *These authors contributed equally to this work. Correspondence and requests for materials should be addressed to H.M. (email: hmatsuo@ndmc.ac.jp)

Estimated ABCG2 function	Rs72552713 (Q126X)	Rs2231142 (Q141K)	Diplotype*	Number of participants		
				Hemodialysis	Health examination[†]	Acute gastroenteritis
Full function	C/C	C/C	*1/*1	51	50	29
3/4 function	C/C	C/A	*1/*2	46	41	30
1/2 function	C/C	A/A	*2/*2	4	8	7
	C/T	C/C	*1/*3	3	5	1
≤1/4 function	C/T	A/C	*2/*3	2	2	0
	T/T	C/C	*3/*3	0	0	0
Total				106	106	67

Table 1. Genotyping results for each estimated ABCG2 function of participants. **1, *2 and *3 represent haplotypes "C-C" (126Q and 141Q), "C-A" (126Q and 141K) and "T-C" (126X and 141Q) of two dysfunctional variants, Q126X (rs72552713) and Q141K (rs2231142), respectively. [†]106 health examination participants were matched for sex- and body-mass index to 106 hemodialysis patients and selected from J-MICC Study.

Estimated ABCG2 function (Diplotype of Q126X and Q141K)*	Hemodialysis						Acute gastroenteritis					
	Case			Control[†]			Acute period			Recovery period		
	N	SUA (mg/dl)	β (SEM)[‡] P value[§]	N	SUA (mg/dl)	β (SEM)[‡] P value[§]	N	SUA (mg/dl)	β (SEM)[‡] P value[‖]	N	SUA (mg/dl)	β (SEM)[‡] P value[‖]
Full function (*1/*1)	51	7.1 ± 0.1		50	5.3 ± 0.2		29	7.5 ± 0.5		24	4.2 ± 0.3	
3/4 function (*1/*2)	46	7.9 ± 0.1		41	5.0 ± 0.2		30	9.6 ± 0.7		24	4.9 ± 0.4	
≤1/2 function (*1/*3, *2/*2, *2/*3 or *3/*3)	9	8.4 ± 0.7		15	6.0 ± 0.3		8	10.6 ± 1.4		7	5.4 ± 0.6	
Total	106	7.5 ± 0.1	0.63 (0.16) $P = 1.1 \times 10^{-4}$	106	5.3 ± 0.1	0.17 (0.18) $P = 0.36$	67	8.8 ± 0.4	1.73 (0.61) $P = 6.3 \times 10^{-3}$	55	4.7 ± 0.2	0.60 (0.36) $P = 0.10$

Table 2. Estimated ABCG2 function and SUA of hemodialysis patients and acute gastroenteritis patients. N, number; SUA, serum uric acid. Plus-minus values are means ± SEM. **1, *2 and *3 represent haplotypes of two dysfunctional variants (Q126X and Q141K) as previously reported. Detailed information on *ABCG2* haplotypes is also shown in Table 1. [†]106 controls were matched for sex- and body-mass index to 106 hemodialysis patients and selected from health examination participants in J-MICC Study. [‡]β means regression coefficient. [§]*P* values were obtained by multiple regression analysis including ABCG2 function and age in the model. [‖]*P* values were obtained by linear regression analysis.

ABCG2 in intestinal diseases, we also performed genotyping of *ABCG2* dysfunctional variants in acute gastroenteritis patients whose ABCG2 function of intestinal urate excretion should be seriously impaired due to damage to the intestinal epithelium.

Results
Genotyping of *ABCG2*.
Genotyping results of the two *ABCG2* dysfunctional variants, Q126X (rs72552713) and Q141K (rs2231142), for 106 hemodialysis patients, 106 sex- and body mass index (BMI)-matched health examination participants and 67 acute gastroenteritis patients, were shown in Table 1. The call rates for both variants were 100%, and they were in Hardy-Weinberg equilibrium ($P > 0.05$). Haplotype frequency of Q126X and Q141K was estimated as shown in Supplementary Table 1. This result indicates that there is no simultaneous presence of the minor allele of Q126X ("T" allele) and Q141K ("A" allele) in one haplotype, which is consistent with our previous study[2]. Therefore, we presumed the diplotypes of all samples as shown in Table 1. In this study, all of the participants were divided into three groups (full function, 3/4 function and ≤1/2 function) based on estimated ABCG2 function for the following analyses.

Analysis of hemodialysis patients.
The estimated ABCG2 function of 106 hemodialysis patients and the mean SUA for each group were shown in Table 2. The less activity the ABCG2 function showed the higher the SUA (7.1 mg/dl for full function, 7.9 mg/dl for 3/4 function and 8.4 mg/dl for ≤1/2 function), and multiple regression analysis revealed that ABCG2 dysfunction significantly elevated SUA ($P = 1.1 \times 10^{-4}$). On the other hand, in 106 sex- and BMI-matched health examination participants, ABCG2 dysfunction tended to elevate SUA (5.3 mg/dl for full function, 5.0 mg/dl for 3/4 function and 6.0 mg/dl for ≤1/2 function), although not significantly ($P = 0.36$, Table 2).

Analysis of acute gastroenteritis patients.
The SUA levels of 67 patients were measured during an acute period of gastroenteritis. Additionally, the SUA levels of 55 patients were measured during the recovery period from gastroenteritis. The mean SUA levels of the acute and recovery period (Table 2) were 8.8 mg/dl and 4.7 mg/dl, respectively, and the paired *t*-test showed a significant difference between them ($P = 2.3 \times 10^{-12}$). The number of patients, who were divided into three groups by estimated ABCG2 function, and the mean SUA levels at the

Estimated ABCG2 function (Diplotype of Q126X and Q141K)[*]	Number			P value[‡]
	Acute gastroenteritis	Dehydration[†]		
		−	+	
Full function (*1/*1)	29	23	6	
3/4 function (*1/*2)	30	20	10	
≤1/2 function (*1/*3, *2/*2, *2/*3 or *3/*3)	8	6	2	
Total	67	49	18	0.50

Table 3. Dehydration in acute gastroenteritis patients for each ABCG2 function. **1, *2 and *3 represent haplotypes of two dysfunctional variants (Q126X and Q141K). Detailed information on *ABCG2* haplotypes is also shown in Table 1. [†]"−" means minimal or no dehydration and "+" means mild to moderate or severe dehydration evaluated according to the criteria recommended by the Center for Disease Control (CDC). [‡]*P* values were obtained by Cochran-Armitage test.

acute and recovery period of gastroenteritis were shown in Table 2. In the acute period, ABCG2 dysfunction significantly elevated SUA (7.5 mg/dl for full function, 9.6 mg/dl for 3/4 function and 10.6 mg/dl for ≤1/2 function, $P = 6.3 \times 10^{-3}$), and the degree of dehydration also affected SUA ($P = 1.6 \times 10^{-3}$, Supplementary Table 2). However, ABCG2 dysfunction was not associated with the degree of dehydration in the acute period ($P = 0.50$, Table 3) and the significant association between ABCG2 dysfunction and SUA remained after the adjustment for the degree of dehydration ($P = 7.8 \times 10^{-3}$), indicating that the association between ABCG2 dysfunction and SUA was not due to dehydration. Regarding the recovery period, there was a trend for SUA to increase by ABCG2 dysfunction (4.2 mg/dl for full function, 4.9 mg/dl for 3/4 function and 5.4 mg/dl for ≤1/2 function, Table 2), but it was not significant ($P = 0.10$).

Discussion

ABCG2, which mediates urate excretion, expresses in both intestine[3] and kidney[4]. About two-thirds of urate is excreted from kidney and about one-third from intestine[11,12]. This is consistent with our previous study using *Abcg2*-knockout mice[8]. However, ABCG2-mediated intestinal urate excretion has not been directly shown by human study. In end-stage renal disease (hemodialysis) patients whose SUA levels are extremely elevated[9,10], renal urate excretion is nearly completely absent, and almost all urate excretion must depend on intestinal excretion *via* ABCG2. Thus, it was supposed that the degree of intestinal ABCG2 dysfunction strongly affects the severity of hyperuricemia in hemodialysis patients (Fig. 1), as was shown by multiple regression analysis in the present study (Table 2). This finding is the first evidence for a physiological role of ABCG2 on intestinal urate excretion in humans.

Besides the physiological role for intestinal urate excretion *via* ABCG2 in humans, we for the first time demonstrated that hyperuricemia in acute gastroenteritis patients is caused by decreased urate excretion in addition to dehydration which is generally considered to be a major cause of hyperuricemia in acute gastroenteritis patients[13]. Pathogens which cause acute gastroenteritis, such as rotaviruses, primarily infect the villus epithelium of the small intestine[14–17]. These viruses induce the destruction of infected intestinal epithelial cells, but they also mediate the down-regulation of the expression of absorptive enzymes, transporters and cytokines, which instigate malabsorption of D-xylose, lipid or lactose[14,17,18]. In acute gastroenteritis patients, intestinal inflammation would also seriously impair the function of intestinal urate excretion of ABCG2, which could be one of the reasons why SUA is markedly increased in acute gastroenteritis patients. Therefore, it is clearly possible that the degree of renal ABCG2 dysfunction affects the severity of hyperuricemia in gastroenteritis patients (Fig. 1), as was first shown by linear regression analysis in acute period gastroenteritis patients in the present study (Table 2).

The evaluation of intestinal urate excretion in humans is very difficult because urate excreted into the intestinal lumen is rapidly metabolized by bacterial flora. Thus, our previous study[8] could reveal the importance of ABCG2 for intestinal urate excretion not using human, but rather *Abcg2*-knockout mice treated with oxonate, an uricase inhibitor. In addition, another study has also reported the decreased intestinal excretion and increased plasma concentration of uric acid in *Abcg2*-knockout mice[19].

Taking into account the results from both hemodialysis and acute gastroenteritis patients in the present study, we for the first time demonstrated that ABCG2 mediates intestinal urate excretion in humans, which suggests the physiological importance of intestinal epithelium as an excretion pathway besides an absorption pathway. In addition, if an end-stage renal disease patient develops acute gastroenteritis, both renal and intestinal urate excretion *via* ABCG2 will extremely decrease, and thereby greatly elevate SUA.

In light of these findings, although further studies would be necessary because of the limited sample size in this study, we proposed a physiological model of urate excretion *via* ABCG2 in humans, and a pathophysiological model of hyperuricemia in intestinal and renal diseases (Fig. 1). Physiologically, ABCG2 mediates urate excretion in both intestine and kidney in humans. Pathophysiologically, in end-stage renal disease patients, the degree of intestinal ABCG2 dysfunction strongly affects the severity of hyperuricemia because urate excretion almost all depends on intestinal excretion *via* ABCG2. Contrarily, in acute gastroenteritis patients, the function of intestinal urate excretion *via* ABCG2 is severely impaired. Therefore, the degree of renal ABCG2 dysfunction clearly affects the severity of hyperuricemia. By this proposed model, physicians will recognize that increased SUA levels could be a useful marker not only for dehydration but also for intestinal impairment which induces urate export failure in intestines. Physicians could also consider "the urate excretion failure due to intestinal impairment" as one of the common causes of hyperuricemia which is often complicated in patients with acute gastroenteritis.
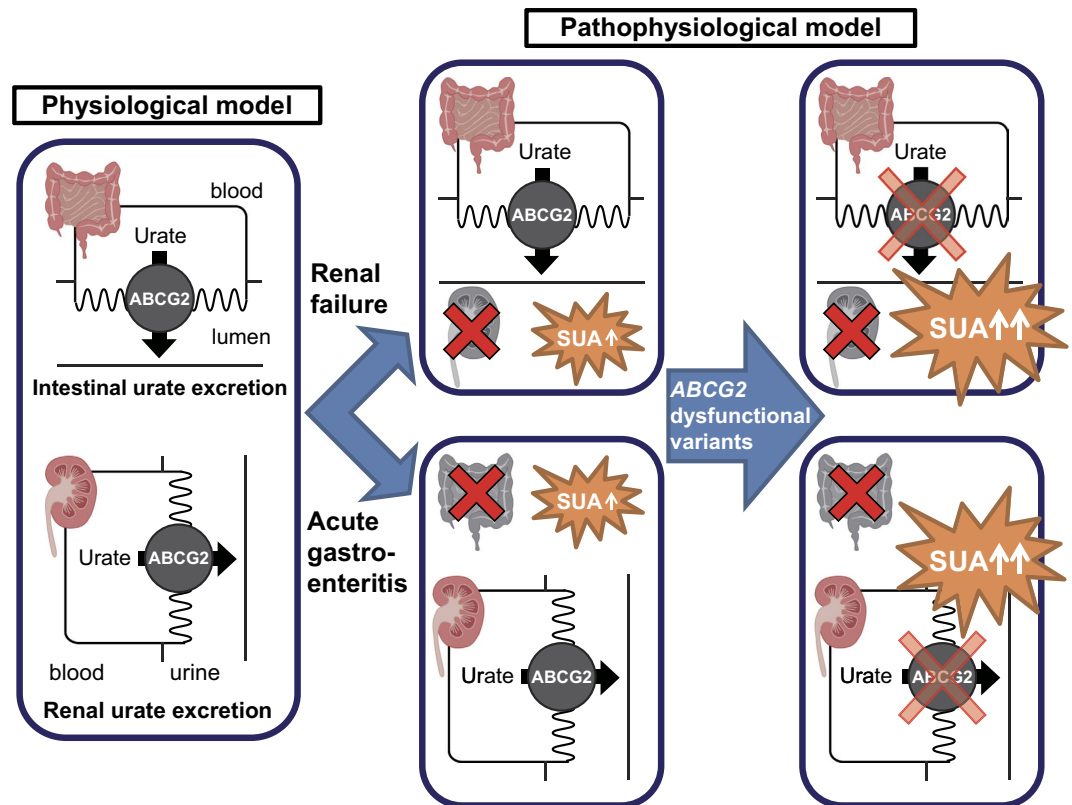
Figure 1. Pathophysiological model of ABCG2-mediated urate excretion in end-stage renal disease and acute gastroenteritis patients. SUA, serum uric acid. ABCG2 physiologically mediates urate excretion in both intestine and kidney. In end-stage renal disease (renal failure) patients, renal urate excretion would be nearly eliminated with urate excretion depending almost entirely on intestinal excretion. Thus, the degree of intestinal ABCG2 dysfunction strongly affects the severity of hyperuricemia in renal diseases such as end-stage renal disease. On the other hand, in acute gastroenteritis patients, intestinal inflammation seriously impairs the intestinal urate excretion *via* ABCG2. Therefore, the degree of renal ABCG2 dysfunction markedly affects the severity of hyperuricemia in intestinal diseases such as acute gastroenteritis patients.

In summary, we revealed that two common dysfunctional variants (Q126X and Q141K) of *ABCG2* have a significant negative effect on both intestinal and renal urate excretion in humans, and that intestinal and renal ABCG2 dysfunction markedly increases SUA in end-stage renal disease and acute gastroenteritis. These findings for the first time demonstrated the physiological and pathophysiological roles of ABCG2 on intestinal urate excretion in humans.

Methods

Participants. This study was approved by the institutional ethical committee of the National Defense Medical College, and all procedures were performed in accordance with the Declaration of Helsinki with written informed consent from each subject. When the participant was a minor, written informed consent was obtained from each parent or guardian of that participant. Degree of dehydration in acute gastroenteritis patients was evaluated by physicians (T. Tsunoda and T.S.) according to the criteria recommended by the Center for Disease Control (CDC)[20], and classified as "minimal or no dehydration", "mild to moderate dehydration", and "severe dehydration".

In order to clarify the physiological role of intestinal urate excretion *via* ABCG2, 106 maintenance hemodialysis patients not taking medications for hyperuricemia were assigned from among the outpatients at Ryougoku East Gate Clinic (Tokyo, Japan). Their SUA levels were measured three times just before each maintenance hemodialysis, and the average was used for analyses. In addition, 106 sex- and BMI-matched subjects were selected from health examination participants in the Shizuoka area in the Japan Multi-Institutional Collaborative Cohort Study (J-MICC Study)[21,22].

Sixty-seven pediatric patients with acute gastroenteritis were also recruited at the Department of Pediatric Hepatology and Gastroenterology in Saiseikai Yokohamashi Tobu Hospital (Yokohama, Japan). Their SUA levels were measured twice at the acute and recovery period of gastroenteritis.

The details of participants in this study are shown in Supplementary Table 3.

Genetic analysis and estimation of ABCG2 function. Genomic DNA was extracted from whole peripheral blood cells[23]. Genotyping of *ABCG2* dysfunctional variants, Q126X (rs72552713) and Q141K (rs2231142), was performed using the TaqMan method (Life Technologies Corporation, Carlsbad, CA, USA) with a LightCycler 480

(Roche Diagnostics, Mannheim, Germany) as previously described[24]. Custom TaqMan assay probes were designed as follows: for Q126X, VIC-CCACTAATACTTACTTGTACCAC and FAM-CCACTAATACTTACTTATACCAC; for Q141K, VIC-CTGCTGAGAACTGTAAGTT and FAM-CTGCTGAGAACTTTAAGTT. To confirm their genotypes, DNA sequencing analysis was performed with the following primers: for Q126X, forward 5′-TGTACAATGAAAAGAGAAAGGTGAG-3′ and reverse 5′-CTGCCTTTTCACATAAGTGTC-3′; for Q141K, forward 5′-ATGGAGTTAACTGTCATTTGC-3′ and reverse 5′-CACGTTCATATTATGTAACAAGCC-3′. Direct sequencing was performed with a 3130xl Genetic Analyzer (Life Technologies Corporation)[23,24].

We previously reported that Q126X is a nonfunctional variant, Q141K is a half-functional variant for urate excretion compared to the wild-type, and that there was no simultaneous presence of the minor alleles of Q126X and Q141K in one haplotype[2], which is confirmed in the participants of the present study (Supplementary Table 1). Thus, three haplotypes were defined as *1 (126Q and 141Q), *2 (126Q and 141K) and *3 (126X and 141Q) as previously reported[25], and all patients could be divided into the following ABCG2 functional groups: full function (*1/*1), 3/4 function (mild dysfunction, *1/*2), 1/2 function (moderate dysfunction, *1/*3 or *2/*2), and ≤1/4 function (severe dysfunction, *2/*3 or *3/*3)[25] as shown in Table 1.

Statistical analysis. For all calculations in the statistical analysis, the software R (version 3.1.1) (http://www.r-project.org/) was used[26]. Comparison of SUA between the acute and recovery period of gastroenteritis was performed with a paired t-test using a two-tailed P value. Linear regression analysis was performed to test the hypothesis that there was no relation between ABCG2 dysfunction and SUA in the analysis of acute gastroenteritis patients. Multiple regression analysis including ABCG2 function and age in the model was used for the analysis of hemodialysis patients and sex- and BMI-matched health examination participants, because age could not be completely matched in the selection from health examination participants. The association between ABCG2 and dehydration was examined using the Cochran-Armitage trend test. Haplotype estimation was performed with the EM algorithm[27] using the package haplo.stats of the software R. We set the significance threshold as $\alpha = 0.05$.

References

1. Feig, D. I., Kang, D. H. & Johnson, R. J. Uric acid and cardiovascular risk. *N. Engl. J. Med.* **359,** 1811–1821 (2008).
2. Matsuo, H. *et al.* Common defects of ABCG2, a high-capacity urate exporter, cause gout: a function-based genetic analysis in a Japanese population. *Sci. Transl. Med.* **1,** 5ra11 (2009).
3. Maliepaard, M. *et al.* Subcellular localization and distribution of the breast cancer resistance protein transporter in normal human tissues. *Cancer Res.* **61,** 3458–3464 (2001).
4. Huls, M. *et al.* The breast cancer resistance protein transporter ABCG2 is expressed in the human kidney proximal tubule apical membrane. *Kidney Int.* **73,** 220–225 (2008).
5. Woodward, O. M. *et al.* Identification of a urate transporter, ABCG2, with a common functional polymorphism causing gout. *Proc. Natl. Acad. Sci. USA* **106,** 10338–10342 (2009).
6. Matsuo, H. *et al.* Common dysfunctional variants in ABCG2 are a major cause of early-onset gout. *Sci. Rep.* **3,** 2014 (2013).
7. Nakayama, A. *et al.* Common dysfunctional variants of ABCG2 have stronger impact on hyperuricemia progression than typical environmental risk factors. *Sci. Rep.* **4,** 5227 (2014).
8. Ichida, K. *et al.* Decreased extra-renal urate excretion is a common cause of hyperuricemia. *Nat. Commun.* **3,** 764 (2012).
9. Krishnan, E. Chronic kidney disease and the risk of incident gout among middle-aged men: a seven-year prospective observational study. *Arthritis Rheum.* **65,** 3271–3278 (2013).
10. Prasad Sah, O. S. & Qing, Y. X. Associations between hyperuricemia and chronic kidney disease: a review. *Nephrourol Mon* **7,** e27233 (2015).
11. Sica, D. A. & Schoolwerth, A. In *Brenner and Rector's The Kidney* (ed Brenner, B. M.) 645–649 (Saunders, 2004).
12. Sorensen, L. B. Role of the intestinal tract in the elimination of uric acid. *Arthritis Rheum.* **8,** 694–706 (1965).
13. Adler, R., Robinson, R., Pazdral, P. & Grushkin, C. Hyperuricemia in diarrheal dehydration. *Am. J. Dis. Child.* **136,** 211–213 (1982).
14. Schreiber, D. S., Blacklow, N. R. & Trier, J. S. The mucosal lesion of the proximal small intestine in acute infectious nonbacterial gastroenteritis. *N. Engl. J. Med.* **288,** 1318–1323 (1973).
15. Ciarlet, M., Conner, M. E., Finegold, M. J. & Estes, M. K. Group A rotavirus infection and age-dependent diarrheal disease in rats: a new animal model to study the pathophysiology of rotavirus infection. *J. Virol.* **76,** 41–57 (2002).
16. Ramig, R. F. Pathogenesis of intestinal and systemic rotavirus infection. *J. Virol.* **78,** 10213–10220 (2004).
17. Greenberg, H. B. & Estes, M. K. Rotaviruses: from pathogenesis to vaccination. *Gastroenterol.* **136,** 1939–1951 (2009).
18. Karst, S. M., Zhu, S. & Goodfellow, I. G. The molecular pathology of noroviruses. *J. Pathol.* **235,** 206–216 (2015).
19. Hosomi, A., Nakanishi, T., Fujita, T. & Tamai, I. Extra-renal elimination of uric acid via intestinal efflux transporter BCRP/ABCG2. *PLoS One* **7,** e30456 (2012).
20. King, C. K., Glass, R., Bresee, J. S. & Duggan, C. Managing acute gastroenteritis among children: oral rehydration, maintenance, and nutritional therapy. *MMWR Recomm. Rep.* **52,** 1–16 (2003).
21. Hamajima, N. & J-MICC Study Group. The Japan Multi-Institutional Collaborative Cohort Study (J-MICC Study) to detect gene-environment interactions for cancer. *Asian Pac. J. Cancer Prev.* **8,** 317–323 (2007).
22. Asai, Y. *et al.* Baseline data of Shizuoka area in the Japan Multi-Institutional Collaborative Cohort Study (J-MICC Study). *Nagoya J. Med. Sci.* **71,** 137–144 (2009).
23. Sakiyama, M. *et al.* Common variant of leucine-rich repeat-containing 16A (LRRC16A) gene is associated with gout susceptibility. *Hum. Cell* **27,** 1–4 (2014).
24. Sakiyama, M. *et al.* Ethnic differences in ATP-binding cassette transporter, sub-family G, member 2 (ABCG2/BCRP): Genotype combinations and estimated functions. *Drug Metab. Pharmacokinet.* **29,** 490–492 (2014).
25. Matsuo, H. *et al.* ABCG2 dysfunction causes hyperuricemia due to both renal urate underexcretion and renal urate overload. *Sci. Rep.* **4,** 3755 (2014).
26. R: A language and environment for statistical computing. (R. Foundation for Statistical Computing, Vienna, 2014).
27. Kitamura, Y. *et al.* Determination of probability distribution of diplotype configuration (diplotype distribution) for each subject from genotypic data using the EM algorithm. *Ann. Hum. Genet.* **66,** 183–193 (2002).

Author Contributions

H.M., T. Tsunoda, K.O. and M.S. conceived and designed this study. H.M., T. Tsunoda, K.O., M.S., T.S., K.W., H.O., A.I. and S.F. collected samples and analyzed clinical data. H.M., M.S., A. Nakayama, M.K. and T.H. performed genetic analysis. H.M. and M.S. performed statistical analyses. A. Nakashima, T. Takada, R.H., H.S., K.I., A.I., S.F. and N.S. provided intellectual input and assisted with the preparation of the manuscript. H.M., T. Tsunoda, K.O. and M.S. wrote the manuscript.

Additional Information

Supplementary information accompanies this paper at http://www.nature.com/srep

Competing financial interests: Yes, there is potential competing interest: H.M., T. Takada, K.I. and N.S. have a patent pending based on the work reported in this paper. Other authors have declared that no competing interests exist.

How to cite this article: Matsuo, H. *et al.* Hyperuricemia in acute gastroenteritis is caused by decreased urate excretion *via* ABCG2. *Sci. Rep.* **6**, 31003; doi: 10.1038/srep31003 (2016).
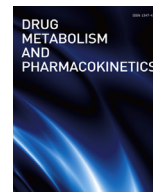
Contents lists available at ScienceDirect

Drug Metabolism and Pharmacokinetics

Note

Common variant of PDZ domain containing 1 (*PDZK1*) gene is associated with gout susceptibility: A replication study and meta-analysis in Japanese population

Toshihide Higashino [a, 1], Hirotaka Matsuo [a, *, 1], Masayuki Sakiyama [a],
Akiyoshi Nakayama [a], Takahiro Nakamura [b], Tappei Takada [c], Hiraku Ogata [a],
Yusuke Kawamura [a], Makoto Kawaguchi [a], Mariko Naito [d], Sayo Kawai [d], Yuzo Takada [e],
Hiroshi Ooyama [f], Hiroshi Suzuki [c], Nariyoshi Shinomiya [a]

[a] *Department of Integrative Physiology and Bio-Nano Medicine, National Defense Medical College, Tokorozawa, Japan*
[b] *Laboratory of Mathematics, National Defense Medical College, Tokorozawa, Japan*
[c] *Department of Pharmacy, The University of Tokyo Hospital, Faculty of Medicine, The University of Tokyo, Tokyo, Japan*
[d] *Department of Preventive Medicine, Nagoya University Graduate School of Medicine, Nagoya, Japan*
[e] *Faculty of Medical Science, Teikyo University of Science, Tokyo, Japan*
[f] *Ryougoku East Gate Clinic, Tokyo, Japan*

ARTICLE INFO

ABSTRACT

PDZ domain containing 1 (PDZK1) is a scaffold protein that organizes a transportsome and regulates several transporters' functions including urate and drug transporters. Therefore, PDZK1 in renal proximal tubules may affect serum uric acid levels through PDZK1-binding renal urate transporters. Two previous studies in Japanese male population reported that a *PDZK1* single nucleotide polymorphism (SNP), rs12129861, was not associated with gout. In the present study, we performed a further association analysis between gout and rs12129861 in a different large-scale Japanese male population and a meta-analysis with previous Japanese population studies. We genotyped rs12129861 in 1210 gout cases and 1224 controls of a Japanese male population by TaqMan assay. As a result, we showed that rs12129861 was significantly associated with gout susceptibility ($P = 0.016$, odds ratio [OR] = 0.80, 95% confidence interval [CI] 0.67–0.96). The result of the meta-analysis among Japanese populations also showed a significant association ($P = 0.013$, OR = 0.85, 95%CI 0.75–0.97). Our findings show the significant association between gout susceptibility and common variant of PDZK1 which reportedly regulates the functions of urate transporters in the urate transportsome.

1. Introduction

PDZ domain containing 1 (PDZK1) is a scaffold protein that binds to various transporters including drug transporters [1–3]. An example of such transporters is the organic anion transporting polypeptide 1A2 (OATP1A2), which is expressed in kidney and functions as a drug transporter [4]. In this scenario, PDZK1 regulates the transport function of OATP1A2 by modulating protein internalization via a clathrin-dependent pathway and by enhancing protein stability [1].

From a different perspective, rs12129861, a single nucleotide polymorphism (SNP), was reported to be associated with serum uric acid (SUA) levels in a genome-wide association study [5]. Rs12129861 is located near *PDZK1* (approximately 2 kb upstream) and may affect the gene expression levels of *PDZK1*. However, in previous Japanese population reports [6,7] of clinically-defined male gout cases, rs12129861 has not shown a significant association with gout susceptibility.

In this study, we performed a further association study between gout and rs12129861 in a different large-scale Japanese population and a meta-analysis with previous Japanese population reports [6,7].

---

* Corresponding author.
  E-mail address: hmatsuo@ndmc.ac.jp (H. Matsuo).
[1] Toshihide Higashino and Hirotaka Matsuo contributed equally to this work.

2. Materials and methods

2.1. Patients and controls

This study was approved by the institutional ethical committees (National Defense Medical College and Nagoya University). All procedures were performed in accordance with the Declaration of Helsinki, and written informed consent was obtained from each subject participating in the study. From the outpatients of Ryougoku East Gate Clinic (Tokyo, Japan), 1210 male Japanese patients with primary gout were recruited. All the patients were diagnosed with gout according to the criteria established by the American College of Rheumatology [8]. As the control group, 1224 Japanese men without gout history or hyperuricemia (SUA levels > 7.0 mg/dL) were selected from participants in the Shizuoka area in the Japan Multi-Institutional Collaborative Cohort Study (J-MICC Study) [9,10]. The mean age of cases and controls was 45.3 ± 10.4 and 53.1 ± 8.8 years old, respectively, and their mean body-mass index was 25.4 ± 3.7 and 23.3 ± 2.7 kg/m^2, respectively.

2.2. Genetic and statistical analyses

Genomic DNA was extracted from whole peripheral blood as previously described [11]. Genotyping of the *PDZK1* polymorphism (rs12129861) was performed using a TaqMan assay (Thermo Fisher Scientific Inc., Waltham, MA) as previously described [7]. All of statistical analyses were performed with SPSS v.22.0J (IBM Japan Inc., Tokyo, Japan) and the software R (version 3.1.1) [12] with meta package [13]. Chi-square test was used for association and Hardy–Weinberg equilibrium analyses. A meta-analysis among present and previous studies [6,7] was performed by the DerSimonian and Laird [14] random-effects model. Cochran's Q test and I^2 were used as measurements of heterogeneity among the present and two previous [6,7] studies. A *P* value < 0.05 was considered statistically significant.

3. Results

The rs12129861 of *PDZK1* genotyping results for 1210 gout cases and 1224 controls are shown in Table 1. The genotyping call rate for rs12129861 was 99.3%. In the control group, this variant was in Hardy–Weinberg equilibrium ($P > 0.05$).

In contrast to previous Japanese studies' results [6,7], the present study shows a statistically significant association between gout and rs12129861 ($P = 0.016$, odds ratio (OR) with 95% confidence interval (CI) 0.80 [0.67–0.96]). In the meta-analysis among the present and previous [6,7] Japanese studies, no apparent heterogeneity was observed (*P* value for Cochran's Q test = 0.65, $I^2 = 0\%$), and rs12129861 also showed a significant association with gout ($P_{meta} = 0.013$, OR with 95% CI: 0.85 [0.75–0.97]; Fig. 1).

4. Discussion

As a component of a transportsome, PDZK1 regulates the function of several transporters including drug [1–3] and urate

Table 1
Association between gout and the *PDZK1* rs12129861 polymorphism.

	Genotype				Allele frequency mode	
	G/G	G/A	A/A	MAF	*P* value	OR (95% CI)
Case	972	212	14	0.10	0.016	0.80 (0.67–0.96)
Control	939	261	18	0.12		

CI, confidence interval; *MAF*, minor allele frequency; *OR*, odds ratio.
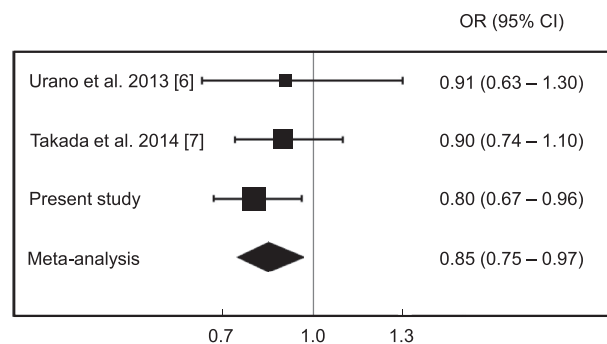
OR (95% CI)

Fig. 1. Meta-analysis of *PDZK1* rs12129861 polymorphism for gout in Japanese male populations. The meta-analysis was performed among results of the present and two previous Japanese male population studies (Urano et al., 2013 [6] and Takada et al., 2014 [7]) by the random-effects (DerSimonian and Laird) model. The sizes of the black boxes are proportional to the inverse of the squared standard error. The horizontal lines indicate the 95% CIs of ORs. The diamond shows the summary OR, and the width indicates the 95% CI. The summary OR was 0.85 (95% CI, 0.75–0.97), which was statistically significant ($P_{meta} = 0.013$). *CI*, confidence interval; *OR*, odds ratio.

transporters [15–17]. A transportsome is a transporting multimolecular complex composed of transporters and scaffold proteins [15–17]. In human kidney, the urate transportsome is located at the apical membrane of proximal tubular cells and contains several urate transporters [15–17], such as ATP-binding cassette transporter, subfamily G, member 2 (ABCG2/BCRP), organic anion transporter 4 (OAT4/SLC22A11), urate transporter 1 (URAT1/SLC22A12), type 1 sodium-dependent phosphate transporter (NPT1/SLC17A1), and multidrug resistance protein 4 (MRP4/ABCC4). Common variants of *ABCG2* [18] significantly increase gout [19–21] and hyperuricemia risks [22,23]. Additionally, *OAT4* [24], *URAT1* [25–28], and *NPT1* [27–30] genes are associated with gout susceptibility. PDZK1 and sodium protein exchanger regulatory factor 1 (NHERF 1) assemble the scaffolding network connecting these transporters in the transportsome [16,17].

To date, two previous reports showed lack of association between the *PDZK1* rs12129861 polymorphism and gout susceptibility in the Japanese population; however, as shown in Fig. 1, the direction of the effect was similar in both studies [6,7]. Therefore, we performed an additional association analysis in a different larger Japanese population. A significant association between rs12129861 and gout susceptibility was evidenced by the present replication study and the meta-analysis with previous reports [6,7]. These findings imply that lack of association between rs12129861 and gout susceptibility was due to the limited number of samples in the previous studies [6,7]. Moreover, other studies report the association between gout and *PDZK1* polymorphisms in Han Chinese [27,31] and New Zealand population [28]. Two of these reports [28,31] showed positive association consistently with the present study results. Since previous genome-wide association studies showed that common variant of PDZK1 are associated with SUA [5,32], PDZK1 variants could be associated with gout susceptibility because of individual differences in SUA levels.

In conclusion, the *PDZK1* rs12129861 showed the association with gout susceptibility which might lead to individual differences in urate transport through the urate transportsome. Our findings also suggest that this *PDZK1* variant might be associated with individual differences in drug transport through the drug transportsome.

Conflict of interest

The authors declare that they have no conflict of interest.

Funding

Acknowledgments

References

[1] Zheng J, Chan T, Cheung FS, Zhu L, Murray M, Zhou F. PDZK1 and NHERF1 regulate the function of human organic anion transporting polypeptide 1A2 (OATP1A2) by modulating its subcellular trafficking and stability. PLoS One 2014;9:e94712. http://dx.doi.org/10.1371/journal.pone.0094712.

[2] Shimizu T, Sugiura T, Wakayama T, Kijima A, Nakamichi N, Iseki S, et al. PDZK1 regulates breast cancer resistance protein in small intestine. Drug Metab Dispos 2011;39:2148—54. http://dx.doi.org/10.1124/dmd.111.040295.

[3] Miyazaki H, Anzai N, Ekaratanawong S, Sakata T, Shin HJ, Jutabha P, et al. Modulation of renal apical organic anion transporter 4 function by two PDZ domain-containing proteins. J Am Soc Nephrol 2005;16:3498—506. http://dx.doi.org/10.1681/ASN.2005030306.

[4] Müller F, Fromm MF. Transporter-mediated drug-drug interactions. Pharmacogenomics 2011;12:1017—37. http://dx.doi.org/10.2217/pgs.11.44.

[5] Kolz M, Johnson T, Sanna S, Teumer A, Vitart V, Perola M, et al. Meta-analysis of 28,141 individuals identifies common variants within five new loci that influence uric acid concentrations. PLoS Genet 2009;5:e1000504. http://dx.doi.org/10.1371/journal.pgen.1000504.

[6] Urano W, Taniguchi A, Inoue E, Sekita C, Ichikawa N, Koseki Y, et al. Effect of genetic polymorphisms on development of gout. J Rheumatol 2013;40:1374—8. http://dx.doi.org/10.3899/jrheum.121244.

[7] Takada Y, Matsuo H, Nakayama A, Sakiyama M, Hishida A, Okada R, et al. Common variant of PDZK1, adaptor protein gene of urate transporters, is not associated with gout. J Rheumatol 2014;41:2330—1. http://dx.doi.org/10.3899/jrheum.140573.

[8] Wallace SL, Robinson H, Masi AT, Decker JL, McCarty DJ, Yü TF. Preliminary criteria for the classification of the acute arthritis of primary gout. Arthritis Rheum 1977;20:895—900. http://dx.doi.org/10.1002/art.1780200320.

[9] Asai Y, Naito M, Suzuki M, Tomoda A, Kuwabara M, Fukada Y, et al. Baseline data of Shizuoka area in the Japan multi-institutional collaborative cohort study (J-MICC study). Nagoya J Med Sci 2009;71:137—44. http://hdl.handle.net/2237/12349.

[10] Hamajima N, Group JMS. The Japan multi-institutional collaborative cohort study (J-MICC study) to detect gene-environment interactions for cancer. Asian Pac J Cancer Prev 2007;8:317—23. http://www.ncbi.nlm.nih.gov/pubmed/17696755.

[11] Matsuo H, Chiba T, Nagamori S, Nakayama A, Domoto H, Phetdee K, et al. Mutations in glucose transporter 9 gene SLC2A9 cause renal hypouricemia. Am J Hum Genet 2008;83:744—51. http://dx.doi.org/10.1016/j.ajhg.2008.11.001.

[12] R Development Core Team. R: a language and environment for statistical computing. Vienna: R. Foundation for Statistical Computing; 2014. http://www.r-project.org/.

[13] Schwarzer G. Meta: meta-analysis with R. R package version 3.7-1. 2014. http://CRAN.R-project.org/package=meta.

[14] DerSimonian R, Laird N. Meta-analysis in clinical trials. Control Clin Trials 1986;7:177—88. http://dx.doi.org/0197-2456(86)90046-2.

[15] Sakiyama M, Matsuo H, Shimizu S, Chiba T, Nakayama A, Takada Y, et al. Common variant of leucine-rich repeat-containing 16A (LRRC16A) gene is associated with gout susceptibility. Hum Cell 2014;27:1—4. http://dx.doi.org/10.1007/s13577-013-0081-8.

[16] Ichida K. What lies behind serum urate concentration? Insights from genetic and genomic studies. Genome Med 2009;1:118. http://dx.doi.org/10.1186/gm118.

[17] Anzai N, Kanai Y, Endou H. New insights into renal transport of urate. Curr Opin Rheumatol 2007;19:151—7. http://dx.doi.org/10.1097/BOR.0b013e328032781a.

[18] Sakiyama M, Matsuo H, Takada Y, Nakamura T, Nakayama A, Takada T, et al. Ethnic differences in ATP-binding cassette transporter, sub-family G, member 2 (ABCG2/BCRP): genotype combinations and estimated functions. Drug Metab Pharmacokinet 2014;29:490—2. http://dx.doi.org/10.2133/dmpk.DMPK-14-SC-041.

[19] Matsuo H, Takada T, Ichida K, Nakamura T, Nakayama A, Ikebuchi Y, et al. Common defects of ABCG2, a high-capacity urate exporter, cause gout: a function-based genetic analysis in a Japanese population. Sci Transl Med 2009;1:5ra11. http://dx.doi.org/10.1126/scitranslmed.3000237.

[20] Woodward OM, Köttgen A, Coresh J, Boerwinkle E, Guggino WB, Köttgen M. Identification of a urate transporter, ABCG2, with a common functional polymorphism causing gout. Proc Natl Acad Sci U. S. A 2009;106:10338—42. http://dx.doi.org/10.1073/pnas.0901249106.

[21] Matsuo H, Ichida K, Takada T, Nakayama A, Nakashima H, Nakamura T, et al. Common dysfunctional variants in ABCG2 are a major cause of early-onset gout. Sci Rep 2013;3:2014. http://dx.doi.org/10.1038/srep02014.

[22] Matsuo H, Nakayama A, Sakiyama M, Chiba T, Shimizu S, Kawamura Y, et al. ABCG2 dysfunction causes hyperuricemia due to both renal urate under-excretion and renal urate overload. Sci Rep 2014;4:3755. http://dx.doi.org/10.1038/srep03755.

[23] Nakayama A, Matsuo H, Nakaoka H, Nakamura T, Nakashima H, Takada Y, et al. Common dysfunctional variants of ABCG2 have stronger impact on hyperuricemia progression than typical environmental risk factors. Sci Rep 2014;4:5227. http://dx.doi.org/10.1038/srep05227.

[24] Sakiyama M, Matsuo H, Shimizu S, Nakashima H, Nakayama A, Chiba T, et al. A common variant of organic anion transporter 4 (OAT4/SLC22A11) gene is associated with renal underexcretion type gout. Drug Metab Pharmacokinet 2014;29:208—10. http://dx.doi.org/10.2133/dmpk.DMPK-13-NT-070.

[25] Taniguchi A, Urano W, Yamanaka M, Yamanaka H, Hosoyamada M, Endou H, et al. A common mutation in an organic anion transporter gene, SLC22A12, is a suppressing factor for the development of gout. Arthritis Rheum 2005;52:2576—7. http://dx.doi.org/10.1002/art.21242.

[26] Sakiyama M, Matsuo H, Shimizu S, Nakashima H, Nakamura T, Nakayama A, et al. The effects of URAT1/SLC22A12 nonfunctional variants, R90H and W258X, on serum uric acid levels and gout/hyperuricemia progression. Sci Rep 2016;6:20148. http://dx.doi.org/10.1038/srep20148.

[27] Zhou ZW, Cui LL, Han L, Wang C, Song ZJ, Shen JW, et al. Polymorphisms in GCKR, SLC17A1 and SLC22A12 were associated with phenotype gout in Han Chinese males: a case-control study. BMC Med Genet 2015;16:66. http://dx.doi.org/10.1186/s12881-015-0208-8.

[28] Phipps-Green AJ, Merriman ME, Topless R, Altaf S, Montgomery GW, Franklin C, et al. Twenty-eight loci that influence serum urate levels: analysis of association with gout. Ann Rheum Dis 2016;75:124—30. http://dx.doi.org/10.1136/annrheumdis-2014-205877.

[29] Urano W, Taniguchi A, Anzai N, Inoue E, Kanai Y, Yamanaka M, et al. Sodium-dependent phosphate cotransporter type 1 sequence polymorphisms in male patients with gout. Ann Rheum Dis 2010;69:1232—4. http://dx.doi.org/10.1136/ard.2008.106856.

[30] Chiba T, Matsuo H, Kawamura Y, Nagamori S, Nishiyama T, Wei L, et al. NPT1/SLC17A1 is a renal urate exporter in humans and its common gain-of-function variant decreases the risk of renal underexcretion gout. Arthritis Rheumatol 2015;67:281—7. http://dx.doi.org/10.1002/art.38884.

[31] Li M, Li Q, Li CG, Guo M, Xu JM, Tang YY, et al. Genetic polymorphisms in the PDZK1 gene and susceptibility to gout in male Han Chinese: a case-control study. Int J Clin Exp Med 2015;8:13911—8. http://www.ncbi.nlm.nih.gov/pmc/articles/PMC4613032.

[32] Köttgen A, Albrecht E, Teumer A, Vitart V, Krumsiek J, Hundertmark C, et al. Genome-wide association analyses identify 18 new loci associated with serum urate concentrations. Nat Genet 2013;45:145—54. http://dx.doi.org/10.1038/ng.2500.

□ CASE REPORT □

A Novel Mutation in a Japanese Family with X-linked Alport Syndrome

Yoshifusa Abe[1], Masayuki Iyoda[2], Kandai Nozu[3], Satoshi Hibino[1], Kei Hihara[2], Yutaka Yamaguchi[4], Tomohiko Yamamura[3], Shogo Minamikawa[3], Kazumoto Iijima[3], Takanori Shibata[2] and Kazuo Itabashi[1]

Abstract

We herein report a novel mutation in a Japanese family with an X-linked Alport syndrome (AS) mutation in *COL4A5*. Patient 1 was a 2-year-old Japanese girl. She and her mother (patient 2) had a history of proteinuria and hematuria without renal dysfunction, deafness, or ocular abnormalities. Pathological findings were consistent with AS, and a genetic analysis revealed that both patients had a heterozygous mutation (c.2767G> C) in exon 32. In summary, the identification of mutations and characteristic pathological findings was useful in making a diagnosis of AS. For a close long-term follow-up, the early detection and treatment of women with X-linked AS are important.

Introduction

Alport syndrome (AS) is a hereditary nephropathy characterized by a family history of hematuria, progressive renal failure, sensorineural hearing loss, and ocular abnormalities (1). Progression to renal failure is predictable in men, whereas the course of renal involvement is much more variable in women, remaining mild in the majority of patients. Approximately 80% of AS is inherited in an X-linked manner and is caused by mutations in the *COL4A5* gene. Nearly all male patients will develop end-stage renal disease (ESRD), whereas heterozygous females exhibit a wide variability in disease severity (2, 3). To date, more than 700 different *COL4A5* mutations have been identified (4, 5). We herein report a novel mutation in a Japanese family with an X-linked AS mutation in *COL4A5*.

Case Report

The patient (patient 1) was a 2-year-old Japanese girl who was the first child of healthy non-consanguineous parents. Her younger brother had no proteinuria or hematuria. Her maternal aunt had an episode of nephritis, and a renal biopsy was performed during childhood, but the findings were uncertain. At 14 months of age, patient 1 was referred to our hospital because of microscopic hematuria that had persisted from the neonatal period. She had no clinically detectable hearing loss or ocular abnormalities. A urine culture revealed no infection. At 15 months of age, enalapril malate was initiated for proteinuria, with a urinary protein/creatinine ratio (P/Cr) of 1.3-3.6 g/gCr. At 21 months of age, she was admitted to our hospital for a renal biopsy. On admission, a urinalysis showed 2+ proteinuria (P/Cr, 1.3 g/gCr) and 3+ hematuria, with the urine sediment containing >100 red cells per high-power field. Her blood urea nitrogen (BUN) level was 17.7 mg/dL, serum creatinine level was
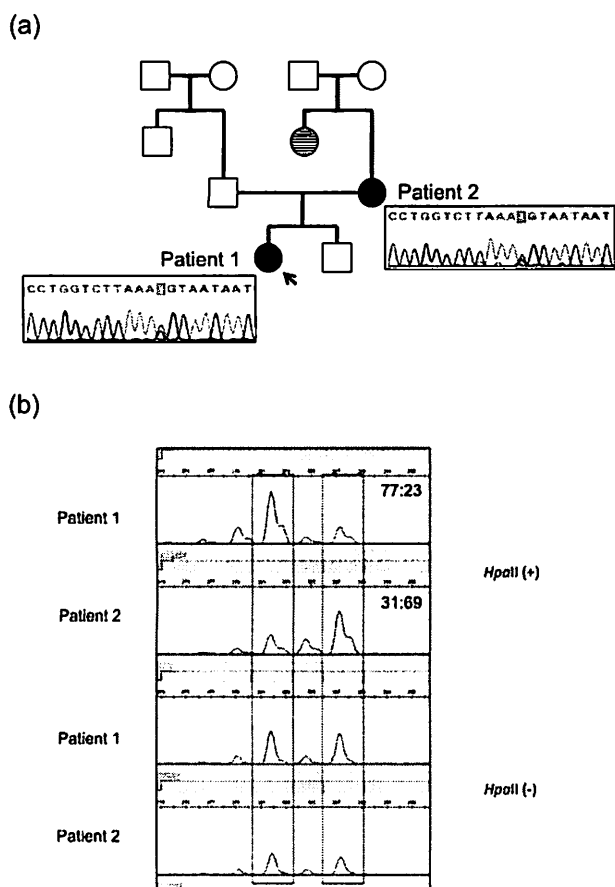
(a)

(b)

Figure 1.   (a) Pedigree and findings of COL4A5 mutation in two patients. The arrow indicates the proband. Unaffected individuals with kidney diseases are denoted by empty squares (men) and circles (women). Affected individuals with X-linked Alport syndrome are denoted by blackened circles (patients 1 and 2). Affected individuals with biopsy-unproven kidney disease are denoted by striped circles. Genetic analyses revealed that both patients had a heterozygous mutation (c. 2,767G>C) in exon 32. (b) X chromosome inactivation assays for our patients. In methylation-sensitive enzymes, a methylated allele is inactivated and cannot be digested by HpaII. Patient 1 and 2 both showed a random pattern with ratios of 77: 23 and 31: 69, respectively. It was impossible to distinguish whether the mutated allele was possessed by an activated or inactivated X chromosome because both had the same number of CAG repeats.

0.22 mg/dL, serum total protein level was 5.9 g/dL, and albumin level was 3.7 g/dL. Serum C3 and C4 levels were 118.2 mg/dL and 24.8 mg/dL, respectively. Antinuclear antibodies were negative. Renal ultrasonography was unremarkable.

Her mother (patient 2) also had a history of proteinuria and hematuria without renal dysfunction, deafness, or ocular abnormalities. The pedigree of her family is shown in Fig. 1a. At 34 years of age, she was admitted to our hospital along with her daughter (patient 1) for a renal biopsy. A urinalysis showed 3+ proteinuria (P/Cr, 1.7 g/gCr) and 2+ he-

maturia, with the sediment containing 10-19 red cells per high-power field. Her BUN level was 20.0 mg/dL, serum creatinine level was 0.59 mg/dL, serum total protein level was 6.8 g/dL, and albumin level was 4.0 g/dL. Serum C3 and C4 levels were 134.4 mg/dL and 34.2 mg/dL, respectively. Antinuclear antibodies were negative. Renal ultrasonography showed a cystic lesion in the right kidney.

The renal biopsy findings of the two patients are shown in Fig. 2. In patient 1, 29 glomeruli were observed on light microscopy; the glomerulus, tubules, and interstitium showed no significant alterations. Immunofluorescence (IF) staining for alpha 5 chains of type IV collagen showed segmental and mosaic patterns in the glomerular basement membrane (GBM). Electron microscopy (EM) demonstrated diffusely thinned-out GBMs (139-143 nm) with focal lamellation and splitting. In patient 2, 40 glomeruli were observed on light microscopy, two of which were globally sclerotic. IF staining for alpha 5 chains of type IV collagen showed segmental and mosaic patterns in the GBM, Bowman's capsule, and distal tubular basement membrane (TBM). EM demonstrated diffusely thinned-out GBMs (149-166 nm) with dense granules and splitting. In both patients, the merged IF staining images for alpha 2 and 5 chains of type IV collagen clarified the findings of segmental and mosaic patterns in the GBM.

A sequence analysis of COL4A5 in the index patient and her mother was performed. The study was approved by the Institutional Review Board of Kobe University School of Medicine, and written informed consent was obtained. Genomic DNA was isolated from each patient's peripheral blood leukocytes using the Quick Gene Mini 80 System (Kurabo Industries, Tokyo, Japan), according to the manufacturer's instructions. Mutational analyses of COL4A5 were performed using polymerase chain reaction (PCR) and direct sequencing of genomic DNA of all exons and exon-intron boundaries. All 51 specific exons of COL4A5 were amplified by PCR. The PCR-amplified products were then purified and subjected to direct sequencing using a Dye Terminator Cycle Sequencing Kit (Amersham Biosciences, Piscataway, USA) with an automatic DNA sequencer (ABI Prism 3130; Perkin Elmer Applied Biosystems, Foster City, USA). The analysis revealed that both patients had a heterozygous mutation (c.2767G>C) in exon 32 (Fig. 1a). To investigate X chromosome inactivation, the human androgen receptor (HUMARA) assay was performed in both patients. Genomic DNA was digested by a methylation-sensitive enzyme, HpaII, at 37°C for 18 hours followed by PCR using DNA with HUMARA primers, as described previously (6). A DNA fragment analysis was performed on a 310 Genetic Analyzer (Thermo Fisher Scientific, Waltham, USA). Fragment data analyses were performed using the Gene Mapper Software program (Thermo Fisher Scientific). The HUMARA assay for patients 1 and 2 revealed that the X chromosome inactivation pattern was 77:23 and 31:69, respectively (Fig. 1b).
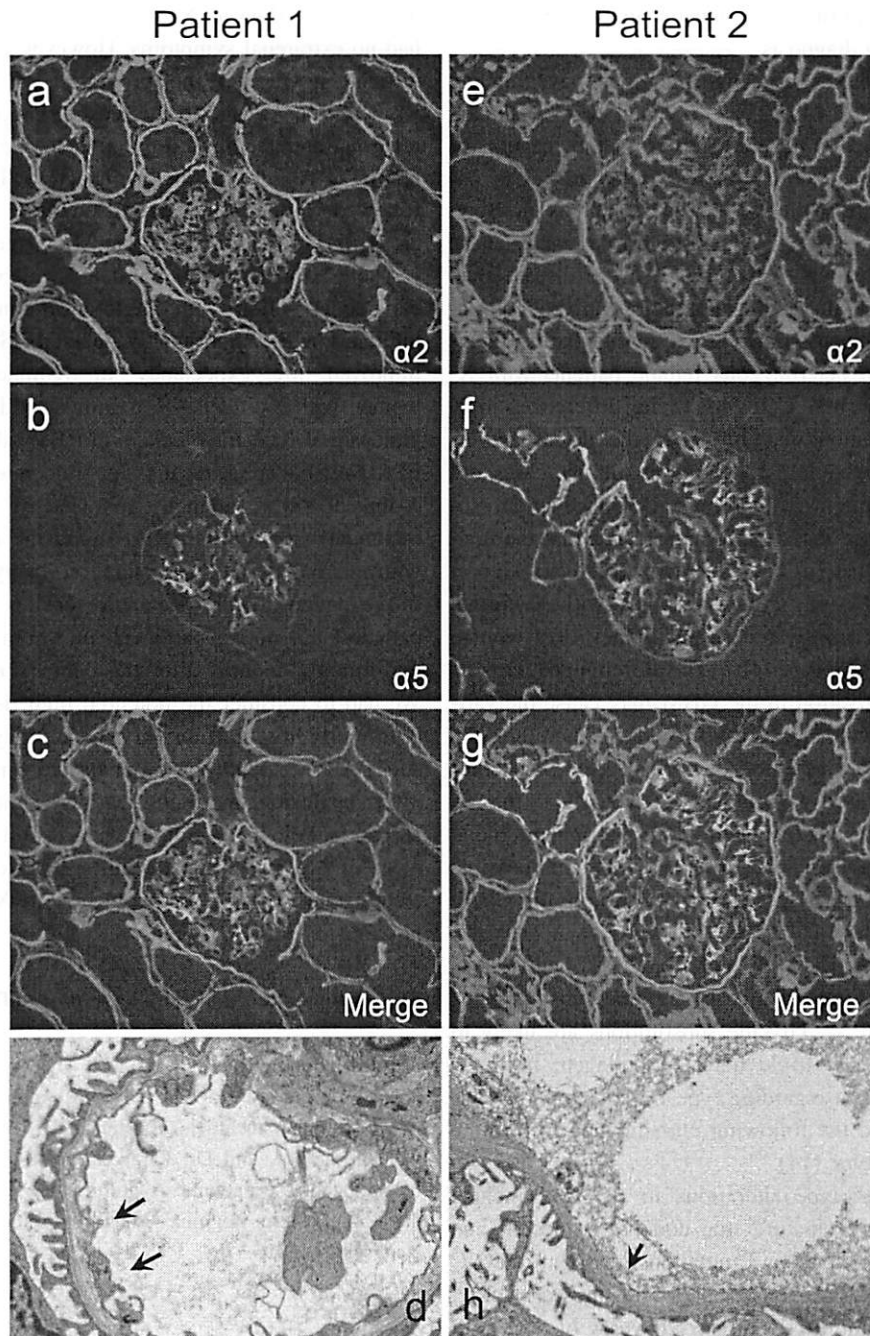
Figure 2.   Renal biopsy findings in X-linked Alport syndrome with a novel mutation. Patient 1 shows (a) a normal pattern of the alpha 2 chain of type IV collagen in the GBM and (b) segmental and mosaic patterns of the alpha 5 chain of type IV collagen in the GBM and the absence of staining in Bowman's capsule and the TBM. (c) The merged findings of the alpha 2 and 5 chains of type IV collagen are shown. (d) Electron microscopy reveals a split lamina densa (arrows) and thin GBM. Patient 2 shows (e) a normal pattern of the alpha 2 chain of type IV collagen in the GBM and (f) a mosaic pattern of the alpha 5 chain of type IV collagen in the GBM and TBM. (g) The merged findings of the alpha 2 and 5 chains of type IV collagen are shown. (h) Electron microscopy reveals a split lamina densa (arrow). GBM: glomerular basement membrane, TBM: tubular basement membrane

Discussion

The index case was a 2-year-old girl with X-linked AS who had inherited a *COL4A5* novel mutation (c.2767G>C) in exon 32 from her mother. Both patients had histories of hematuria and proteinuria without sensorineural hearing loss or ocular abnormalities. Renal biopsy findings indicated he-

reditary glomerulonephritis, and genetic analyses were useful in making a final diagnosis.

More than 700 disease-causing mutations have already been reported in COL4A5 (2, 5). In men with X-linked AS, clinical features can be predicted from the location of COL4A5 mutations (3). Hematuria was noted earlier in patient 1. Pathologically, patient 1 had less signals in Bowman's capsule and the TBM compared with patient 2. These findings imply that patient 1 had more severe disease than patient 2. It reported that the genotype-phenotype correlations are not observed in women, even among family members (2, 7). Although heterozygous female patients with X-linked AS have a normal COL4A5 allele, differences in X chromosome inactivation may influence the disease severity (2, 8). However, the HUMARA assay in our cases did not confirm non-random X chromosome inactivation, so-called skewed X, since it is usually considered that the non-random inactivation pattern is >80:20 or <20:80 (9). Guo et al. reported that 90% of X chromosomes with a normal COL4A5 allele were inactivated in the kidney of a woman with a severe AS phenotype (10). The different patterns of X chromosome inactivation in the GBM may cause the variable phenotypes in women with X-linked AS. Therefore, the inactivation of a high proportion of normal X chromosomes in critical tissues could be clinically severe (11). In this study, skewed X was not detected in the peripheral blood cells of both patients 1 and 2. However, it remains possible that skewed X operates in specific tissue, namely the GBM, more strongly in patient 1 than in patient 2.

The mutation identified in our patient's family was c.2767G>C, resulting in a glycine to arginine substitution at position 923 in exon 32. Glycine substitutions are likely to alter the folding of the triple helix of collagen; however, solid evidence is absent regarding type IV collagen (12, 13). Gross et al. proposed the following classification to link the phenotype and genotype (14):

i. Severe AS. Genotype alterations in COL4A5 include large rearrangement, premature stop codons, frameshift and donor splice site mutations, and mutations involving the NC 1 domain. The phenotype is associated with the early onset of end-stage renal failure (ESRF) at -20 years of age, with 80% presenting with hearing loss and 40% presenting with ocular lesions.

ii. Moderate-severe AS. The genotype is characterized by non-glycine-X-Y missense, glycine-X-Y substitutions involving exons 21-47, and in-frame and acceptor splice site mutations. The phenotype is associated with ESRF at -26 years of age, with 65% presenting with hearing loss and 30% presenting with ocular lesions.

iii. Moderate AS. The genotype is characterized by glycine-XY substitutions involving exons 1-20. The phenotype is associated with ESRF at -30 years of age, with 70% presenting with hearing loss, and 30% presenting with ocular lesions.

According to this classification, our patients were classified as having moderate-severe AS. Taken together with no

detection of skewed X, this may explain why our patients had no extrarenal symptoms. However, it would be clinically difficult to predict the prognosis of kidney function in women with AS due to the lack of genotype-phenotype correlations and the intra-familial heterogeneity of the phenotype (2). Therefore, our patients should be longitudinally followed while paying careful attention to a progressive increase in proteinuria, as previously suggested (2).

There is no specific treatment available for AS; however, early intervention with angiotensin-converting enzyme inhibitors (ACEI) significantly delayed ESRD progression and improved life expectancy in X-linked AS (15, 16). In women with X-linked AS, treatment with either ACEI or angiotensin II receptor blockers (ARBs) inhibits progression to ESRD (15). Therefore, it is recommended that patients with X-linked AS are annually followed by a nephrologist, and treatment with ACEIs/ARBs should be initiated for patients with microalbuminuria, proteinuria, or hypertension (15, 17). In our patients, ACEI (enalapril malate) was administered to patient 1 but not to patient 2, in whom a renal biopsy was performed 3 months after the delivery of her second child. We had to consider the potential high risk of fetal and newborn morbidity and mortality, which may be associated with ACEI/ARB fetopathy in pregnant women (18, 19).

In conclusion, the identification of mutations and characteristic pathological findings were useful in making the diagnosis of AS. For a close long-term follow-up, the early detection and treatment of women with X-linked AS are important.

The authors state that they have no Conflict of Interest (COI).

References

1. Alport AC. Hereditary familial congenital haemorrhagic nephritis. Br Med J 1: 504-506, 1927.
2. Jais JP, Knebelmann B, Giatras I, et al. X-linked Alport syndrome: natural history and genotype-phenotype correlations in girls and women belonging to 195 families: a "European Community Alport Syndrome Concerted Action" study. J Am Soc Nephrol 14: 2603-2610, 2003.
3. Jais JP, Knebelmann B, Giatras I, et al. X-linked Alport syndrome: natural history in 195 families and genotype- phenotype correlations in males. J Am Soc Nephrol 11: 649-657, 2000.
4. Barker DF, Denison JC, Atkin CL, Gregory MC. Efficient detection of Alport syndrome COL4A5 mutations with multiplex genomic PCR-SSCP. Am J Med Genet 98: 148-160, 2001.
5. Savige J, Ars E, Cotton RG, et al. DNA variant databases improve test accuracy and phenotype prediction in Alport syndrome. Pediatr Nephrol 29: 971-977, 2014.
6. Allen RC, Zoghbi HY, Moseley AB, Rosenblatt HM, Belmont JW.

Methylation of HpaII and HhaI sites near the polymorphic CAG repeat in the human androgen-receptor gene correlates with X chromosome inactivation. Am J Hum Genet 51: 1229-1239, 1992.

7. Rheault MN. Women and Alport syndrome. Pediatr Nephrol 27: 41-46, 2012.

8. Shimizu Y, Nagata M, Usui J, et al. Tissue-specific distribution of an alternatively spliced COL4A5 isoform and non-random X chromosome inactivation reflect phenotypic variation in heterozygous X-linked Alport syndrome. Nephrol Dial Transplant 21: 1582-1587, 2006.

9. Kubota T. A new assay for the analysis of X-chromosome inactivation in carriers with an X-linked disease. Brain Dev 23 (Suppl 1): S177-S181, 2001.

10. Guo C, Van Damme B, Vanrenterghem Y, Devriendt K, Cassiman JJ, Marynen P. Severe alport phenotype in a woman with two missense mutations in the same COL4A5 gene and preponderant inactivation of the X chromosome carrying the normal allele. J Clin Invest 95: 1832-1837, 1995.

11. Nakanishi K, Iijima K, Kuroda N, et al. Comparison of alpha5(IV) collagen chain expression in skin with disease severity in women with X-linked Alport syndrome. J Am Soc Nephrol 9: 1433-1440, 1998.

12. Persikov AV, Pillitteri RJ, Amin P, Schwarze U, Byers PH, Brodsky B. Stability related bias in residues replacing glycines within the collagen triple helix (Gly-Xaa-Yaa) in inherited connective tissue disorders. Hum Mutat 24: 330-337, 2004.

13. Raghunath M, Bruckner P, Steinmann B. Delayed triple helix formation of mutant collagen from patients with osteogenesis imperfecta. J Mol Biol 236: 940-949, 1994.

14. Gross O, Netzer KO, Lambrecht R, Seibold S, Weber M. Meta-analysis of genotype-phenotype correlation in X-linked Alport syndrome: impact on clinical counselling. Nephrol Dial Transplant 17: 1218-1227, 2002.

15. Temme J, Peters F, Lange K, et al. Incidence of renal failure and nephroprotection by RAAS inhibition in heterozygous carriers of X-chromosomal and autosomal recessive Alport mutations. Kidney Int 81: 779-783, 2012.

16. Gross O, Licht C, Anders HJ, et al. Early angiotensin-converting enzyme inhibition in Alport syndrome delays renal failure and improves life expectancy. Kidney Int 81: 494-501, 2012.

17. Savige J, Gregory M, Gross O, Kashtan C, Ding J, Flinter F. Expert guidelines for the management of Alport syndrome and thin basement membrane nephropathy. J Am Soc Nephrol 24: 364-375, 2013.

18. Miura K, Sekine T, Iida A, Takahashi K, Igarashi T. Salt-losing nephrogenic diabetes insipidus caused by fetal exposure to angiotensin receptor blocker. Pediatr Nephrol 24: 1235-1238, 2009.

19. Shotan A, Widerhorn J, Hurst A, Elkayam U. Risks of angiotensin-converting enzyme inhibition during pregnancy: experimental and clinical evidence, potential mechanisms, and recommendations for use. Am J Med 96: 451-456, 1994.

Case Reports in **Nephrology and Dialysis**

Karger **Open access**

Case Report

A Case of *Transforming Growth Factor-β-Induced* Gene-Related Oculorenal Syndrome: Granular Corneal Dystrophy Type II with a Unique Nephropathy

Yoichi Iwafuchi[a]   Tetsuo Morioka[b]   Yuko Oyama[a]   Kandai Nozu[c]
Kazumoto Iijima[c]   Ichiei Narita[d]

[a]Department of Internal Medicine, Koseiren Sanjo General Hospital, Sanjo, Japan;
[b]Department of Internal Medicine, Kidney Center, Shinrakuen Hospital, Niigata, Japan;
[c]Department of Pediatrics, Kobe University Graduate School of Medicine, Kobe, Japan;
[d]Division of Clinical Nephrology and Rheumatology, Niigata University Graduate School of Medical and Dental Sciences, Niigata, Japan

Keywords
Granular corneal dystrophy type II · *Transforming growth factor-β-induced* gene · Oculorenal syndrome · Next-generation sequencing · Extracellular matrix · Protein-protein interactions

Abstract
Many types of inherited renal diseases have ocular features that occasionally support a diagnosis. The following study describes an unusual example of a 40-year-old woman with granular corneal dystrophy type II complicated by renal involvement. These two conditions may coincidentally coexist; however, there are some reports that demonstrate an association between renal involvement and granular corneal dystrophy type II. Granular corneal dystrophy type II is caused by a mutation in the *transforming growth factor-β-induced (TGFBI)* gene. The patient was referred to us because of the presence of mild proteinuria without hematuria that was subsequently suggested to be granular corneal dystrophy type II. A kidney biopsy revealed various glomerular and tubular basement membrane changes and widening of the subendothelial space of the glomerular basement membrane by electron microscopy. How-

KARGER

Dr. Yoichi Iwafuchi
Department of Internal Medicine, Koseiren Sanjo General Hospital
Tsukanome 5-1-62
Sanjo 955-0055 (Japan)
E-mail iwafuchiy@hotmail.com

Case Reports in Nephrology and Dialysis

Case Rep Nephrol Dial 2016;6:106–113		107
DOI: 10.1159/000449129	© 2016 The Author(s). Published by S. Karger AG, Basel www.karger.com/cnd	

Iwafuchi et al.: A Case of *Transforming Growth Factor-β-Induced* Gene-Related Oculorenal Syndrome: Granular Corneal Dystrophy Type II with a Unique Nephropathy

ever, next-generation sequencing revealed that she had no mutation in a gene that is known to be associated with monogenic kidney diseases. Conversely, real-time polymerase chain reaction, using a simple buccal swab, revealed *TGFBI* heteromutation (R124H). The TGFBI protein plays an important role in cell-collagen signaling interactions, including extracellular matrix proteins which compose the renal basement membrane. This mutation can present not only as corneal dystrophy but also as renal disease. *TGFBI*-related oculorenal syndrome may have been unrecognized. It is difficult to diagnose this condition without renal electron microscopic studies. To the best of our knowledge, this is the first detailed report of nephropathy associated with a *TGFBI* mutation.

© 2016 The Author(s)
Published by S. Karger AG, Basel

Introduction

Many types of inherited renal diseases have ocular features that are helpful in diagnosis [1]. We have observed a case of renal involvement complicated by granular corneal dystrophy type II (GCD2). GCD2, also known as Avellino corneal dystrophy (CD), is an autosomal dominant disorder caused by a mutation in the transforming growth factor-β-induced *(TGFBI)* gene [2]. This mutation can be found in several distinct autosomal dominant genetically determined cases of CD; however, it is not known whether this mutation produces other clinical manifestations other than CD. TGFBI proteins (TGFBIp) interact with several extracellular matrix (ECM) components [3, 4]. A mutation in this gene may actually influence basement membrane organization.

We believe that our study was a type of oculorenal syndrome associated with a *TGFBI* mutation, which remains to be acknowledged.

Case Report

A 40-year-old woman was evaluated for a 20-year history of proteinuria. She was not taking any medication, and her physical examination was unremarkable. She did not have any deafness or visual disturbances. She presented with a urinary protein level of 1.5 g/day. Her urinary sediment demonstrated <1 erythrocytes and leukocytes per high-power field. Complete blood cell results were normal. The following clinical laboratory values were noted: serum urea nitrogen (BUN), 14.9 mg/dl; creatinine (Cre), 0.79 mg/dl; total cholesterol, 189 mg/d; total protein, 6.4 g/dl; and albumin, 3.9 g/dl. The levels of C-reactive protein, immunoglobulins (Ig), and total complement, C3, C4, and C1q were all normal. Tests for antinuclear antibody, hepatitis B virus surface antigen, hepatitis C virus antibody, and cryoglobulins were all negative. All other laboratory tests were within normal limits. Results of a chest X-ray and an electrocardiogram were normal. Renal ultrasound and computed tomography revealed normal kidneys.

A kidney biopsy, performed using light microscopy, revealed 11 glomeruli, 1 of which was obsolete or sclerosed (fig. 1a). Light microscopy did not demonstrate any remarkable changes in the glomeruli (fig. 1b). Focal tubular atrophy with dilation of peritubular capillaries and focal infiltration of small round cells were observed. Immunostaining revealed no significant deposits of IgG, IgA, or C3. Clinical and histopathological findings confirmed the diagnosis of minor glomerular lesions. We observed the patient without the administration of drugs. After 7 years, the patient developed mild hypertension and began taking 4 mg/day of losartan potassium. The patient's mild proteinuria (1–1.5 g/g Cre) continued, and her

Case Reports in Nephrology and Dialysis

Case Rep Nephrol Dial 2016;6:106–113

108

DOI: 10.1159/000449129 | © 2016 The Author(s). Published by S. Karger AG, Basel
www.karger.com/cnd

Iwafuchi et al.: A Case of *Transforming Growth Factor-β-Induced* Gene-Related Oculorenal Syndrome: Granular Corneal Dystrophy Type II with a Unique Nephropathy

renal function was mildly decreased. After 10 years, the patient was re-admitted for additional evaluation of proteinuria. Laboratory testing revealed the following: urinary protein level of 1.5 g/day, BUN level of 15.0 mg/dl, and Cre level of 0.94 mg/dl. Approximately 2 years before her second admission, the patient complained of mild blurred vision and was diagnosed with CD. Slit-lamp examination revealed a large number of gray-white central granular and linear opacities in both eyes (fig. 2); therefore, we diagnosed her condition as GCD2. A second kidney biopsy was performed under light microscopy, revealing 18 glomeruli, 6 of which were obsolete or sclerosed (fig. 3a). The glomeruli were slightly enlarged with segmental mesangial proliferation (fig. 3b). Segmental double contours of the glomerular capillary walls were also observed (fig. 3c). Focal tubular atrophy with mild interstitial inflammation, dilation of peritubular capillaries, and segmental thickening of tubular basement membranes (TBM) were observed. Several foam cells were noted in the interstitium (fig. 3d). Immunofluorescent examination revealed no significant deposits of immunoglobulins or complement components. Congo red staining was negative for amyloid. Electron microscopic examination of the second biopsy revealed no electron dense deposits. The subendothelial space was widened, and irregularity of the glomerular basement membrane (GBM) was segmentally observed. Segmental irregular thinning, basket-waving, duplication, lamellation, and reticulation of GBM and TBM were observed partially and slightly (fig. 3e–i). Immunostaining of the α-5 chains of type IV collagen was normal.

Upon her renal pathological findings, we assumed the existence of a genetic cause. After obtaining informed consent, we collected DNA from the patient. The genome DNA was extracted from the whole blood, and targeted next-generation sequencing of candidate genes for inherited renal diseases was negative (online suppl. table S1; for all online suppl. material, see www.karger.com/doi/10.1159/000449129). Real-time polymerase chain reaction using a simple buccal swab (Avellino Labs Universal Test®; ALUT) revealed *TGFBI* heteromutation (R124H). We speculated that this condition was a novel case of oculorenal syndrome associated with *TGFBI* mutation. Because of the patient's condition, we analyzed her parents and daughter. Her 74-year-old father had the same mutation of *TGFBI* (R124H) and was diagnosed with relatively mild GCD2. Her 77-year-old mother and 26-year-old daughter, however, did not have mutated *TGFBI* (R124H) or GCD2. Her father had no proteinuria but had a slightly elevated level of urinary N-acetyl-β-D-glucosaminidase (3.0 U/g Cre); however, his renal function was normal (serum Cre, 0.79 mg/dl).

Subsequently, the patient was again treated in our outpatient clinic with 4 mg/day of losartan potassium but with no immunosuppressive agents.

Discussion

We have reported an unusual case of renal involvement and GCD2 with *TGFBI* heteromutation. These two conditions may coincidentally coexist; however, findings demonstrating an association between renal involvement and GCD2 have been presented.

The TGFBIp (also known as βig-h3, keratoepithelin) is a 68-kDa ECM protein with four evolutionary conserved fasciclin-1 domains and a carboxy-terminal Arg-Gly-Asp sequence [5]. This protein participates in many physiological processes, including morphogenesis, adhesion/migration, tumorigenesis, angiogenesis, wound healing, and inflammation [6]. TGFBIp is found in ECM of several human tissues and is abundant in the cornea. Mutations of the human *TGFBI* gene have been linked to several autosomal dominant multiple types of CD, including GCD2. Almost all cases of GCD2 are caused by *TGFBI* gene mutations (5q31),

KARGER

Iwafuchi et al.: A Case of *Transforming Growth Factor-β-Induced* Gene-Related Oculorenal Syndrome: Granular Corneal Dystrophy Type II with a Unique Nephropathy

particularly p.Arg124His (R124H) [2]. In a previous study, *TGFBI* gene mutation was estimated to have a prevalence of at least 11.5 affected people per 10,000 individuals in Korea [7].

According to embryonic expression studies using a mouse knock-out model of *TGFBI*, Schorderet et al. [8] speculated that functional loss of *TGFBI* affects several mesoderm-derived structures. TGFBIp is associated with adhesion/migration and ECM interactions. Mutations in adhesion and ECM molecules, such as integrins and laminin-β2, play an important role in the pathogenesis of focal segmental glomerulosclerosis [9]; however, thus far, the relationship between *TGFBI* mutation and kidney disease has not been established.

In an autopsy patient with *TGFBI*-related CD, pathologic deposits caused by TGFBIp accumulation were only observed in the cornea and in no other tissue or organ, including the kidney; however, an electromicroscopic examination was not performed in that report [10]. TGFBIp was present in the capsule and TBM of the developing kidney [11] and was predominantly localized in the epithelial cells of the collecting ducts as well as the distal proximal tubules [12]. TGFBIp is secreted into the extracellular space and may bind to fibronectin, laminin, and type I, II, and IV collagens [13] as well as integrins [12, 13]. Proteomic analysis revealed that TGFBIp is a component of glomerular ECM [3, 4], and it exhibits protein-protein interactions between the following ECM proteins: α-2 macroglobulin; α-1, α-2 chain type I collagen; α-1 chain type II collagen; α-1, α-2, α-3, and α-4 chain type IV collagen; fibronectin; and fibrillin-1 [3]. Proteoglycans directly bind to TGFBIp and affect collagen VI aggregation and possibly the interaction between integrin and collagen VI [14]. Binding allows TGFBIp, including ECM proteins, to play an important role in cell-collagen signaling interactions that comprise BM, bone formation, and development as well as cell migration and growth.

In our patient, various pathological findings of GBM and TBM and widening of the subendothelial space of GBM were observed by electron microscopy. A negative genetic analysis of well-known monogenic kidney diseases prompted us to consider that *TGFBI* mutation could affect the BM of the developing kidneys and produce such BM findings. The findings of TBM were more obvious than those of GBM. The pathophysiological mechanisms and the incidence of this condition or genotype-phenotype correlation for *TGFBI* mutations are not obvious.

Visual disturbances preceded by proteinuria occurred in our patient during her clinical evaluation. If detailed examination of the corneas is not performed, GCD2 may not be observed until middle-age and older. It should be noted that detailed ocular examinations, including cornea assessments, are valuable when diagnosing nephropathy associated with *TGFBI* mutations. Presently, ALUT testing is beneficial for laser-assisted in situ keratomileusis to protect patients from accelerated vision loss. As demonstrated with our patient, this test is easy and safe to perform when diagnosing patients with nephropathy associated with *TGFBI* mutations.

In conclusion, we have reported the first case of a unique nephropathy complicated by *TGFBI*-related CD. We consider that our case was probably a novel type of oculorenal syndrome. *TGFBI*-related nephropathy remains unknown and is difficult to diagnose without electron microscopic examination. Further reports should be accumulated to determine whether the incidence of renal diseases associated with this mutation may presently be more frequent. Patients with *TGFBI*-related CDs, including GCD2, should be examined for renal abnormalities.

Case Reports in Nephrology and Dialysis

Case Rep Nephrol Dial 2016;6:106–113		110
DOI: 10.1159/000449129	© 2016 The Author(s). Published by S. Karger AG, Basel www.karger.com/cnd	

Iwafuchi et al.: A Case of *Transforming Growth Factor-β-Induced* Gene-Related Oculorenal Syndrome: Granular Corneal Dystrophy Type II with a Unique Nephropathy

Acknowledgement

Statement of Ethics

The authors have no ethical conflicts to disclose, and the patient provided informed consent.

Disclosure Statement

The authors declare that they have no relevant financial interests.

References

1   Izzedine H, Bodaghi B, Launay-Vacher V, Deray G: Eye and kidney: from clinical findings to genetic explanations. J Am Soc Nephrol 2003;14:516–529.

2   Klintworth GK: Corneal dystrophies. Orphanet J Rare Dis 2009;4:7.

3   Randles MJ, Woolf AS, Huang JL, Byron A, Humphries JD, Price KL, Kolatsi-Joannou M, Collinson S, Denny T, Knight D, Mironov A, Starborg T, Korstanje R, Humphries MJ, Long DA, Lennon R: Genetic background is a key determinant of glomerular extracellular matrix composition and organization. J Am Soc Nephrol 2015;26:3021–3034.

4   Lennon R, Byron A, Humphries JD, Randles MJ, Carisey A, Murphy S, Knight D, Brenchley PE, Zent R, Humphries MJ: Global analysis reveals the complexity of the human glomerular extracellular matrix. J Am Soc Nephrol 2014;25:939–951.

5   Kawamoto T, Noshiro M, Shen M, Nakamasu K, Hashimoto K, Kawashima-Ohya Y, Gotoh O, Kato Y: Structural and phylogenetic analyses of RGD-CAP/βig-h3, a fasciclin-like adhesion protein expressed in chick chondrocytes. Biochim Biophys Acta 1998;1395:288–292.

6   Thapa N, Lee BH, Kim IS: TGFBIp/βig-h3 protein: a versatile matrix molecule induced by TGF-β. Int J Biochem Cell Biol 2007;39:2183–2194.

7   Lee JH, Cristol SM, Kim WC, Chung ES, Tchah H, Kim MS, Nam CM, Cho HS, Kim EK: Prevalence of granular corneal dystrophy type 2 (Avellino corneal dystrophy) in the Korean population. Ophthalmic Epidemiol 2010;17:160–165.

8   Schorderet DF, Menasche M, Morand S, Bonnel S, Büchillier V, Marchant D, Auderset K, Bonny C, Abitbol M, Munier FL: Genomic characterization and embryonic expression of the mouse Bigh3 (Tgfbi) gene. Biochem Biophys Res Commun 2000;274:267–274.

9   Chen YM, Liapis H: Focal segmental glomerulosclerosis: molecular genetics and targeted therapies. BMC Nephrol 2015;16:101.

10 El Kochairi I, Letovanec I, Uffer S, Munier FL, Chaubert P, Schorderet DF: Systemic investigation of keratoepithelin deposits in TGFBI/BIGH3-related corneal dystrophy. Mol Vis 2006;12:461–466.

11 Billings PC, Whitbeck JC, Adams CS, Abrams WR, Cohen AJ, Engelsberg BN, Howard PS, Rosenbloom J: The transforming growth factor-β-inducible matrix protein βig-h3 interacts with fibronectin. J Biol Chem 2002;277:28003–28009.

12 Kim JE, Jeong HW, Nam JO, Lee BH, Choi JY, Park RW, Park JY, Kim IS: Identification of motifs in the fasciclin domains of the transforming growth factor-β-induced matrix protein βig-h3 that interact with the αvβ5 integrin. J Biol Chem 2002;277:46159–46165.

13   Kim MO, Yun SJ, Kim IS, Sohn S, Lee EH: Transforming growth factor-β-inducible gene-h3 (βig-h3) promotes cell adhesion of human astrocytoma cells in vitro: implication of α6β4 integrin. Neurosci Lett 2003;336:93–96.
14   Reinboth B, Thomas J, Hanssen E, Gibson MA: Big-h3 interacts directly with biglycan and decorin, promotes collagen VI aggregation, and participates in ternary complexing with these macromolecules. J Biol Chem 2006;281:7816–7824.
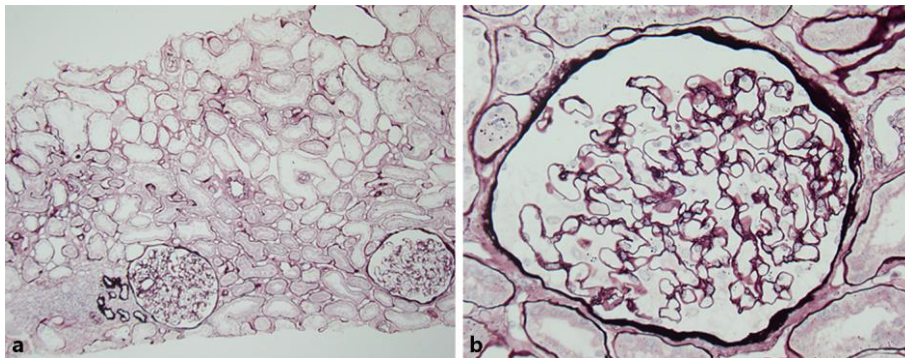
Fig. 1. a Normal appearance of the glomeruli. Focal tubular atrophy with dilation of the peritubular capillaries and focal infiltration of small round cells (periodic acid-silver methenamine stain, original magnification ×48). **b** Glomeruli revealing unremarkable changes by light microscopic examination (periodic acid-silver methenamine stain, original magnification ×400).
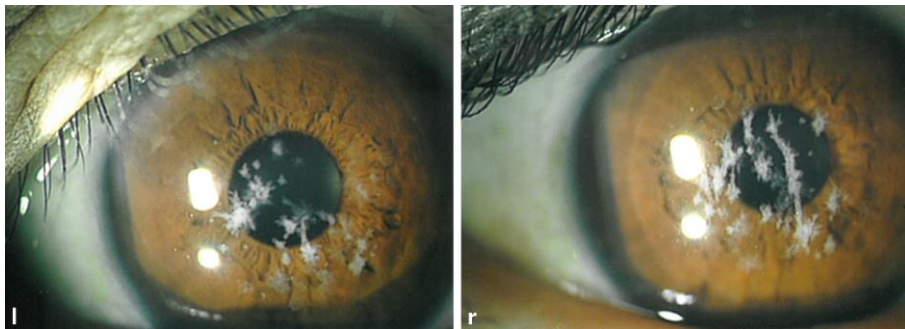

Fig. 2. Bilateral slit-lamp examination demonstrating areas of fused crumb-like white stromal opacities resulting in elongated and stellate shapes. l = Left; r = right.
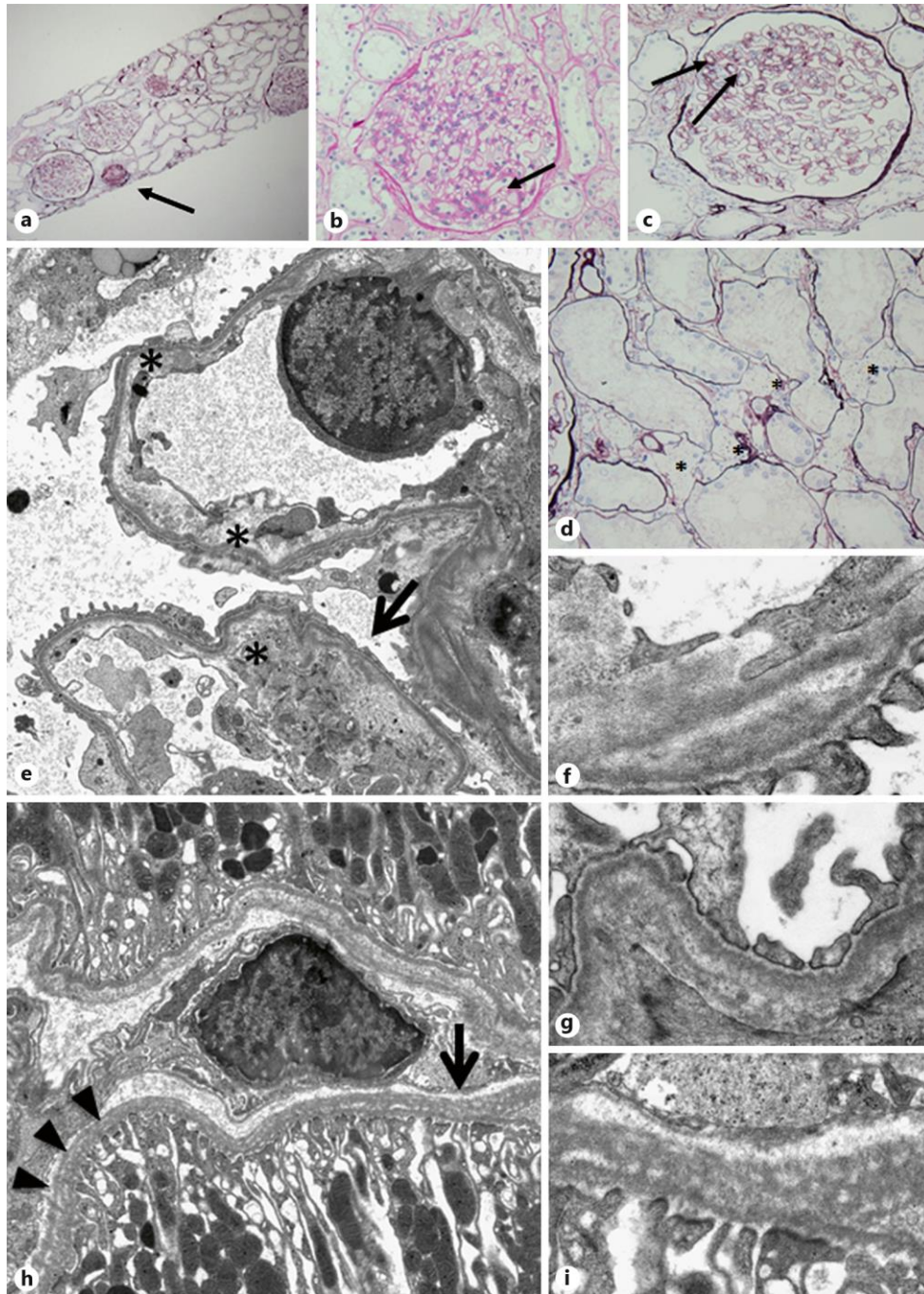
KARGER

Iwafuchi et al.: A Case of *Transforming Growth Factor-β-Induced* Gene-Related Oculorenal Syndrome: Granular Corneal Dystrophy Type II with a Unique Nephropathy

Iwafuchi et al.: A Case of *Transforming Growth Factor-β-Induced* Gene-Related Oculorenal Syndrome: Granular Corneal Dystrophy Type II with a Unique Nephropathy

Fig. 3. a Light microscopic examination revealing 18 glomeruli. Six (arrow) were obsolete or sclerosed. The glomeruli were slightly enlarged with segmental mesangial proliferation. Focal tubular atrophy with mild interstitial inflammation was noted (periodic acid-silver methenamine stain, original magnification ×48). **b** The glomerulus displaying a mild segmental increase in the mesangial matrix (arrow) (periodic acid-Schiff stain, original magnification ×400). **c** Slightly enlarged glomerulus with segmental mesangial proliferation. Segmental double contours of the glomerular capillary walls (arrows) were observed (periodic acid-silver methenamine stain, original magnification ×400). **d** Several foam cells (asterisks) were noted in the interstitium. Focal tubular atrophy with dilation of peritubular capillaries was also noted (periodic acid-silver methenamine stain, original magnification ×400). **e** Separation of the endothelial cell from the underlying GBM (asterisks). Slightly irregular appearance, such as partial thinning and duplication of the GBM with partial effacement of foot processes (arrow) (electron microscopy, original magnification ×2,000). **f** Higher magnification displaying partial duplication of the GBM (electron microscopy, original magnification ×12,000). **g** Higher magnification displaying partial irregularity of the GBM (electron microscopy, original magnification ×10,000). **h** Diffuse irregular distribution with reticulation (arrows) and lamellation (arrowheads) of the TBM (electron microscopy, original magnification ×2,000). **i** Higher magnification displaying reticulation of the TBM (electron microscopy, original magnification ×10,000).

SHORT COMMUNICATION

Cryptic exon activation in *SLC12A3* in Gitelman syndrome

Kandai Nozu[1], Yoshimi Nozu[1], Keita Nakanishi[1], Takao Konomoto[2], Tomoko Horinouchi[1], Akemi Shono[1], Naoya Morisada[1], Shogo Minamikawa[1], Tomohiko Yamamura[1], Junya Fujimura[1], Koichi Nakanishi[3], Takeshi Ninchoji[1], Hiroshi Kaito[1], Ichiro Morioka[1], Mariko Taniguchi-Ikeda[1], Igor Vorechovsky[4] and Kazumoto Iijima[1]

Gitelman syndrome (GS) is an autosomal recessive renal tubulopathy characterized by hypokalemic metabolic alkalosis with hypocalciuria and hypomagnesemia. GS clinical symptoms range from mild weakness to muscular cramps, paralysis or even sudden death as a result of cardiac arrhythmia. GS is caused by loss-of-function mutations in the solute carrier family 12 member 3 (*SLC12A3*) gene, but molecular mechanisms underlying such a wide range of symptoms are poorly understood. Here we report cryptic exon activation in *SLC12A3* intron 12 in a clinically asymptomatic GS, resulting from an intronic mutation c.1669+297 T > G that created a new acceptor splice site. The cryptic exon was sandwiched between the L3 transposon upstream and a mammalian interspersed repeat downstream, possibly contributing to inclusion of the cryptic exon in mature transcripts. The mutation was identified by targeted next-generation sequencing of candidate genes in GS patients with missing pathogenic *SLC12A3* alleles. Taken together, this work illustrates the power of next-generation sequencing to identify causal mutations in intronic regions in asymptomatic individuals at risk of developing potentially fatal disease complications, improving clinical management of these cases.
Journal of Human Genetics advance online publication, 27 October 2016; doi:10.1038/jhg.2016.129

INTRODUCTION

Gitelman syndrome (GS, OMIM 263800) is one of the most common autosomal recessive kidney tubulopathies, with an estimated prevalence of 1:40 000 in Caucasians.[1,2] GS is characterized by hypokalemia, hypomagnesemia, metabolic alkalosis and hypocalciuria, and usually manifests as mild weakness, cramps and general fatigue. However, some GS cases are clinically asymptomatic or are not diagnosed until late childhood or adulthood,[3] but molecular mechanisms for the variable penetrance and age of onset are poorly understood.

GS is caused by mutations in the solute carrier family 12 member 3 (*SLC12A3*) gene[4] that encodes the thiazide-sensitive sodium-chloride cotransporter.[4] The loss of sodium-chloride cotransporter function leads to a decrease in sodium and chloride reabsorption in the distal convoluted tubule, causing salt-wasting tubulopathy. To date, more than 400 different *SLC12A3* mutations have been identified in GS; however, as many as 20–41% patients were found only with a single pathogenic allele, suggesting that the mutation screening is unsatisfactory.[3–8] Although using reverse transcription-PCR (RT-PCR) may help identify deep intronic mutations resulting in RNA processing abnormalities,[9,10] this method may not identify all aberrant mRNAs. The reason for the large fraction of missing GS alleles is poorly understood.

Here we report a case of latent GS caused by a partial cryptic exon activation in *SLC12A3* intron 12. Identification of the new exon was facilitated by next-generation sequencing (NGS) followed by *in silico* analysis and RT-PCR validation of aberrant transcripts. The case highlights the importance of detecting intronic variants in low-penetrance genetic conditions at risk of potentially fatal complications, permitting a more focused management of affected families.

MATERIALS AND METHODS

The proband was a 5-year-old girl diagnosed by chance with mild proteinuria (urinary protein/creatinine: $0.4 \, \mathrm{g \, gCr^{-1}}$), hypokalemia ($2.7 \, \mathrm{mEq \, l^{-1}}$), hypomagnesemia ($1.5 \, \mathrm{mg \, dl^{-1}}$), metabolic alkalosis ($\mathrm{HCO_3^-}$: $26.7 \, \mathrm{mEq \, l^{-1}}$) and hypocalciuria (urinary calcium/creatinine: $0.005 \, \mathrm{mg \, mg^{-1}}$). The laboratory findings were indicative of GS, but she had not suffered any overt clinical symptoms.

All procedures were reviewed and approved by the Institutional Review Board of Kobe University School of Medicine. Informed consent was obtained from all patients or their parents.

NGS samples were prepared using a HaloPlex Target Enrichment System Kit (Agilent Technologies, Santa Clara, CA, USA) according to the manufacturer's instructions to capture 12 genes (Supplementary Table 1), including *SLC12A3*, *CLCNKB*, *SLC12A1*, *KCNJ1* and other

[1]Department of Pediatrics, Kobe University Graduate School of Medicine, Kobe, Japan; [2]Department of Pediatrics, Faculty of Medicine, University of Miyazaki, Miyazaki, Japan; [3]Department of Pediatrics, Wakayama Medical University, Wakayama, Japan and [4]University of Southampton Faculty of Medicine, Southampton, UK
Correspondence: Dr K Nozu, Department of Pediatrics, Kobe University Graduate School of Medicine, 7-5-1 Kusunoki-cho, Chuo, Hyogo, Kobe 6500017, Japan.
E-mail: nozu@med.kobe-u.ac.jp

2

genes associated with hypokalemia. Amplified target libraries were sequenced using MiSeq (Illumina, San Diego, CA, USA), which was followed by variant analysis with SureCall (v.3.0; Agilent Technologies). The *SLC12A3* reads were mapped to the human reference sequence NC_000015.9 and NM_000338.2. Exons were numbered according to a previous report.[11] Rare variants with a frequency <1% were analyzed using the Human Splicing Finder v.3.0 software (http://www.umd.be/HSF3/).

RESULTS

Conventional mutation screening of *SLC12A3* in the proband revealed only a single pathogenic allele on the maternal chromosome (c.2927C>T, p.Ser976Phe), which was previously reported in two patients.[12,13] We next used the HaloPlex target enrichment system analysis of candidate genes for tubulopathies/pseudo-GS, including *SLC12A3*. NGS detected a total of 88 heterozygous intronic *SLC12A3* variants (Figure 1a). Analysis of variants with a minor allele frequency of <1% using the Human Splicing Finder (v.3.0) software[14] revealed a single heterozygous variant predicted to create a new 3′ splice site, c.1567+297 T>G, located in intron 12. This change had a potential of activating a cryptic exon with a high-score cryptic

5′ splice site further downstream (Supplementary Figures 1A and B). Validation of the putative cryptic exons using RT-PCR with primers in exons 12 and 13 revealed a 108-bp insertion of the new coding sequence in the patient's *SLC12A3* mRNA (Figures 1c and d), confirming the *in silico* prediction. The new exon was sandwiched between the L3 transposon and a mammalian interspersed repeat located upstream and downstream, respectively (Figures 1c and d and Supplementary Figures 2 and 3). The presence of each mutation was confirmed in parental samples (Figure 1e). These results indicated that the GS proband was a compound heterozygote for *SLC12A3* mutations, one resulting in amino-acid substitution S976F in the C-terminal domain of sodium-chloride cotransporter and the other in protein truncation through cryptic exon activation.

We then used NGS in two more GS cases with previously reported deep intronic splicing mutations. In Case 1, NGS detected a total of 30 heterozygous intronic *SLC12A3* variants, including mutation c.1670−191C>T, which created a new 5′ splice site (Supplementary Figures 4A–C) and activated the cryptic exon, as reported.[10] In Case 2, NGS detected a total of 27 heterozygous intronic
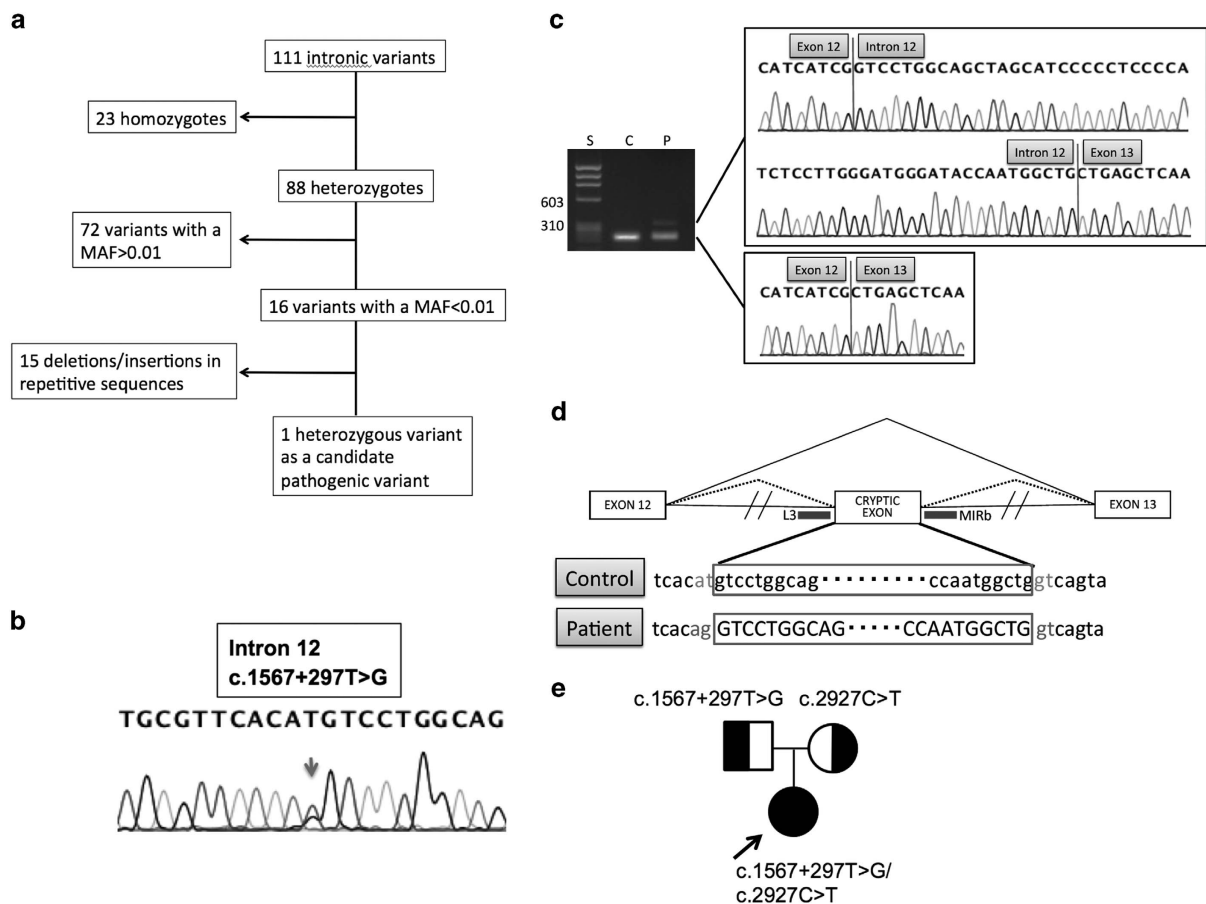

Figure 1 Cryptic exon activation in solute carrier family 12 member 3 (*SLC12A3*) in Gitelman syndrome (GS). (**a**) Flow chart illustrates the step-wise identification of the intronic mutation in our proband. MAF, minor allele frequency. (**b**) Genomic sequence of *SLC12A3* intron 12 in the proband. Mutation c.1567+297 T>G was detected by next-generation sequencing and confirmed by Sanger sequencing. (**c**) Transcript analysis by reverse transcription-PCR (RT-PCR). Left panel: S, size marker with fragment sizes shown to the left; C, control; P, patient. The fraction of aberrant transcripts was ~ 12% of the total signal from polyadenylated RNAs. Right panel: Direct sequencing of the larger transcript showed a 108-bp insertion between exons 12 and 13. (**d**) Schematics of the cryptic exon activation. Exons are shown as boxes, introns as lines and aberrant transcripts as dotted lines. Transposed elements are schematically shown by green rectangles and correspond to alignments in Supplementary Figure 3. (**e**) Pedigree of the GS family. The proband is denoted by an arrow. Each GS allele was inherited from the parents. A full color version of this figure is available at the *Journal of Human Genetics* journal online.

SLC12A3 variants, including variant c.2548+253C > T, which creates a new 3′ splice site (Supplementary Figures 5A–C).[9]

DISCUSSION

Previously, we reported two deep intronic *SLC12A3* mutations, both of which were hotspots for Japanese and Taiwanese GS patients, suggesting that these cases might be observed more frequently.[9,10] In this report, we used NGS to detect missing alleles in a suspected GS. Our results clearly demonstrate that NGS can facilitate their identification in asymptomatic cases that may develop potentially life-threatening complications later in life. As an example, arrhythmia as a result of hypokalemia can develop in GS children as young as 6 years of age.[15] To confirm the utility of this method, NGS successfully identified known variants in two other GS cases possessing deep intronic variants that affected splicing.

Interestingly, the novel cryptic exon was activated in a region closely flanked by a long interspersed repeat upstream and a mammalian interspersed repeat downstream (Supplementary Figure 3). Mammalian interspersed repeats have a propensity to exonize by a single mutation, and have very high exonization levels compared with other transposable elements,[16] although it remains to be seen if this element facilitated usage of the new 3′ splice site.

Although NGS is still more expensive compared with conventional direct sequencing, NGS of DNA samples may complement RT-PCR approaches and facilitate identification of aberrant transcripts missed by conventional techniques. Definite genetic diagnosis of GS will permit better management of patients and improve their quality of life.

In conclusion, we identified a novel *SLC12A3* allele in GS that activates a cryptic exon flanked by interspersed repeats deep in intron 12. Our study illustrates the power of NGS to fully define the mutation pattern in GS and also improve our understanding of the phenotypic variability of this condition. This approach can be used more widely to identify individuals at risk of fatal complications in many other genetic disorders, providing a better support for their clinical management.

CONFLICT OF INTEREST

The authors declare no conflict of interest.

ACKNOWLEDGEMENTS

1 Seyberth, H. W. An improved terminology and classification of Bartter-like syndromes. *Nat. Clin. Pract. Nephrol.* **4**, 560–567 (2008).
2 Seyberth, H. W. & Schlingmann, K. P. Bartter- and Gitelman-like syndromes: salt-losing tubulopathies with loop or DCT defects. *Pediatr. Nephrol.* **26**, 1789–1802 (2011).
3 Cruz, D. N., Shaer, A. J., Bia, M. J., Lifton, R. P., Simon, D. B., Yale, G. S. *et al.* Gitelman's syndrome revisited: an evaluation of symptoms and health-related quality of life. *Kidney Int.* **59**, 710–717 (2001).
4 Simon, D. B., Nelson-Williams, C., Bia, M. J., Ellison, D., Karet, F. E., Molina, A. M. *et al.* Gitelman's variant of Bartter's syndrome, inherited hypokalaemic alkalosis, is caused by mutations in the thiazide-sensitive Na-Cl cotransporter. *Nat. Genet.* **12**, 24–30 (1996).
5 Colussi, G., Bettinelli, A., Tedeschi, S., De Ferrari, M. E., Syren, M. L., Borsa, N. *et al.* A thiazide test for the diagnosis of renal tubular hypokalemic disorders. *Clin. J. Am. Soc. Nephrol.* **2**, 454–460 (2007).
6 Lemmink, H. H., Knoers, N. V., Karolyi, L., van Dijk, H., Niaudet, P., Antignac, C. *et al.* Novel mutations in the thiazide-sensitive NaCl cotransporter gene in patients with Gitelman syndrome with predominant localization to the C-terminal domain. *Kidney Int.* **54**, 720–730 (1998).
7 Lin, S. H., Shiang, J. C., Huang, C. C., Yang, S. S., Hsu, Y. J. & Cheng, C. J. Phenotype and genotype analysis in Chinese patients with Gitelman's syndrome. *J. Clin. Endocrinol. Metab.* **90**, 2500–2507 (2005).
8 Monkawa, T., Kurihara, I., Kobayashi, K., Hayashi, M. & Saruta, T. Novel mutations in thiazide-sensitive Na-Cl cotransporter gene of patients with Gitelman's syndrome. *J. Am. Soc. Nephrol.* **11**, 65–70 (2000).
9 Lo, Y. F., Nozu, K., Iijima, K., Morishita, T., Huang, C. C., Yang, S. S. *et al.* Recurrent deep intronic mutations in the SLC12A3 gene responsible for Gitelman's syndrome. *Clin. J. Am. Soc. Nephrol.* **6**, 630–639 (2011).
10 Nozu, K., Iijima, K., Nozu, Y., Ikegami, E., Imai, T., Fu, X. J. *et al.* A deep intronic mutation in the SLC12A3 gene leads to Gitelman syndrome. *Pediatr. Res.* **66**, 590–593 (2009).
11 International Human Genome Sequencing, C. Finishing the euchromatic sequence of the human genome. *Nature* **431**, 931–945 (2004).
12 Jang, H. R., Lee, J. W., Oh, Y. K., Na, K. Y., Joo, K. W., Jeon, U. S. *et al.* From bench to bedside: diagnosis of Gitelman's syndrome—defect of sodium-chloride cotransporter in renal tissue. *Kidney Int.* **70**, 813–817 (2006).
13 Nakamura, A., Shimizu, C., Nagai, S., Yoshida, M., Aoki, K., Kondo, T. *et al.* Problems in diagnosing atypical Gitelman's syndrome presenting with normomagnesaemia. *Clin. Endocrinol. (Oxf)* **72**, 272–276 (2010).
14 Desmet, F. O., Hamroun, D., Lalande, M., Collod-Beroud, G., Claustres, M. & Beroud, C. Human Splicing Finder: an online bioinformatics tool to predict splicing signals. *Nucleic Acids Res.* **37**, e67 (2009).
15 Bettinelli, A., Tosetto, C., Colussi, G., Tommasini, G., Edefonti, A. & Bianchetti, M. G. Electrocardiogram with prolonged QT interval in Gitelman disease. *Kidney Int.* **62**, 580–584 (2002).
16 Vorechovsky, I. Transposable elements in disease-associated cryptic exons. *Hum. Genet.* **127**, 135–154 (2010).